博 士 学 位 論 文
Doctoral Thesis

論文題目

Thesis Title

Interference Coordination for A Cellular System with Distributed MU-MIMO

(セルラ分散 MU-MIMO 通信システムの干渉制御)

東 北 大 学 大 学 院 工 学 研 究 科

Graduate School of Engineering,

TOHOKU UNIVERSITY

専攻/Department: Communications Engineering

学籍番号/ ID No: C0TD2301

氏 名 /Name: GE CHANG

Interference Coordination for A Cellular System with Distributed MU-MIMO

(セルラ分散MU-MIMO通信システムの干渉制御)

by

Ge Chang（葛 暢）

A Dissertation
for Doctor of Philosophy (Engineering)

Submitted to
Department of Communications Engineering
Graduate School of Engineering
Tohoku University

June, 2023

Supervised by Prof. Chen, Qiang （陳 強）

Abstract

In 5G and beyond, the application of distributed MU-MIMO has garnered considerable interest due to its potential in resolving challenges associated with utilizing the mm-wave band, such as radio link blockage. To address the computational complexity issues posed by large-scale distributed MU-MIMO systems, a cluster-wise distributed MU-MIMO approach has been devised. Nonetheless, the adoption of cluster-wise distributed MU-MIMO in cellular system brings about an unintended consequence of introducing additional intracell and intercell interference, which significantly impacts system capacity. Consequently, this study aims to explore interference coordination (IC) within the cellular system with cluster-wise distributed MU-MIMO, with the goal of enhancing overall system capacity.

Taking inspiration from recent advancements in utilizing graph coloring algorithms (GCA) for interference coordination (IC), this study explores the application of GCA-based IC in cellular systems with cluster-wise distributed MU-MIMO. However, within the context of the O-RAN architecture, the conventional framework for implementing GCA-based IC exhibits certain limitations. Employing GCA-based IC based on the fully centralized (FC) framework effectively mitigates both intracell and intercell interference, but its computational complexity surpasses practical constraints. Conversely, employing GCA-based IC based on the fully decentralized (FD) framework offers computational flexibility, yet it only addresses intracell interference, leaving intercell interference stemming from color collisions unresolved. Hence, there is a need of an enhanced GCA-based IC and also an improved framework to enable the simultaneous mitigation of both the intracell interfernce and intercell interference.

In this study, based on the O-RAN architecture, a 2-layer IC framework is proposed and two upgraded GCA-based ICs that can be used under this 2-layer IC framework are also proposed. The application of these two methods under the 2-layer IC framework has been verified to successfully mitigate both intercell interference and intracell interference, while maintaining a

computational complexity similar to that of the FD framework.

One of the proposed approaches is to integrate GCA with FFR (Frequency and Fractional Reuse) scheme, thereby combining the intracell IC advantages of GCA with the intercell IC advantages of FFR. Based on this idea, in Chapter 3, a modified GCA-based IC is proposed. All the clusters in each cell are categorized into two types: cell-edge clusters and inner-cell clusters. Each type is colored separately using distinct color options. In order to realize the above-mentioned idea, the following task has been done. Firstly, based on computational geometry (CG), a method to abstract the IC problem as a graph is first proposed, which is able to circumvent the threshold optimization problem of traditional graph construction methods, while at the same time, automatically distinguish the clusters that locates near the cell boundaries. Then, with the constructed graph, a new GCA, named as the restricted conditional GCA (RC-GCA) is also proposed in this chapter, in which it enables the separate coloring of the cell-edge clusters and the inner-cell clusters. Based on RC-GCA, the cell-edge clusters can be colored with restrictions of color options so as to minimize the occurrence of color collisions, while the inner-cell clusters can be colored under conditions so as to self-adapt to the existing cell-edge colors. Finally, based on the O-RAN architecture, a 2-layer IC framework, which relies on the cooperation of non-real-time (non-RT) radio access network intelligent controller (RIC) and near-RT RICs, is also proposed in this chapter. The proposed 2-layer IC framework combines the strengths of the FC framework and the FD framework. It preserves the global perspective of the FC framework while ensuring that the specific IC execution process resembles the FD framework, taking place at each near-RT RIC. When the proposed modified GCA-based IC is appllied under this 2-layer IC framework, a reasonable allocation of cell-edge color options to each cell ie enabled. The effectiveness of the proposed 2-layer IC framework based on modified GCA is verified by the fact that it can further mitigate the intercell interference, building on the successful mitigation of intracell interference, thus enhancing the system capacity even further. It is also demonstrated that our proposed 2-layer IC framework based on GCA outperforms the well-known fractional frequency reuse (FFR) scheme, the fully decentralized (FD) framework and no IC case, and is able to achieve performance comparable to the fully centralized (FC) framework.

The other proposed approach is to combine the GCA-based IC with the rapidly advancing field of artificial intelligence (AI), particularly Deep Reinforcement Learning (DRL). In Chapter 4, considering the dynamics of the environment, a new joint IC method is proposed. The

proposed joint IC includes a GCA-based intracell IC and a DRL-based intercell IC. Based on online training, our proposed joint IC can follow the time-varying environment and thus achieve dynamic IC control based on the real-time feedback from the environment. Considering of the training overhead in practical application, a strategy to apply the proposed joint IC under the 2-layer IC framework is also proposed. By selectively activating the DRL-based intercell IC only in non-adjacent cells, not only the capacity enhancement can be guaranteed but also the training overhead can be controlled. The validation of the computer simulation reveals that our proposed 2-layer IC framework based on joint IC can dramatically increase the capacity and obtain a performance close to the FC framework. At the same time, the analysis of its convergence proves that the DQN can converge within a dozen of time instants and thus our proposed joint IC can adapt to the fast-changing environment with strong environmental adaptability.

Contents

Chapter 1

Introduction

1.1 Background of Research

Due to the continuous growth of mobile data traffic, commercial deployments of 5G have commenced in numerous countries [1]. The exponential rise in the number of users and devices has led to the densification of the radio access network (RAN) [2]. One approach to RAN densification is the deployment of a large number of small-cell base stations (BSs) within the macro-cell area. However, frequent handoffs resulting from user mobility can lead to increased control signaling traffic, thereby reducing the system capacity for data services [3]. To address this issue, RAN densification based on massive multi-user multi-input multi-output (MU-MIMO) technology has been a promissing subject of study [4].

There are two main approaches in massive MU-MIMO: co-located MU-MIMO and distributed MU-MIMO [5]. As shown in Figure 1.1, in co-located MU-MIMO, a base station (BS) is equipped with an array antenna that consists of a large number of antenna elements. Narrow beams are formed to serve users within the coverage area of the base station (cell). On the other hand, in distributed MU-MIMO, a massive number of distributed antennas (DAs), each with its own radio unit, are spatially deployed throughout the cell. These antennas are connected to the BS through optical fronthaul.

In the context of using mm-wave bands in 5G and beyond, which is becoming necessary due to the increasing utilization of the sub-6GHz band [6], distributed MU-MIMO offers a distinct advantage over co-located MU-MIMO. With a spatial deployment of multiple distributed an-

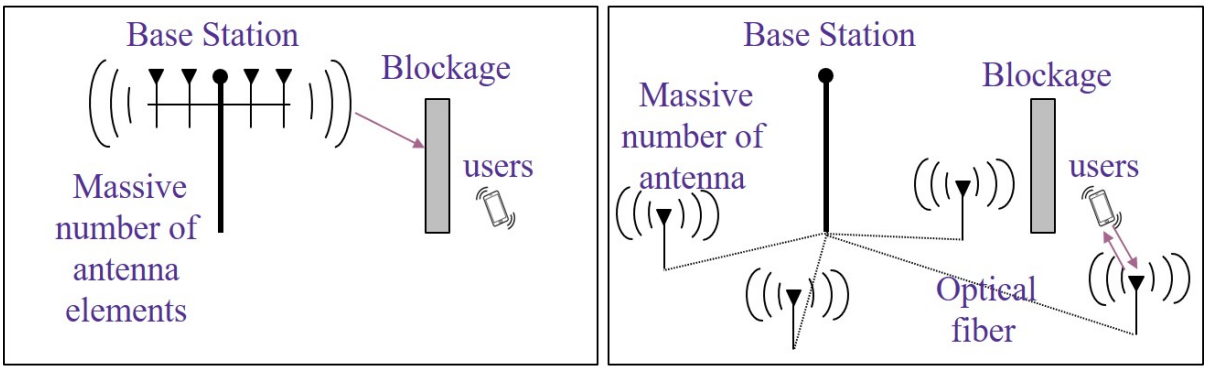

Figure 1.1: Co-located MU-MIMO and the distributed MU-MIMO.

tennas (DAs) across the cell, distributed MU-MIMO can effectively address the issue of radio link blockage caused by rectilinear propagation characteristics [7]. As a result, distributed MU-MIMO has captured great attention for further investigation.

The main drawback of large-scale massive MU-MIMO, no matter it is co-located or distributed, lies in the extremely high computational complexity associated with multi-user signal processing. One possible way to alleviate this computational complexity challenge is to form user-centric virtual small-cell known as user-clusters (referred to as clusters hereafter) [8]. Clusters are created by grouping nearby users that generate significant interference to one another. By dividing a large-scale cell-based MU-MIMO into several smaller-scale cluster-based MU-MIMOs operating in parallel, the computational complexity can be effectively reduced. This system is named as the cellular system with cluster-wise distributed MU-MIMO as shown in Figure 1.2.

However, the introduction of clusters brings a new kind of interference to the system, known as the inter-cluster interference. The inter-cluster interference can be categorized into two types: intracell interference and intercell interference [9]. Intracell interference occurs between clusters within the same cell, while intercell interference occurs between clusters from different cells that face each other along a cell boundary. The intracell and intercell interference are coupled with each other, rendering interference coordination (IC) in cluster-wise distributed MU-MIMO a complex task.

Therefore, the aim of this study is to propose an inter-cluster IC that can effectively handle

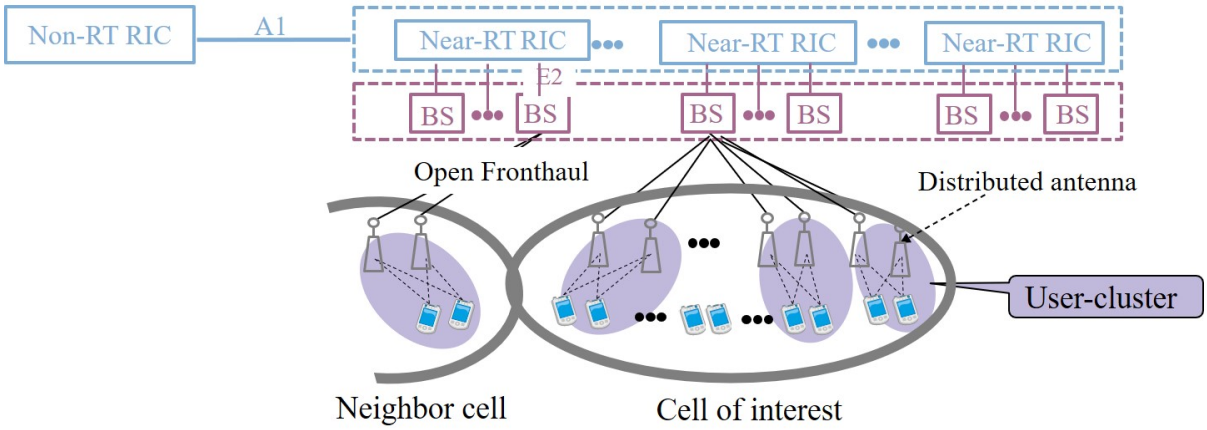

Figure 1.2: Cellular system with cluster-wise distributed MU-MIMO under O-RAN architecture.

both the intracell interference and the intercell interference at the same time, thereby enhance the system capacity.

1.2 Introduction of Cellular System with Cluster-wise Distributed MU-MIMO in O-RAN Architecture

The cellular system with cluster-wise distributed MU-MIMO is designed to be applied under the Open RAN (O-RAN) architecture [10] as shown in Figure 1.2. The O-RAN, through its disaggregated, hierarchical, adaptive network function processing architecture, aims to build a radio network that is intelligent, multi-vendor, software-driven, flexible, and dynamic, so as to fulfill the needs of the next generation mobile networks [11]. The key functional components introduced by O-RAN architecture is the non-RT RIC and the near-RT RIC [12].

The non-RT RIC, with a control loop on the order of seconds or minutes, is responsible for global monitoring and optimization, as well as providing policy-based guidance to support the operation of near-RT RICs. While the near-RT RICs, whose control loop is between 10ms to 1s, is the specific executor, and is responsible to perform tasks such as policy enforcement or radio resource management for one or several cells [13] - [18].

	Control loop	Responsibility
non-RT RIC	seconds or minutes	global monitoring and optimization, as well as providing policy-based guidance to **support the operation of near-RT RICs**.
near-RT RIC	between 10ms to 1s	**specific executor** to perform tasks such as policy enforcement or radio resource management for one or several cells.

Figure 1.3: The comparison of non-RT RIC and near-RT RIC in O-RAN.

In cellular system with cluster-wise distributed MU-MIMO, The wide communication service area, which comprises a large number of DAs, is divided into a prescribed number of cells. The non-RT RIC, with its broaden perspective on the network, is used to perform cellular construction based on the location of DAs. The near-RT RIC, which is connected with the O-DU, O-CU-CP/Up via the E2 interface, is responsible for forming user-clusters inside a cell, and cluster-wise MU-MIMO is carried out in parallel. In such a cellular system, there are two types of interferences: intercell interference and intracell interference. Both these interferences are essentially inter-cluster interferences, but because some clusters belong to the same cell and other clusters belong to neighboring cells, the problem of IC becomes very complicated.

1.3 Challenge of Applying Inter-cluster IC in Cellular System with Cluster-wise Distributed MU-MIMO

In real communication scenarios, the users ' locations will change frequently, leading to periodic updates of user-clusters. Therefore the required inter-cluster IC should be dynamic and can self-adapt to the ever-changing clusters ' topology. In recent years, the successful application of graph coloring algorithm (GCA)-based IC has showed promising potentials. In a small-cell network, H. Zhang, et al.[19] and L. Chen, et al. [20] applied GCA to mitigate the co-tier interference. D. Qu, et al. [21] applied GCA to control the intercell interference so

as to enhance the spectrum efficiency and user experience for an ultra-dense cellular network. Additionally, J. Mu, et al. [22] applied GCA to solve for IC in fast-changing wireless body area networks (WBANs) of the topology to enhance frequency resource utilization and system stability. In [23] , B. Wang, et al. applied GCA to realize co-channel interference management in unmanned aerial vehicle (UAV)-assisted disaster relief networks.

GCA is an algorithm that can assign different colors to neighboring vertices. When GCA is applied for IC, it can serve as a resource scheduling method. In this study, the GCA-based IC is applied in frequency-domain. When GCA-based IC is applied, the available bandwidth is divided into several sub-bands, each of which represents a corresponding color. Thus, applying GCA ensures that the different sub-bands are assigned to neighboring clusters, which as a result, mitigating the inter-cluster interference.

However, the use of GCA pre-assumes the construction of a graph, which requires centralized information gathering. This centralized approach is feasible inside each cell, but considering the system scalability and flexibility for deployment, also the limitations of computational complexity in practical, it is hard to be deployed in the entire system-level. As a result, a practical solution is to utilize GCA-based IC in a parallel manner as a localized intracell IC solution inside each cell.

By applying GCA independently in each cell as an intracell IC solution, the interference among clusters within the same cell can be effectively mitigated. However, a challenge arises when considering the interference between clusters belonging to different cells, particularly in the vicinity of cell boundaries. Since the coloring results are not shared among BSs, there is a possibility of color collision occurring among clusters from different cells. As a result, the issue of intercell interference persists in these areas. Hence, the main challenge of this study is to modify the existing GCA-based IC approach to address both intracell interference and intercell interference simultaneously, while at the same time, make sure the IC is applied in each cell with only the locally observed information and no information exchange among the neighboring cells.

1.4 Proposal of this Studies

In this study, two upgraded GCA-based IC is proposed to solve the above-mentioned challenges. The first method is to modify the coloring process to avoid the occurrence of color

collision during the coloring process, which has been named as the modified GCA-based IC. The second method is to eliminate the occurred color collision after the coloring process, which has been named as the joint IC.

1.4.1 Modified GCA-based IC

The first idea comes up with a well-known radio resource allocation-based IC, namely the fractional frequency reuse (FFR) scheme [24]. In cellular systems, the FFR and its variations, such as soft frequency reuse (SFR) [25] and adaptive soft frequency reuse (ASFR) [26], are well-known intercell ICs. The key idea of FFR is to divide users in each cell into two groups, known as inner-cell users and cell-edge users. A frequency reuse factor of n is then applied to cell-edge users, while a reuse factor of one is applied to the inner-cell users. In this way, a different frequency band is allocated to cell-edge users of a different neighboring cell. Therefore, the FFR scheme can realize the intercell IC. However, it should be noted that the use of a reuse factor of n reduces the transmission bandwidth to one part in n accordingly. Therefore, the application of FFR needs to be carefully considered.

Until now, there have been many reports on the successful application of FFR. For example, L. Yang, et al. [27] applied FFR-based IC to enhance the coverage and capacity of a wireless heterogeneous network (HetNet). Furthermore, L. Eslami, et al. [28] proposed a new FFR architecture for IC in a single-cell HetNet containing macro cellular users, D2D users and femto-cell users. A.D. Firouzabadi, et al. [29] demonstrated that FFR techniques significantly improve downlink coverage probability in hybrid full/half duplex (FD/HD) small cell networks. To mitigate the additional intercell interference due to the flexibility of traffic configuration, M. Song, et al. [30] proposed an FFR-based IC for dynamic time-division duplex (D-TDD) small cell networks. In addition, M. Nafees, et al. [31] adopted the FFR scheme in UAV networks to improve the signal-to-interference plus noise ratio (SINR) level of cell-edge users.

In [32], X. Li, et al. proposed an FFR scheme for multi-cell full-dimension MIMO (FD-MIMO) systems, and confirmed that the FFR-based IC scheme can significantly improve the cell-edge performance while maintaining a relatively high total throughput. In [33], T. Saito, et al. applied the FFR scheme to distributed MU-MIMO to enhance the capacity of cell-edge users.

Inspired by the core idea of FFR, In this study, I try to combine the advantage of GCA-based

IC in intracell IC and the advantage of FFR in intercell IC together to modified the existing GCA-based IC, thereby to make it possible to mitigate the intracell interference and the intercell interference at the same time.

1.4.2 Joint IC (GCA-based Intracell IC + DRL-based Intercell IC)

The second idea draws inspiration from the recent surge in artificial intelligence (AI), particularly in the field of reinforcement learning (RL). Some new progresses for intercell IC in cellular system based on RL have emerged. As early as in 2015, M. Simsek, et al. [34] have tried to apply the Q-learning algorithm to solve the intercell IC among macrocells and picocells in a Heterogeneous network (HetNet). In order to overcome the memory and computational limitation problems that come with tabular-based Q-learning algorithm, the authors proposed to store the probability distribution over all actions instead of the state-action combination in Q table.

In more recent years, with the development of deep learning technology, deep reinforcement learning (DRL) embedded with updatable neural networks has been able to solve large-scale problems more efficiently than tabular-based RL. In 2020, in order to solve the intercell IC problem in an ultra-dense network with small-cell BSs deployed in a residential area, Y. Wang, et al. [35] applied the actor-critic (AC) algorithm to minimize each BS ' s transmit power so as to reduce the intercell interference to the user equipments (UEs) of the surrounding BSs. In order to realize a fully decentralized scheme without information exchange between BSs, the Mean Field Theory is employed together with AC algorithm. Similarly, in 2021, in order to solve the intercell IC problem in HetNets, M. Yan, et al. [36] applied the Double DQN to schedule sub-channels to individual users. In order to improve the robustness of Double DQN, Wasserstein Generative Adversarial Networks (W-GANs) is incorporated together.

Inspired by the above-mentioned contributions, I also want to explore the application of DRL for intercell IC in the cellular system with cluster-wise distributed MU-MIMO. In this study, I strive to combine the strengths of GCA-based IC in intracell IC with the potential of DRL for intercell IC, proposing a joint IC approach. This joint IC approach aims to further mitigate intercell interference while building upon the promising achievements in intracell IC.

1.5 Construction of Dissertation

This dissertation is divided into 6 chapters.

In Chapter 2, the conventional heuristic GCA and the application of GCA-based IC is firstly introduced. Then, the performance of GCA-based IC is evaluated under two commonly used frameworks: fully centralized (FC) and fully decentralized (FD). Finally, the problem statement is established: under the condition that each cell operates in a decentralized manner, there is a pressing need for a novel GCA-based IC that can mitigate intracell interference while considering intercell interference as well.

In order to realize this motivation, two GCA-based method is proposed, which is explained in Chapter 3 and Chapter 4.

In Chapter 3, the concept of Fractional Frequency Reuse (FFR) is incorporated into the GCA algorithm, resulting in a modified GCA-based IC approach. The clusters are categorized into two types: cell-edge clusters and inner-cell clusters. Each type is colored separately using distinct color options. In order to realize the above-mentioned idea, the following task has been done. Firstly, based on computational geometry (CG), a method to abstract the IC problem as a graph is first proposed. Then, a new GCA, named as the restricted conditional GCA (RC-GCA) is also proposed in this chapter. Finally, based on the O-RAN architecture, a 2-layer IC framework, which relies on the cooperation of non-real-time (non-RT) radio access network intelligent controller (RIC) and near-RT RICs, is also proposed in this chapter. The effectiveness of our proposed 2-layer IC framework based on GCA is verified by the fact that it can further mitigate the intercell interference, building on the successful mitigation of intracell interference, thus enhancing the system capacity even further.

In Chapter 4, the possibility of combining GCA with DRL is explored in depth in this chapter, and a new joint IC method is proposed. The proposed joint IC includes a GCA-based intracell IC and a DRL-based intercell IC. Based on online training, our proposed joint IC can follow the time-varying environment and thus achieve dynamic IC control based on the real-time feedback from the environment. Also, a strategy to apply the proposed joint IC under the 2-layer IC framework is proposed. The validation of the computer simulation reveals that our proposed 2-layer IC framework based on joint IC can dramatically increase the capacity and obtain a performance close to the FC framework. At the same time, the analysis of its convergence proves that the DQN can converge within a dozen of time instants and thus our

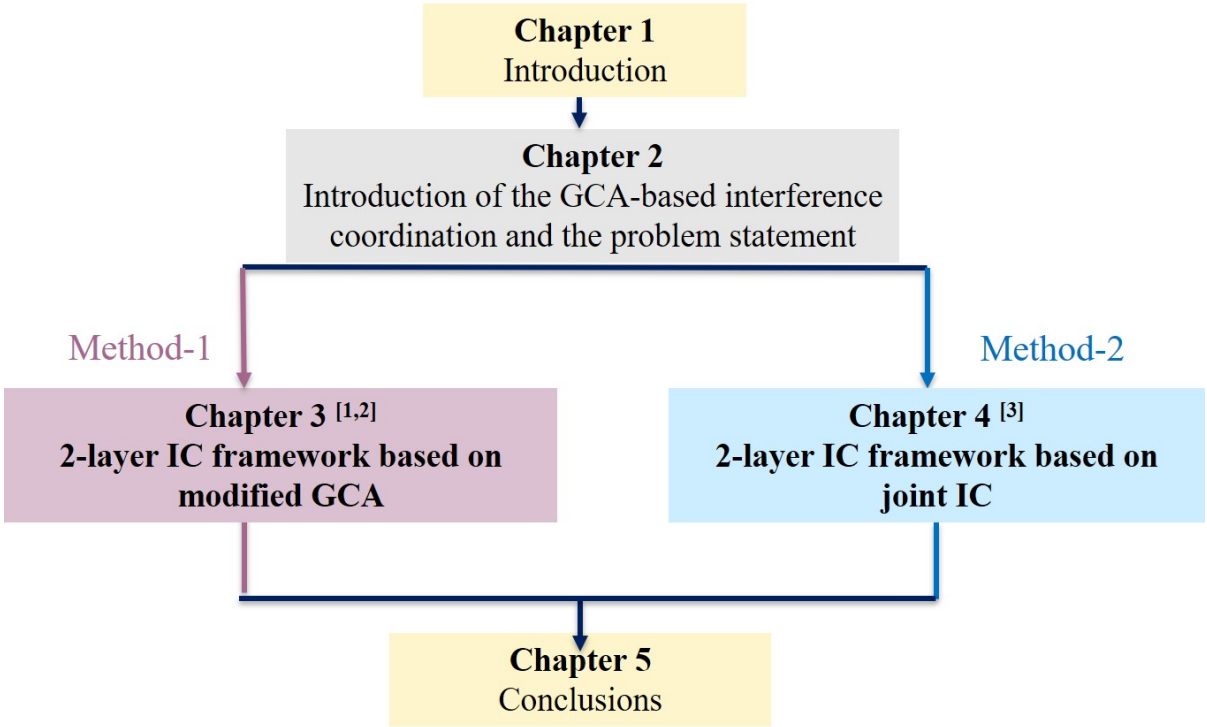

Figure 1.4: Construction of dissertation.

proposed joint IC can quickly adapt to the changing environment.

Chapter 5 concludes this dissertation, and highlights the remaining work to be done in the future research.

The construction of this dissertation is given in Figure 1.4.

Chapter 2

Introduction of GCA-based IC and Problem Statement

In this chapter, the fundamental knowledge required to implement IC using GCA, as well as common approaches to use GCA-based IC in cellular systems with cluster-wise distributed MU-MIMO, are presented. In Section 2.1, the conventional heuristic GCA and how to apply the GCA for IC in cellular system is introduced. Then in Section 2.2, the performance of GCA-based IC is evaluated under two commonly-used frameworks, known as the fully centralized (FC) and the fully decentralized (FD), to verified the performance and better clarity the research problem.

2.1 Conventional GCA-based IC

The graph coloring problem is a classical combinatorial optimization problem, which usually relies on heuristic algorithms to obtain sub-optimal solutions developed for engineering applications. To facilitate understanding, the pseudo code for the conventional heuristic GCA is shown in Algorithm-1, and Figure 2.1 illustrates the working diagram of the heuristic GCA.

Because the graph coloring problem is derived from graph theory. Therefore, the application of GCA pre-assume the construction of a graph $G = (V, E)$, where V and E denote the set of vertices and edges, respectively.

Then, based on graph G, the coloring process of heuristic GCA follows a specific order

Algorithm 1: Heuristic graph coloring algorithm

Input: $\mathbf{A}, \mathbf{c}$

```
Initialize δ
Sort all vertices by decending order of δ, and set the obtained vertex set as 𝒱.
for v_i = v_1 : v_N do
    m = 1
    if m ∉ c ⊙ A^(v_i, :) then
        c_{v_i} ← m
    else
        m = m + 1
    end if
    Reset the vertex set 𝒱.
end for
```

(Note that $\odot$ marks the Hadamard product; $\mathbf{X}^{(y,:)}$ indicates the yth row vectors of the matrix $\mathbf{X}$.)

of processing the vertices, which is known as the coloring sequence as shown in Figure 2.1. Therefore, the most important step in heuristic GCA is to determine the coloring sequence. The difference between different heuristic GCA lies in how to determine the coloring sequence of all the vertices in the graph. For example, the Large Degree Order (LDO) sorts the vertices based on their degrees, while the DSATUR algorithm sorts them based on the degree of saturation. [37]

After that, during coloring process, all the vertex is colored one by one according to the coloring sequence, and at the same time, all the colors are assigned a fixed label, which are represented by numbers 0, 1, 2, and so on. For each vertex, the color with the smallest label that is not already used by any of its neighboring vertices will be assigned

When GCA is used for IC, similarly at first, the IC problem we faced need to be abstracted as a graph. Because the interference in a wireless communication system is bidirectional, therefore, it can be simplified as an undirected graph $G = (V, E)$, where V and E denote the set of vertices and edges, respectively. The vertex (V), represent clusters, which in actually consist of multiple users and therefore has a certain shape. However, for the sake of simplicity, in this

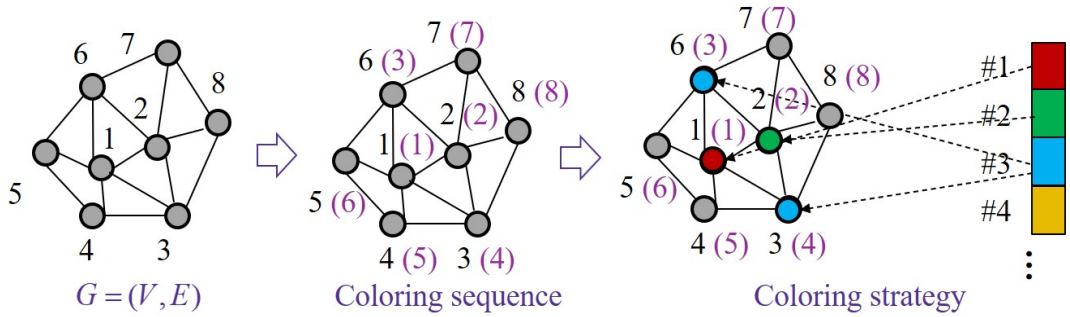

Figure 2.1: The introduction of the heuristic GCA.

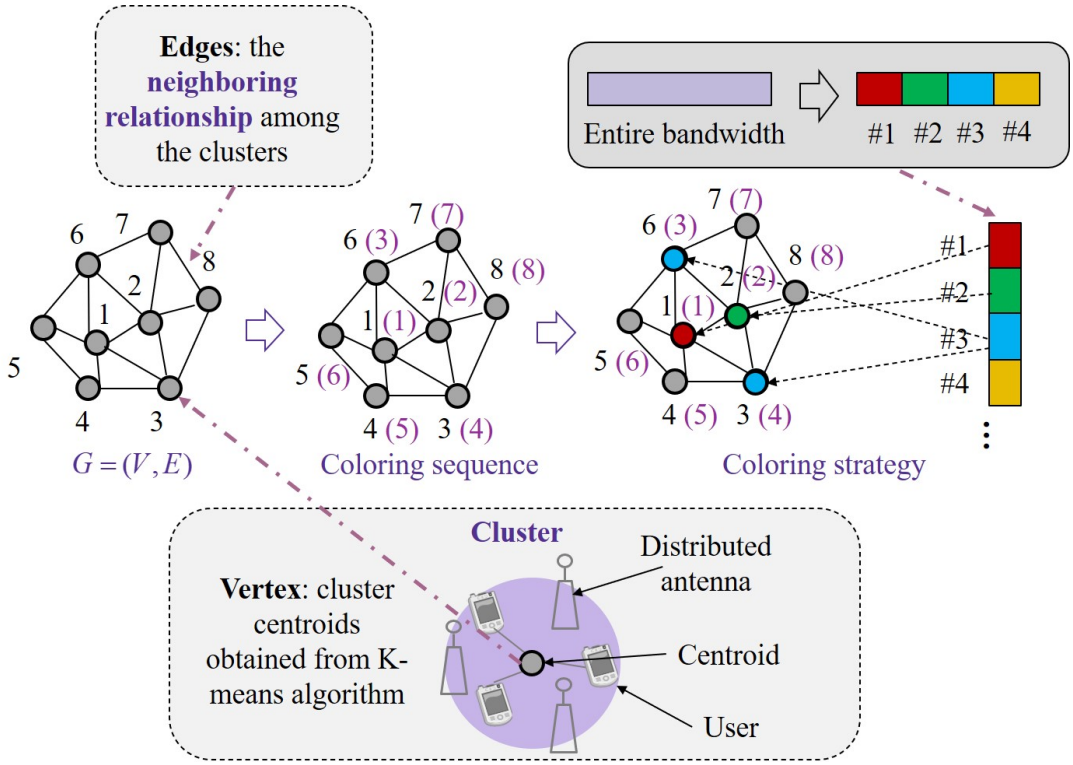

Figure 2.2: The application of GCA for interference coordination.

study, we use the cluster centroid's location to represent the corresponding vertex. Edges(E), on the other hand, represent the interrelation between clusters. Since the most severe interference occurs between neighboring clusters, the edges are further simplified to represent the adjacent relationships between clusters, as illustrated in Figure 2.2.

Besides graph G, the colors also need to be prepared. in this study, we apply the frequency domain scheduling, so the entire available bandwidth will be divided into several sub-bands, and each sub-band will correspond to a specific color.

Therefore, when applying GCA on the graph G, the different sub-band can be assigned to the neighboring clusters, so that since any two neighboring clusters will not share the same sub-band, the severe inter-cluster interference can be mitigated.

2.2 Problem Statement

The performance of the conventional GCA-based IC under existing framework in the cellular system with cluster-wise distributed MU-MIMO will firstly be verified. Therefore, in Section 2.2.1 of this chapter, the construction of a cellular structure will be described first. Then, two typical framework for the application of GCA-based IC, known as the fully centralized (FC) framework and the fully decentralized (FD) framework, will be verified to better illustrate the challenges faced when applying GCA-based IC in cellular system with cluster-wise distributed MU-MIMO.

2.2.1 Generation of Cellular Structure

In this study, we consider a normalized area of 5×5 over which 3,200 DAs are randomly located and a cellular structure of 25 cells is constructed. First, K-means algorithm is applied to obtain the cell centroids using the location information of DAs. Based on the cell centroids, the cellular structure is constructed by using the centroidal Voronoi tessellations (CVT) [38]. An example of cellular structure is shown in Figure 2.3. To accurately estimate the link capacity under the intercell interference environment, the centermost cell which experience the intercell interference from every direction is chosen as the cell of interest in this study.

Inside each cell, user-clusters are formed by K-means algorithm [39]. In this study, we assume 8 clusters are formed in each cell. The clustering result is also shown in Figure

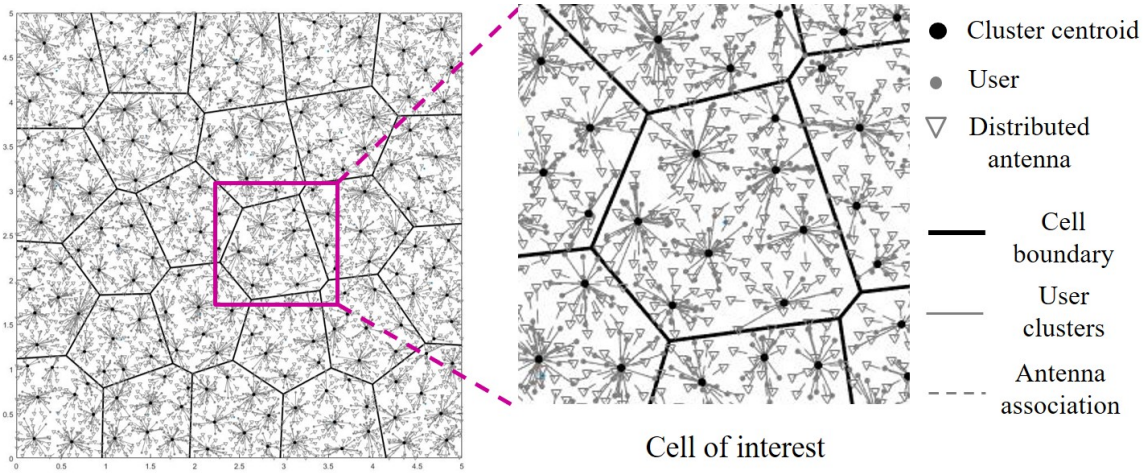

Figure 2.3: Cellular structure with user-clusters in each cell.

2.3, where the users in the same cluster are connected to the cluster centroid by solid lines. The serving DAs are then assigned to each user-cluster based on the principle of proximity for conducting cluster-wise distributed MU-MIMO. The DA assignment results are shown as dashed lines in Figure 2.3. Finally, because ZF precoding [40] is going to be applied, the number of DAs in each cluster must not be less than the number of users, and the assignment of DAs is further optimized based on the previously proposed trading algorithm [41].

2.2.2 Verification of Fully Centralized (FC) Framework Under the O-RAN Architecture

As explained in the Chapter 1, in order to apply GCA-based IC to mitigate both the intracell interference and the intercell interference thoroughly, the GCA-based IC should be applied in a centralized manner with all the information been collected by one single control point. We named this application scenario as the fully centralized (FC) framework. To apply FC framework under the O-RAN architecture, the non-RT RIC should be used to directly control all the clusters in every cells as shown in Figure 2.4.

After the user-clustering is conducted by each near-RT RICs, the non-RT RIC collects the information of all the clusters via A1 interface, and then, is responsible for conducting

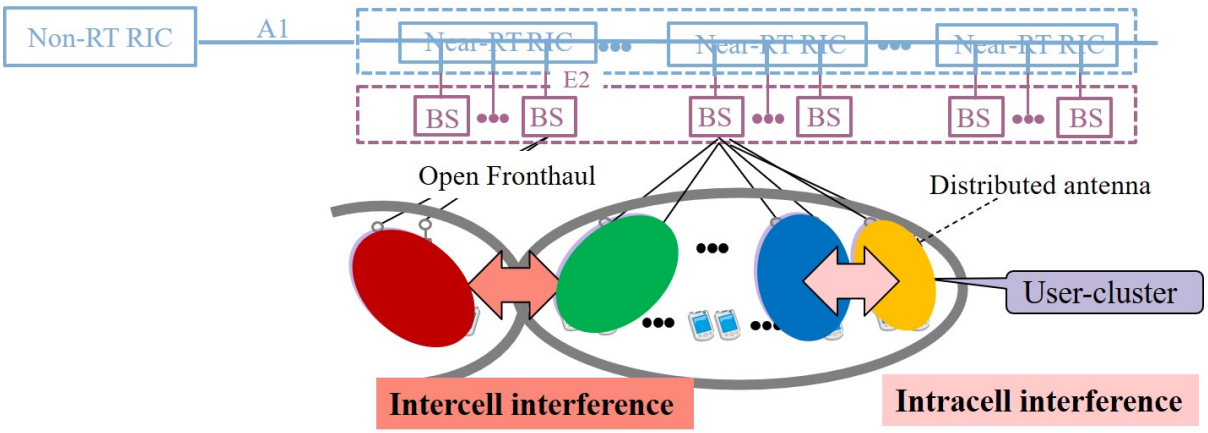

Figure 2.4: Apply GCA-based IC based on the fully centralized (FC) framework under the O-RAN architecture.

GCA-based IC for all clusters inside the entire service area. One example of coloring results under the FC framework is shown in Figure 2.5. From the results in Figure 2.5, it is clearly illustrated that applying GCA-based IC under FC framework is able to assign different colors to the neighboring clusters no matter in the cell-edge or the inner-cell, therefore the intercell interference and the intracell interference can be both considered at the same time.

However, it is also obvious that applying GCA-based IC under the FC framework has a very high computational complexity. The computational complexity of GCA is $O(n^2)$, when GCA-based IC is applied under the FC framework, n equals the number of clusters in the entire multicell system. Meanwhile, for the users with high mobility, it is difficult to apply GCA-based IC by the non-RT RIC. Another major drawback is that this centralized manner is not recommended in O-RAN architecture. According to the original designer of RIC in O-RAN, the non-RT RIC provides a broader system perspective but has a larger control loop. It is specifically designed to support the operation of the non-RT RIC. While the near-RT RIC is desinged as the real executor. By letting each near-RT RIC to be the real executor, it is able to guarantee the system ' s scalability and flexibility for deployment.

Therefore, the results of FC framework can only be regarded as an ideal benchmark, and is difficult to be utilized in practical applications. The GCA-based IC is better to be applied by each near-RT RICs in a decentralized manner.

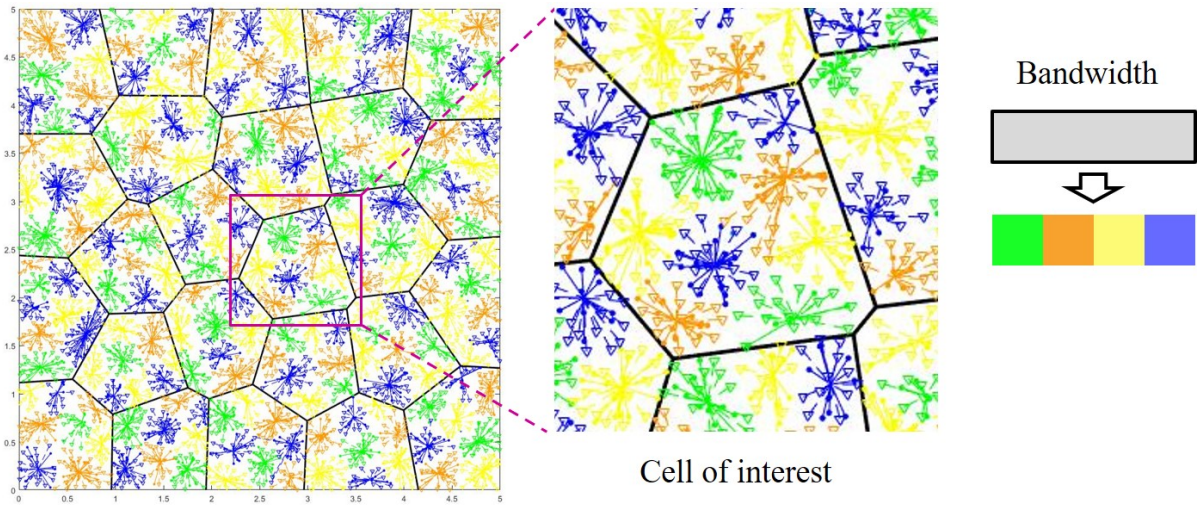

Figure 2.5: Coloring results for GCA-based IC based on the fully centralized (FC) framework.

2.2.3 Verification of Fully Decentralized (FD) Framework Under the O-RAN Architecture

As mentioned above, the FC framework is not suitable for real applications, while a practical alternative is the fully decentralized (FD) framework. In FD framework, after the user-clustering is conducted by each near-RT RICs independently, the GCA-based IC is then directly been conducted by each near-RT RIC, and the non-RT RIC does not need to participate (as shown in Figure 2.6).

The FD framework distributes the computational load from the non-RT RIC to each near-RT RICs, however, because the cells are considered isolated from each other, the coloring results will not shared among the neighboring cells, so the intercell interference cannot be taken into account, and thus it remains. The coloring results of the FD framework is shown in Figure 2.7. Compared with the FC framework shown in Figure 2.5, a lot of color collision can be found near the cell-edge area, indicating that the intercell interference cannot be mitigated thoroughly. Therefore, applying GCA-based IC under the FD framework cannot achieve a similar good interference mitigation as the FC framework, and accordingly, the link capacity obtained by the FC framework is higher than that by the FD framework.

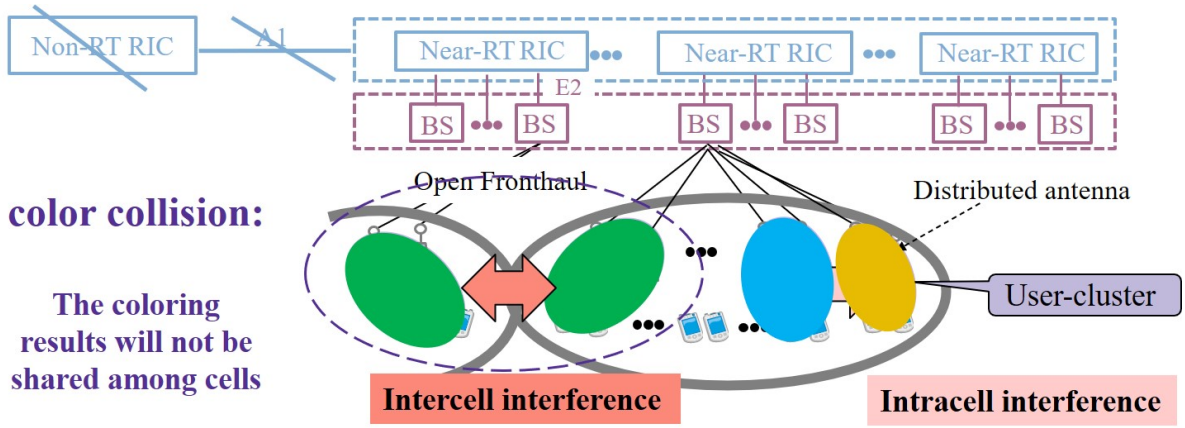

Figure 2.6: Apply GCA-based IC based on the fully decentralized (FD) framework under the O-RAN architecture.

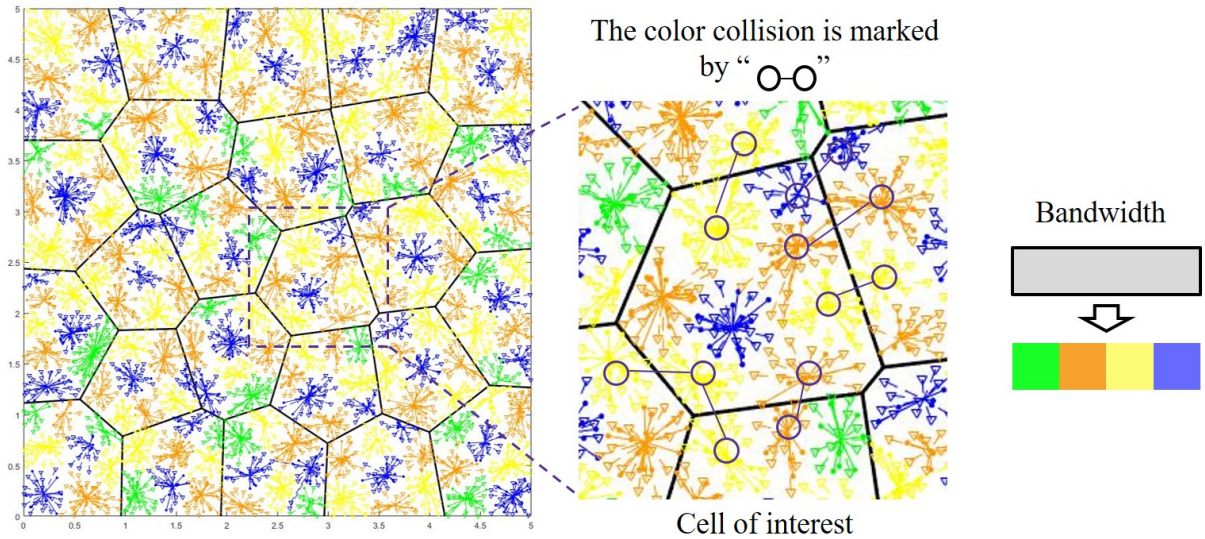

Figure 2.7: Coloring results for GCA-based IC based on the fully decentralized (FD) framework.

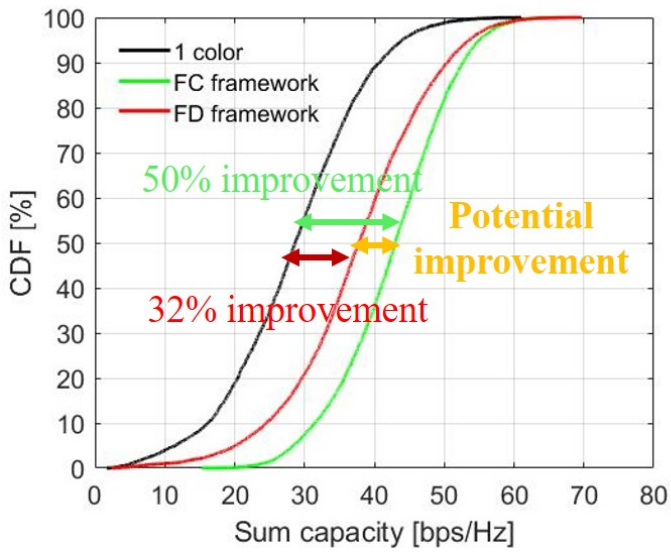

Figure 2.8: CDF of sum capacity achievable by the FC and FD framework.

In order to understand the influence of color collision on system capacity, in Figure 2.8, the cumulative distribution function (CDF) of sum capacity achievable by the FC and FD frameworks is verified. (Note that the detailed simulation setting is explained in Chapter 3.) From the results in Figure 2.8, it is clearly illustrated that the FC framework is able to improve the system capacity by 50% compared with the 1-color case (no interference coordination case). While the FC framework can only achieve 32% due to the existence of the color collision in the cell-edge area. Therefore the aim of this study is to to fill this performance gap caused by color collision while maintaining the computational complexity at a low level, or in other words, to solve the contradiction between the FC and FD framework.

In this study, a novel 2-layer IC framework is proposed, which allows the two kinds of RICs to cooperate with each other to fully exploit their respective advantages. Besides that, two GCA-based method is also proposed to be applied under this 2-layer IC framework, and the detailed explanation is provided in Chapter 3 and Chapter 4.

2.3 Summary

In this chapter, we presented the fundamental knowledge required to implement IC using GCA, as well as common approaches to using GCA-based IC in cellular systems with cluster-wise distributed MU-MIMO. Through computer simulations, we demonstrated the limitations of the existing approaches, providing a clearer understanding of the research challenges we aim to address.

Firstly, the conventional heuristic GCA and how to apply the GCA for IC in cellular system was introduced.

Then, the performance of GCA-based IC was evaluated under two commonly used frameworks: fully centralized (FC) and fully decentralized (FD). The verification leads to the fact that the GCA-based IC under FC framework can mitigate both the intracell interference and the intracell interference, but its computational complexity exceeds practical limits. On the other hand, the GCA-based IC under FD framework is computational flexible, but it can only mitigate the intracell interference, leaving intercell interference caused by color collision unresolved.

Furthermore, the future requirements for scalability and flexibility for deployment in cellular systems were highlighted. It is highly desirable for cells to operate independently without information exchange between them.

Therefore, the problem statement was established: under the condition that each cell operates in a decentralized manner, there is a pressing need for a novel GCA-based IC that can mitigate intracell interference while considering intercell interference as well.

Chapter 3

2-layer IC Framework based on Modified GCA

3.1 Introduction

The core idea of the first method is to combine the advantage of intercell IC in FFR and the advantage of intracell IC in GCA-based IC together to modify the existing GCA-based IC, so as to minimize the occurrence of color collision during the coloring process. Therefore in the first method of the modified GCA-based IC, the idea of cell-edge classification from FFR will be integrated into GCA-based IC, thereby taking intercell IC into consideration while ensuring the effect of intracell IC.

1. Firstly, as shown in Figure 3.1, all the clusters needs to be divided into two categories, known as the cell-edge clusters and the inner-cell clusters. Therefore, to enable effective cell-edge/inner-cell classification, a graph construction method is proposed in Section 3.3 with help of the computational geometry (CG).

2. Secondly, the cell-edge clusters and the inner-cell clusters need to be colored separately. The cell-edge clusters experienced both the intracell interference and the intercell interference, therefore needs to be colored first. Similar as the FFR scheme, when coloring the cell-edge clusters, only part of the color options can be used, therefore the restrictions of the color options should be introduced to the original GCA-based IC. Also, when

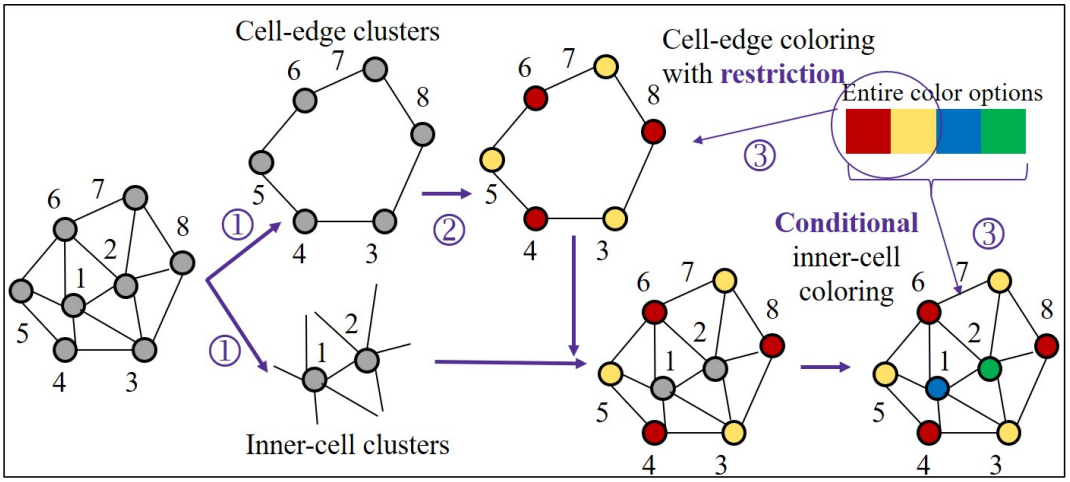

Figure 3.1: The overal concept of the modified GCA-based IC.

coloring the inner-cell clusters, the inner-cell clusters should self-adapt to the existing cell-edge colors, therefore, the idea of conditional GCA is also introduced to the original GCA-based IC. As a result, a new restricted conditional GCA (RC-GCA) is also proposed in Section 3.4 to enable the cell-edge coloring and the inner-cell coloring.

3. Finally, to enable the practical application of this modified GCA-based IC, the number of colors been restricted for the cell-edge clusters should be decided. Therefore, based on O-RAN architecture, a 2-layer IC framework is also proposed in Section 3.5 to provide hierarchical support for the application of modified GCA-based IC.

Therefore in this chapter, we firstly provide the brief introduction of the FFR scheme, and then the proposed graph construction method, the RC-GCA, and the 2-layer IC framework will be explained one by one in the following sections in details.

3.2 Understanding of FFR Scheme

The Fractional Frequency Reuse (FFR) scheme is a well-known technique employed in cellular networks to mitigate intercell interference and improve overall system performance. It

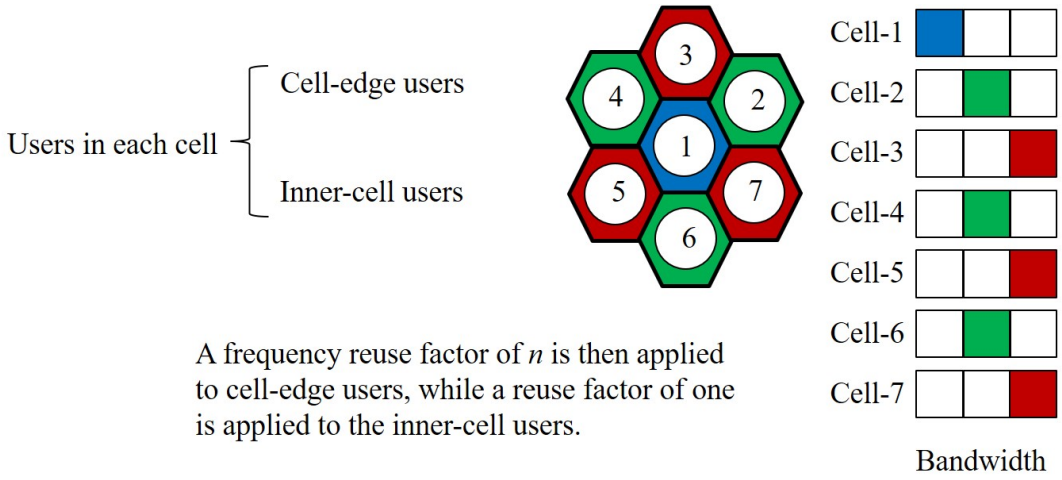

Figure 3.2: The introduction of FFR scehme.

divides the available frequency spectrum into multiple sub-bands and allocates them to different areas within a cell based on their interference characteristics. FFR aims to strike a balance between cell-edge user performance and system capacity by dynamically allocating frequency resources. In FFR, the cell is partitioned into two or more regions, typically an inner-cell region and an cell-edge region, each with different frequency reuse factors as shown in Figure 3.2.

FFR enhances system capacity by effectively managing intercell interference in cellular networks. It allows for better utilization of available frequency resources by adapting the frequency reuse pattern according to the varying user density and traffic distribution within the cell. By assigning different frequency resources to different regions of the cell, FFR enables improved signal quality, reduced interference, and enhanced user experience, especially at cell edges where interference is typically more pronounced. Additionally, FFR can be implemented in a flexible manner, allowing operators to adjust the frequency allocation based on the specific network conditions and user demands. Overall, the FFR scheme is an important tool in optimizing the performance of cellular networks and maximizing their capacity.

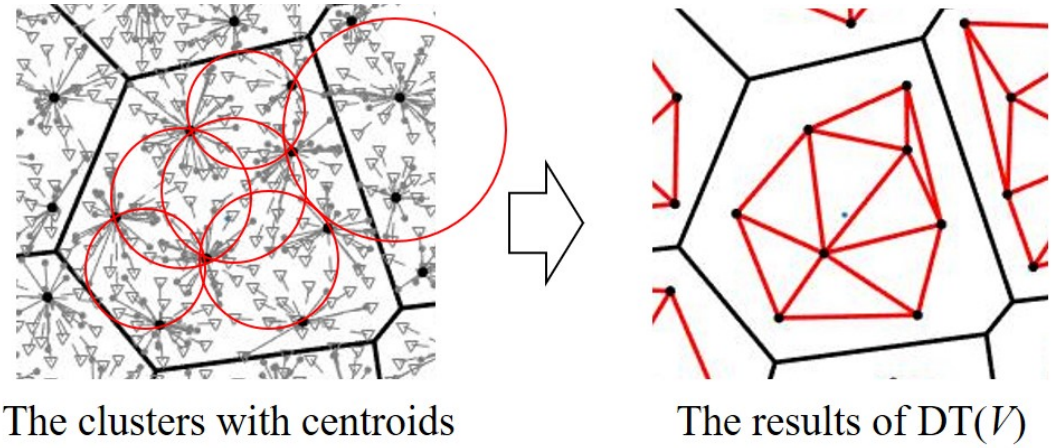

Figure 3.3: Graph construction based on delaunay triangulation.

3.3 Proposed Graph Construction Method

As mentioned in the chapter 2, the application of GCA-based IC pre-assume the construction of a graph $G = (V, E)$, where V and E denote the set of vertices and edges, respectively. In this study, it is assumed that the non-RT RIC form cells and each near-RT RICs form user-clusters based on the K-means algorithm [39]. Each cell and cluster can be represented by their corresponding centroids in geometric position. Therefore, V denotes the centroids of clusters or cells. E denotes the mutual adjacency relationship among the vertices, as the most severe interference exists between neighboring vertices. V is easily obtained because once each near-RT RICs apply the K-means algorithm, the location information of the centroids is known; however, E cannot be obtained directly. To define E, we need to derive the relative adjacency relationship from the position information of the centroids.

A commonly used method is to use the threshold [19][20][21]. However, the optimum threshold value is usually obtained via optimization algorithm, which is not applicable in the case of dynamically changing user locations and cluster topology. Therefore, in this study, we propose to apply the Delaunay Triangulation [42] from CG to help decide the adjacency relationship and thus circumvent the threshold optimization problem. The Delaunay Triangulation is a classic triangulation method with linearithmic time complexity. For the

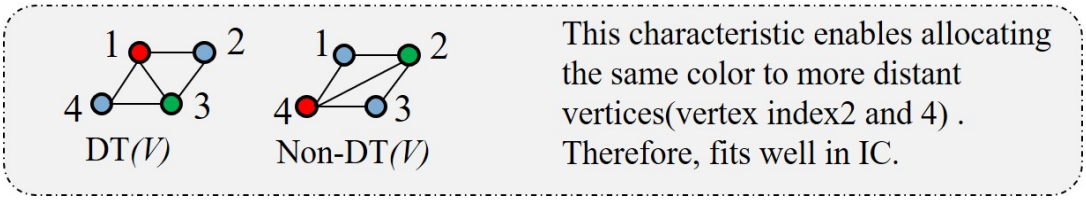

Figure 3.4: The characteristic of delaunay triangulation.

given three vertices in V, if the circle circumscribing them does not contain any other vertex, the Delaunay Triangulation is satisfied and the result of such triangulation is denoted as DT(V). We apply Delaunay Triangulation on the centroids. If there is a triangle edge connecting two vertices, these two vertices are regarded as neighbors. In this way, the adjacency relationship, or E of graph, can be determined without using the threshold as shown in Figure 3.3.

The reason why DT(V) can be used to define the adjacency relationship is explained below. There are several characteristics of DT(V), among which the most important one is that it can maximize the minimum angle and avoid sliver triangles (triangles with extremely acute angles) [42]. This characteristic enables allocating the same color to more distant vertices, therefore, fits well in IC. We take vertices with index 1–4 in Figure 3.4 for illustrating this point. In Figure 3.4, we provide two triangulation results for the vertices 1–4. DT(V), which is the left one, defines the vertices 1 and 3 as neighbors, while non-DT(V) defines 2 and 4 as neighbors. Thus, using DT(V) can assign the same color to more distant vertices, which fits well in the application scenario of IC.

Furthermore, other characteristics of DT(V) are also worth mentioning. Firstly, the nearest neighbor graph (NNG) has been demonstrated to be a subgraph of DT(V) [42], and because the nearest neighbors usually provide the strongest interference, it can be ensured that the strongest interference will be mitigated. Another characteristic of DT(V) is that the change of any one vertex will only affect its nearby triangles, while the far located vertex ' s triangulation results remain unchanged. Because of this characteristic, adding or removing several vertices has no effect on the far away vertices, thereby maintaining the system scalability [42].

Applying DT(V) as a graph construction method also has another irreplaceable advantage. In our proposed modified GCA-based IC, the clusters needs to be classified into cell-edge clusters and inner-cell clusters, and then, colored separately. For the cell-edge classification

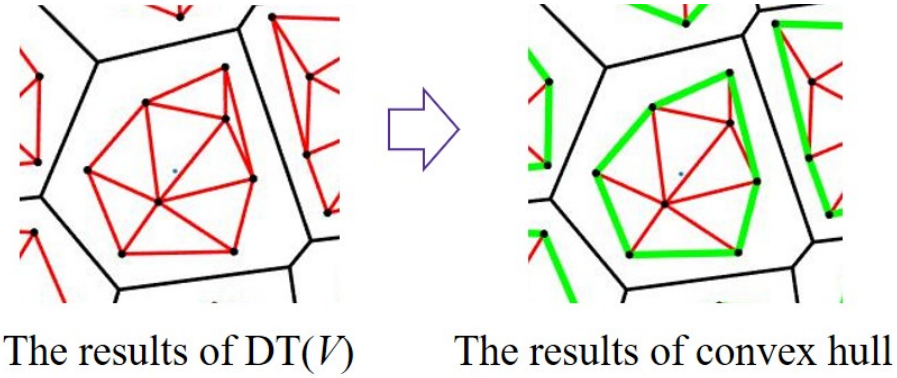

Figure 3.5: The classification of cell-edge clusters based on the construction of convex hull.

method, the construction of convex hull [42] is a very promising way. The convex hull has been proved to have good performance in the similar scenarios such as boundary detection in wireless sensor networks [43]. Because the convex hull is a subgraph of DT(V) [44] as shown in Figure 3.5, if the graph is constructed based on the DT(V), the convex hull is directly obtained with no further computational complexity, and the problem of cell-edge/ inner-cell clusters classification can be solved directly.

In addition, in the proposed idea of the modified GCA-based IC, the number of the color options is decided in advance. Because of the structural advantage of triangles, the graph constructed by DT(V) can cope well with the case when the number of color options is greater than or equal to three, However, when the number of color options is restricted to two, the structural advantage of Delaunay triangulation no longer exists. Therefore, we need to extend further on the basis of the adjacency relationship determined by DT(V) to construct the bipartite graph.

A bipartite graph is a graph whose vertices can be divided into two disjoint sets such that all edges connect vertices from different sets. In the graph coloring problem, the case when the number of color options equals two is known as the 2-colorable problem, and the bipartite graph is proven to be 2-colorable [45].

The construction of bipartite graph on the basis of DT(V) is illustrated in Figure 3.6. Firstly, based on the undirected unweighted graph G, the weights are introduced to further construct the undirected weighted graph $G' = (V', E', W')$, where V', E', and W' denote the set of vertices,

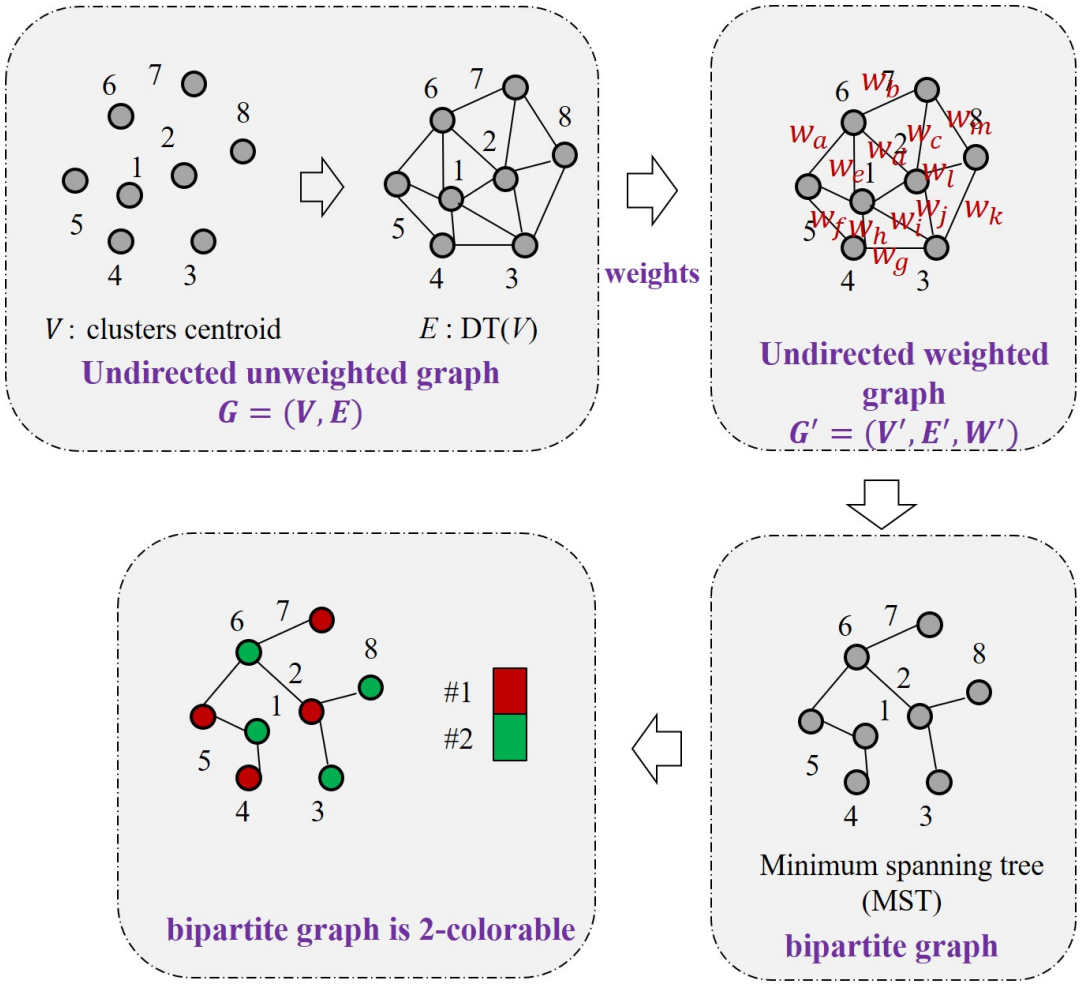

Figure 3.6: Construction of MST on the basis of delaunay triangulation.

edges, and weights, respectively. The weights are determined based on the distance between the centroids in this study.

Based on graph G', minimum spanning tree (MST) [42] is applied to construct the bipartite graph, note that the Prim ' s algorithm or Kruskal ' s algorithm [46] can be used as faster approaches to solve MST on the basis of DT(V). MST is a spanning tree with minimum sum of weights. Because the weights are defined as distance and the pathloss is inversely proportional to distance, MST actually connects the paths where the vertices interfere the most with each other.

The application of MST has been considered mainly in adhoc networks to improve the connectivity while solving the tradeoff of power conservation [47][48][49]. It should be noted that to the best of the authors ' knowledge, this is the first time to apply MST to solve graph coloring-based ICs. In adhoc networks, MST is used to determine the strongest link of connection. Whereas, in our case, MST is used to determine the strongest link of interference between vertices, and interference mitigation is achieved by breaking these links when different colors are offered.

According to our previous study [50], using CG-based graph construction can achieve the same good result in defining E as using the optimized threshold. Therefore, in the case of dynamically changing user locations and cluster topology, using our proposed method is considered more feasible compared to using the threshold method. Based on the results of DT(V) and MST or convex hull, the adjacency matrix $\mathbf{A} = (a_{ij}) \in \mathbb{R}^{N \times N}$ can be defined as in (3.1). The adjacency matrix records the information of V and E in graph, and is the basis of GCA-based IC.

$$a_{ij} = \begin{cases} 1, & \text{vertex } i \text{ and } j \text{ are connected by DT}(V) \\ 0, & \text{vertex } i \text{ and } j \text{ are not connected by DT}(V) \end{cases} \tag{3.1}$$

3.4 Proposed Restricted Conditional GCA (RC-GCA)

After the graph G is constructed, the GCA can be carried out based on the graph G. In order to realize the proposed idea of modified GCA-based IC, the cell-edge clusters and the inner-cell clusters need to be colored separately. For the cell-edge coloring, according to the requirement of FFR, only part of the bandwidth can be used so as to mitigate the intercell interference. In this way, when coloring the cell-edge clusters, we can only use part of the color options. Therefore,

the restrictions of the color options must be introduced into the conventional heuristic GCA. While for the inner-cell coloring, because the inner-cell clusters need to be colored to adapt to the existing cell-edge clusters, the conditions of the pre-coloring results also need to be introduced to the conventional heuristic GCA. Therefore in this section, a new heristic GCA named as the restricted conditional GCA (RC-GCA) is proposed, which is designed for both the cell-edge coloring and the inner-cell coloring.

The proposed RC-GCA is shown in Algorithm 2, in which the famous DSATUR [37] is used as an example to explain how to add restriction and conditions to heuristic GCA. We assume that all vertices that are allocated the same color belong to one color group. Representing the total number of vertices by N, κ_m denotes a set of vertices in the mth color group, $m \in \{1, 2, \ldots, M, \}$, where M is the restricted maximum number of colors. The prior coloring result obtained after the 1st layer IC is expressed by the vector $\mathbf{c} = [c_1 \cdots c_N]$ with $c_i \in \{0, 1, 2, \cdots, M\}$ where $c_i = 0$ indicates that vertex i has not been colored. The proposed RC-GCA is modified based on DSATUR, and all the vertices are first arranged as $v_1, v_2, \ldots, v_N$ in descending order of degree δ in steps 1–2, then reset based on the degree of saturation $\delta^{'}$ [37] in step 14 after been colored sequentially in steps 3–13.

During the coloring process in steps 3–13, the conditional GCA with restricted color labels from $M^{'}$ to M is first conducted in steps 5–9. For a vertex v_i, the setting of the restriction $M^{'}$ to M clarifies the available color pool, while the prior coloring results $\boldsymbol{c}$ and adjacency matrix $\mathbf{A}$ together decide the pre-colored conditions, that is, they decide which colors have been pre-colored by neighbors and thus cannot be used. The remaining colors with smallest label will then be assigned to v_i.

After performing steps 5–9, because the adding of restrictions will decrease the degree of freedom, a few vertices may remain uncolored. Steps 10–12 are designed to recolor these uncolored vertices. During the recoloring process, color collision with one or more neighbors is inevitable. To minimize the interference among the inevitable color collision, it is better to assign the same color to the vertices with the least interference between them. As mentioned before, the interference becomes weaker on average if the distance is longer, and therefore, the most distant neighbors should be chosen. Assuming that the location information of cluster centroids is known to each near-RT RICs, it is better to assign the same color to the most distant neighbors.

To find the most distant neighbors, we define a relative distance matrix $\widetilde{\mathbf{D}} = (\widetilde{d_{ij}}) \in \mathbb{R}^{N \times N}$),

Algorithm 2: Restricted conditional graph coloring algorithm (RC-GCA)

Input: $\mathbf{A}, \mathbf{D}, \mathbf{c}, M^{'}, M$

Output: $\kappa_m, \forall m \in M$

1: Initialize δ
2: Sort all vertices in decending order of δ, and set the obtained vertex set as $\mathcal{V}$.
3: **for** $v_i = v_1 : v_N$ **do**
4: **while** $c_{v_i} = 0$ **do**
5: **for** $m = M^{'} : M$ **do**
6: **if** $m \notin \mathbf{c} \odot \mathbf{A}^{(v_i,:)}$ **then**
7: $c_{v_i} \leftarrow m$
8: **end if**
9: **end for**
10: **if** $c_{v_i} = 0$ **then**
11: $c_{v_i} \leftarrow c_{\arg\max(\tilde{\mathbf{D}} \odot \mathbf{A}^{(v_i,:)})}$
12: **end if**
13: **end while**
14: Reset the vertex set $\mathcal{V}$ based on the degree of Saturation δ'.
15: $\kappa_{c_{v_i}} = \kappa_{c_{v_i}} \bigcup v_i$ % Assigning the vertex to color group.
16: **end for**

(Note that $\odot$ denotes the Hadamard product; $\mathbf{X}^{(y,:)}$ indicates the yth row vectors of the matrix $\mathbf{X}$.)

where

$$\tilde{d}_{ij} = \frac{d_{ij}}{\sum_{j=1, j \neq i}^{N} d_{ij}}, i, j = 1 \sim N \tag{3.2}$$

with d_{ij} denoting the distance from the centroid of cluster j to that of cluster i. Based on $\widetilde{\mathbf{D}}$, the recoloring process (steps 10–12) is performed. The recoloring process allows the existence of color collision, but minimizes its impact on interference by ensuring that the color collision happens only between the most distant neighbors.

3.5 Proposed 2-layer IC Framework

Based on the graph construction method proposed in Section 3.3, the newly proposed RC-GCA is able to realize the separate coloring of the cell-edge clusters and the inner-cell clusters, as required by the idea of modified GCA-based IC. However in real application, how to decide the restricted color options for cell-edge clusters remains unsolved. Therefore, a novel 2-layer IC framework based on O-RAN architecture is further proposed to provide hierarchical support for the application of the modified GCA-based IC.

The proposed 2-layer IC framework is illustrated in Figure 3.7. In the 1st layer of IC, the location information of DAs is gathered by the O1 interface to the non-RT RIC, and the so-called non-RT RIC applications (rApps) are responsible for constructing cells based on the location of DAs, and coordinating the intercell interference with the help of cell centroid information. The results of intercell IC will be passed via A1 interface to the near-RT RICs. Because the DAs ' locations are stable in general, the 1st layer IC is only carried out when cellular reconfiguration is updated, therefore this kind of large-timescale operation task fits well with the control loop of non-RT RIC.

In the 2nd layer of IC, each near-RT RIC, which is connected with the O-CU-CP/UP and O-DU via the high-speed E2 interface, is responsible to obtain the information of users ' location. Then the near-RT RIC applications (xApps) are responsible for forming clusters and coordinating the intracell interference under the conditions of the result of the 1st layer IC.

For the application of the modified GCA-based IC, the proposed RC-GCA will be used as both the rApp and the xApp, and the details are illustrated in Figure 3.8. In the 1st layer IC, the available frequency band will be divided into several sub-bands (named as total color pool), and the motivation of 1st layer IC is to specify the sub-color pool that can be used by cell-edge clusters of each cell. We assume that the number of total color pool is N_{color}^{total}. Additionally, we assume that the total color pool is divided into N_{sub} sub-color pools, and each sub-color pool has the same number N_{color}^{sub} of colors. Therefore, $N_{color}^{total} = N_{color}^{sub} \times N_{sub}$.

In the 1st layer of intercell IC, the non-RT RIC applies RC-GCA-based rAPP for global intercell IC by assigning one of the sub-color pools to each cell. The results of the sub-color pool assignment are passed to the corresponding near-RT RICs as a guidance information to support the operation of near-RT RICs in the 2nd layer IC. Thus, when applying RC-GCA-based rAPP in the 1st layer IC, M is set to N_{sub}. Because the cell structure is stable in general if the

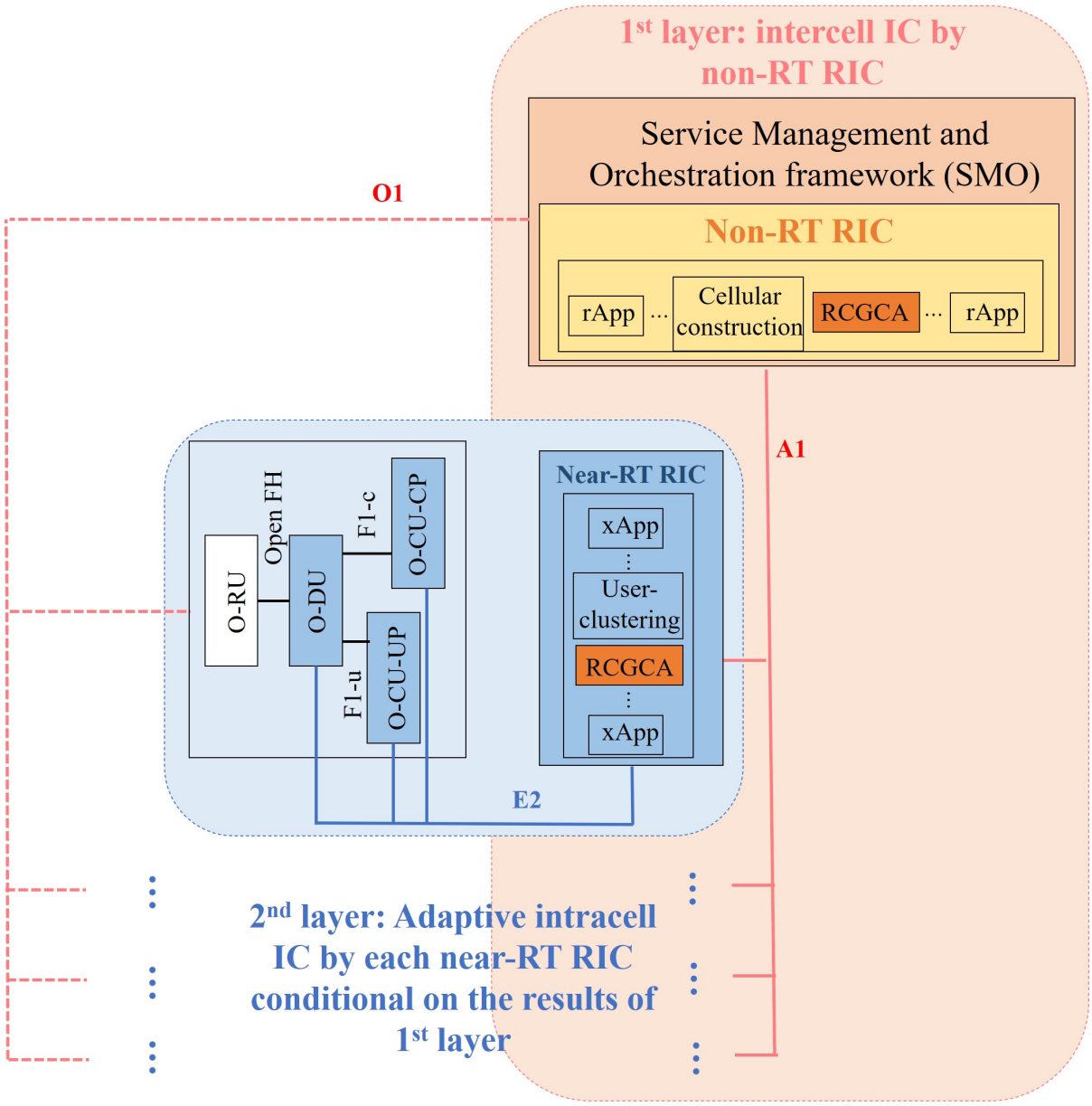

Figure 3.7: 2-layer IC framework based under O-RAN architecture.

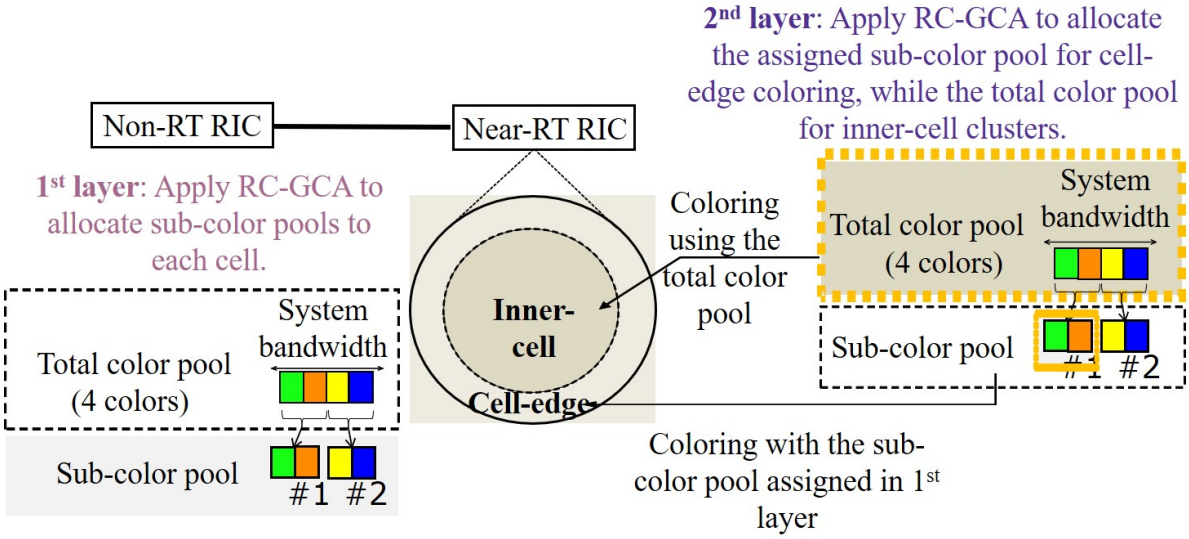

Figure 3.8: 2-layer IC framework based on RC-GCA.

cellular reconfiguration is not considered, the 1st layer IC is carried out only once.

In the 2nd layer of intracell IC, each near-RT RICs, as the specific IC executors, applies RC-GCA-based xAPP to realize the idea of modified GCA-based IC, that is to perform intracell IC independently under the conditions of the results of intercell IC in 1st layer.

The 2-layer IC framework can be classified as a semi-decentralized framework that adds an additional centralized layer on top of the decentralized layer. Compared with the FC framework, the 2-layer IC framework is feasible in practical because the non-RT RIC only needs to coordinate the relationship among cells rather than coordinating all the clusters, and the task of coordinating the clusters is delegated to each corresponding near-RT RICs. Compared with the FD framework, the 2-layer IC framework is able to consider intercell interference without information sharing among the cells.

The ”openness” of O-RAN enables substantial flexibility of its deployment, and each near-RT RIC can be flexibly configured with one or several cells [51]. Our proposed 2-layer IC framework works the same way regardless of the number of cells. For the sake of simplicity and without loss of generality, in the following sections of this paper, in order to enable easy illustration of how our proposed 2-layer IC framework works based on RC-GCA, we assume

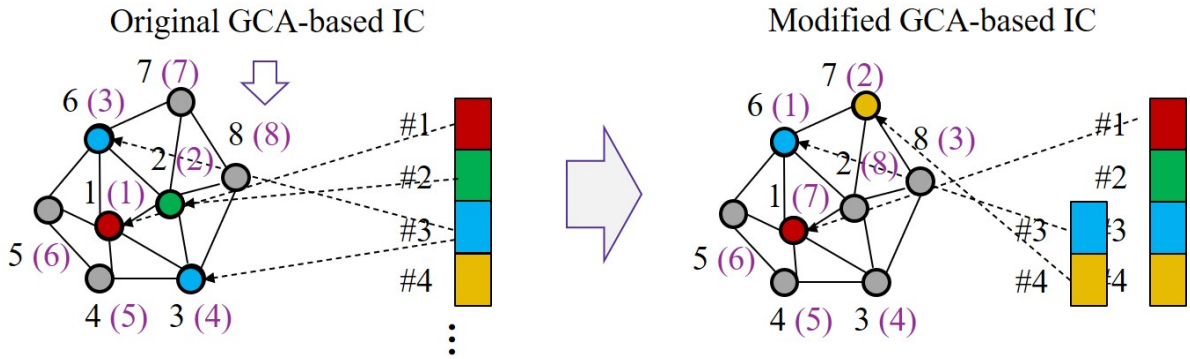

Figure 3.9: The comparison between the modified GCA-based IC and the conventional GCA-based IC.

each near-RT RIC controls one cell independently.

3.6 Comparison between Modified GCA-based IC and Conventional GCA-based IC

In this section, we will illustrate the difference between the proposed modified GCA-based IC and the original GCA-based IC. As shown in Figure 3.9, compared with the original GCA-based IC, the coloring sequence of all the clusters are firstly modified. The original GCA-based IC typically relies on the degree or degree-related values to determine the coloring sequence, thus the coloring process are usually starts from the inner-cell clusters. In contrast, the modified GCA-based IC prioritizes coloring the cell-edge clusters.

Also, in the original GCA, all clusters use the same set of color options. However, after modification, different clusters will have different sets of color options, as shown in Figure 3.9.

However, the computational complexity of the proposed modified GCA-based IC has not been increased compared to the original GCA-based IC. This is because none of these modifications altered the loop structure within the algorithm or increased the number of loop iterations.

3.7 Simulation Results Analysis

In this section, we will demonstrate the performance evaluation of our proposed 2-layer IC framework based on RC-GCA. First, the downlink capacity formula will be explained. Then, the optimized parameter setting (N_{sub} and N_{color}^{sub}) for applying RC-GCA under the 2-layer IC framework will be discussed. Finally, computer simulations are conducted using optimized parameter settings to evaluate the performance of the proposed 2-layer IC framework based on RC-GCA. The simulation results of the proposed method is compared with the dynamic FFR, no IC case, FC framework based on GCA, and FD framework based on GCA to validate its effectiveness.

3.7.1 Link Capacity Formula

In this section, we evaluate the downlink sum capacity and user capacity. As described in Section 3.4, after applying GCA-based IC, each cluster is assigned one color from the total color pool of N_{color}^{total} colors, and all clusters that are assigned the same color belong to one color group. Because a different color corresponds to a different frequency sub-band, the interference exists only inside the color group. Assuming that the number of clusters in each cell is N_C^{cell}, and each cell has the same number of clusters, the total number of clusters in the service area can be obtained as $N_C^{total} = N_C^{cell} \times N_{cell}$. Similarly, the total number of users and DAs in the service area can be denoted as N_U^{total} and N_A^{total}, respectively. In the mth color group, $m \in \{1, 2, \cdots, N_{color}^{total}\}$, the numbers of clusters, users, and DAs are denoted by N_C, N_U, and N_A, respectively. Furthermore, the ith user and j^{th} DA in the kth cluster are denoted by U_i^k and A_j^k , respectively. N_{U^k} and N_{A^k} are the number of users and DAs in the kth cluster, respectively.

In a cellular system with cluster-wise distributed MU-MIMO, the received signal is the superposition of the desired signal, interference, and noise. The interference comprises multi-user interference within each cluster and inter-cluster interference from other clusters (irrespective of being in the same cell or in neighbor cells) that are assigned the same color. Because ZF precoding is used for cluster-wise MU-MIMO, only the inter-cluster interference is considered

in this study. The downlink received signal of user U_i^k can be expressed as

$$\begin{aligned} y_{U_i^k} =& \mathbf{H}_k^{(i,:)} \mathbf{W}_k^{(:,i)} \sqrt{P_k} x_{U_i^k} + \\ & \sum_{l=1, l\neq k}^{N_C} \sum_{j=1}^{N_{Ul}} \mathbf{H}_{k,l}^{(j,:)} \mathbf{W}_l^{(:,j)} \sqrt{P_l} x_{U_j^l} + n_{U_i^k} \end{aligned} \tag{3.3}$$

where the first, second, and third terms are the desired signal, inter-cluster interference, and noise, respectively. Note that the matrices are represented as bold upper case letters and the superscripts $(i, :)$ and $(:, i)$ represent the ith row and column vectors of the matrix, respectively.

In (3.3), $x_{U_i^k}$ and $n_{U_i^k}$ are the transmit signal and noise, respectively. P_k and P_l are the power allocated to the kth and l^{th} clusters, respectively, and can be expressed as

$$P_{k \text{ or } l} = \frac{N_{U^{k \text{ or } l}} P}{\|\mathbf{W}_{k \text{ or } l}\|_F^2} \tag{3.4}$$

where $\|\cdot\|_F$ stands for the Frobenius norm. P is the normalized transmit signal power-to-noise ratio equal to all N_U users. P is set to 0 dB, indicating that the received signal-to-noise ratio becomes 0 dB when the distance between the transmitter and receiver is equal to unit length of a cell. Furthermore, $\mathbf{W}_k$ and $\mathbf{W}_l$ are the ZF precoder matrices, which can be expressed as

$$\mathbf{W}_{k \text{ or } l} = (\mathbf{H}_{k \text{ or } l})^{\dagger} = \mathbf{H}_{k \text{ or } l}^{\mathsf{H}} \left(\mathbf{H}_{k \text{ or } l} \mathbf{H}_{k \text{ or } l}^{\mathsf{H}} \right)^{-1} \tag{3.5}$$

where $(\cdot)^{\mathrm{H}}$ denotes the conjugate transposition of a matrix.

In (3.5), $\mathbf{H}_k \in \mathbb{C}^{N_{U^k} \times N_{A^k}}$ is the channel matrix and $\mathbf{H}_{k,l} \in \mathbb{C}^{N_{U^k} \times N_{A^l}}$ is the interference channel matrix between N_{U^k} users of the kth cluster and N_{A^l} DAs of the lth cluster. $\mathbf{H}_k$ and $\mathbf{H}_{k,l}$ can be expressed as

$$\mathbf{H}_k = \begin{pmatrix} h_{11} & \cdots & h_{1N_{A^k}} \\ \vdots & & \vdots \\ h_{N_{U^k}1} & \cdots & h_{N_{U^k}N_{A^k}} \end{pmatrix} \tag{3.6}$$

$$\mathbf{H}_{k,l} = \begin{pmatrix} h_{11} & \cdots & h_{1N_{A^l}} \\ \vdots & & \vdots \\ h_{N_{U^k}1} & \cdots & h_{N_{U^k}N_{A^l}} \end{pmatrix} \tag{3.7}$$

In (3.6) and (3.7), $h_{a,b}$ is given as

$$h_{a,b} = \sqrt{{d_{a,b}}^{-\alpha}}\sqrt{10^{-\frac{\varphi_{dB}}{10}}}z \tag{3.8}$$

where $d_{a,b}$ is the distance between the ath user and b^{th} DA, α is the pathloss exponent, φ_{dB} is the shadowing loss, which is characterized by a real-valued zero-mean Gaussian random variable with standard deviation of σ, and z is the Rayleigh fading gain, which is characterized by a complex-valued zero-mean Gaussian random variable with unit variance. In this study, we assume that $\mathbf{H}_k$ and $\mathbf{H}_{k,l}$ are perfectly known.

The received signal-to-interference-plus-noise-ratio ($SINR_{U_i^k}$) of the ith user in the kth cluster is computed by approximating the sum of inter-cluster interference and noise as a complex Gaussian process, and is given as

$$SINR_{U_i^k} = \frac{\left\|\mathbf{H}_k^{(i,:)}\mathbf{W}_k^{(:,i)}\right\|^2 P_k}{\sum_{l=1,l\neq k}^{N_C}\sum_{j=1}^{N_{U^l}}\left\|\mathbf{H}_{k.l}^{(j,:)}\mathbf{W}_l^{(:,j)}\right\|^2 P_l + 1} \tag{3.9}$$

The U_i^kth user capacity $C_{U_i^k}^m$[bps/Hz], m^{th} color group ' s sum capacity C_{sum}^m[bps/Hz], and system sum capacity C [bps/Hz] are obtained as

$$\begin{cases} C_{U_i^k}^m = \frac{1}{N_{color}^{total}}\log_2\left(1 + SINR_{U_i^k}\right) \\ C_{sum}^m = \sum_{k=1}^{N_C}\sum_{i=1}^{N_{U^k}} C_{u_i^k}^m \\ C = \sum_{m=1}^{N_{color}^{total}} C_{sum}^m \end{cases} \tag{3.10}$$

The parameter setting for computer simulation is shown in Table 3.1. Because the user movement in a small range will not affect the clustering results, in this studies, we adopted the quasi-static simulation. For simulation, a quasi-static environment is considered, implying that user locations remain the same during their communication duration. The quasi-static channel is realized by generating shadowing loss and Rayleigh fading gain for each user location. The user locations are generated randomly for 100 times. For each generation of user locations, the shadowing loss of each user is generated 10 times, and for each generation of shadowing loss, the Rayleigh fading gain for each user is generated 10 times. As a consequence, the total number of channel realizations is 10,000. For each generation of user locations, clustering and modified GCA-based IC are carried out and the user capacity, sum capacity per color group,

Table 3.1: Simulation Setting

Total number of DAs in service area, N_A^{total}	3200
Total number of users in service area, N_U^{total}	2400
Number of clusters in each cell, N_C^{cell}	5-11
Pathloss exponent,α	3.5
Shadowing standard deviation, σ[dB]	8
Fading type	Rayleigh fading
Number of user location patterns	100
Number of shadowing generation per user location pattern	10
Number of fading generation per shadowing generation	10

and system sum capacity are then computed using (3.10) for obtaining their CDF. N_{color}^{total}, N_{sub}, and the corresponding N_{color}^{total} will be determined after optimization, as shown in the following subsection.

3.7.2 Parameter Optimization

When applying the proposed modified GCA-based IC under the 2-layer IC framework, the number of colors N_{color}^{sub} in each sub-color pool and the number of sub-color pools N_{sub} need to be determined. In Table 3.2, six possible cases obtained from different combinations of N_{color}^{sub} and N_{sub} are listed. The 50% sum capacity (which is the sum capacity at CDF of 50%) obtained for each case when eight clusters are formed in each cell is plotted in Figure 3.10. It can be seen clearly that the highest capacity is obtained when $N_{sub} = N_{color}^{sub} = 2$. Accordingly, the restricted maximum number of colors M should be set to $M = N_{sub} = 2$ for the 1st layer IC, and $M = N_{color}^{total} = N_{color}^{sub} \times N_{sub} = 4$ for the 2nd layer IC.

More colors usually means that the interference can be mitigated more thoroughly, so why the capacity obtained by the restricted color options overwhelm the non-restriction case?

Actually, there is a tradeoff between interference mitigation and capacity improvement. Although increasing the total number of colors N_{color}^{total} can achieve better interference mitigation, the transmission bandwidth is made narrower, and therefore, increasing N_{color}^{total} does not necessarily result in a higher capacity. To restrict the value of N_{color}^{total}, N_{sub} needs to be restricted

Table 3.2: Parameter Setting

N_{color}^{sub} \ N_{sub}	2	3	4
2	case #1	case #2	case #3
3	case #4	case #5	case #6

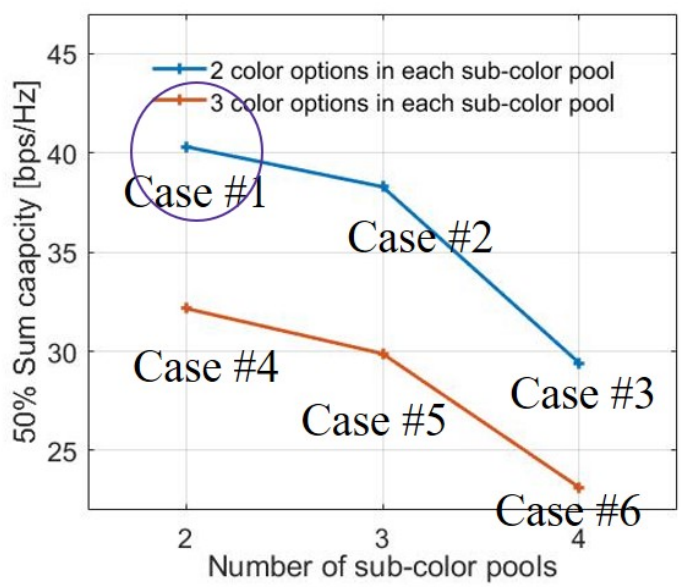

Figure 3.10: 50% sum capacity comparison for different settings of N_{sub} and N_{color}^{sub}.

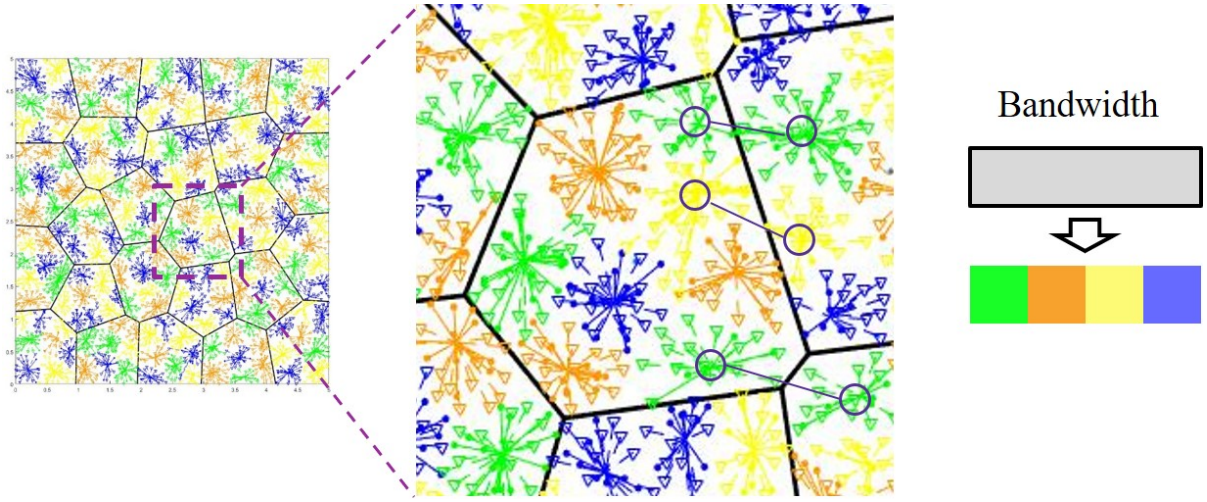

Figure 3.11: Coloring results for 2-layer IC framework based on modified GCA-based IC.

first in the 1st layer IC. Therefore, $N_{sub} = 2$ is considered to be a good compromise between interference mitigation and bandwidth reduction. In the 2nd layer IC, because the cell-edge clusters are along the cell boundary, most of the intracell interference among them can be mitigated by assigning two colors in the sub-color pool in turn. Therefore, $N_{color}^{sub} = 2$ can be used for cell-edge coloring. For coloring the inner-cell clusters, the total available color pool $N_{color}^{total} = 4$ can be used.

The coloring results with eight clusters is illustrated in Figure 3.11. From the results, Compared with the coloring results of applying GCA-based IC under the fully decentralized (FD) framework in Figure 2.7, it can be seen that a lot of the color collision can be mitigated at the cell boundary. Therefore, better intercell IC performance and the higher capacity can be expected.

3.7.3 Sum Capacity Analysis

In this section, we focus on comparing the sum of user capacities in the cell of interest. From the results of CDF in sum capacity in Figure 3.12, it can be observed that the proposed 2-layer IC framework based on modified GCA (marked as the blue curve) can achieve higher capacity than the fully decentralized (FD) framework (marked as the red curve), while maintaining a

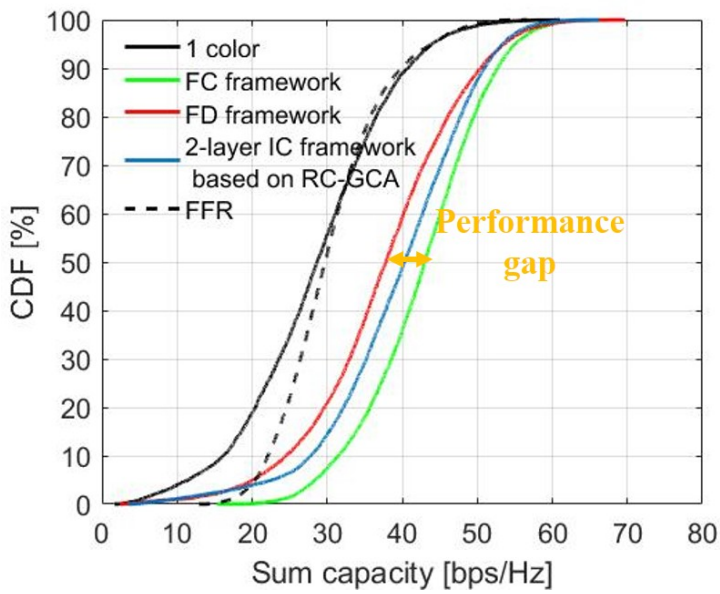

Figure 3.12: The CDF comparison of the proposed 2-layer IC framework based on modified GCA.

similar computational complexity.

As for the capacity at CDF=50 %, we can see that the proposed 2-layer IC framework based on modified GCA improves by 6.5% compared to the FD framework and achieves 94% of the FC framework. Therefore, the conclusion can be draw that the proposed 2-layer IC framework based on modified GCA can significantly reduce the color collision, thereby further improve system sum capacity.

3.8 Summary

In this chapter, in order to mitigate both the intracell interference and the intercell interference, the first method named the 2-layer IC framework based on modified GCA was proposed. The overall idea of this method is to minimize the occurrence of color collision during the coloring process, thereby enhancing the performance of intracell IC and intercell IC at the same time.

To facilitate this idea, a 2-layer IC framework based on the O-RAN architecture, a modified heuristic GCA and a graph construction method were proposed.

1. The proposed 2-layer IC framework, based on the O-RAN architecture, aims to provide hierarchical support for the decentralized application of the modified GCA-based IC in a cellular system with cluster-wise distributed MU-MIMO. This framework relies on the cooperation between the non-RT RIC and the near-RT RICs, enabling it to achieve performance comparable to the fully centralized (FC) framework while maintaining computational complexity similar to the fully decentralized (FD) framework. In the 1st layer, the near-RT RICs are ensured to operate under the overall control of the non-RT RIC, thereby creating the conditions for achieving intercell IC. While in the 2nd layer, each near-RT RIC are ensured to apply IC in a decentralized manner with no information exchange with each other.

2. The newly proposed heuristic GCA is called the Restricted Conditional GCA (RC-GCA). Compared with the conventional GCA, the idea of the color options restriction and also the idea of conditional coloring on a pre-colored graph is introduced. The introduced restrictions on color options ensure that the coloring of cell-edge clusters effectively reduces the occurrence of color collisions, thereby enhancing intercell IC performance. Meanwhile, the introduced idea of conditional coloring ensures that the coloring of inner-cell clusters self-adapts to the coloring results of cell-edge clusters, guaranteeing the effectiveness of intracell IC. As a result, the proposed RC-GCA enables both cell-edge coloring and inner-cell coloring, realizing the concept of the modified GCA-based IC.

3. The proposed graph construction method, based on computational geometry (CG), provides significant support to the application of the 2-layer IC framework based on modified GCA. It effectively addresses the threshold optimization problem during graph construction and enables the classification of cell-edge clusters and inner-cell clusters.

Chapter 4

2-layer IC Framework based on Joint IC

4.1 Introduction

In the first proposed method of the 2-layer IC framework based on modified GCA in Chapter 3, the motivation is to try to modify the coloring process so that to avoid the occurrence of color collision during the coloring process. Recognizing the recent advancements in artificial intelligence (AI), I was inspired to explore how this emerging technology could be utilized to address the traditional issue of IC.

Initially, the first endeavor was to continue with the approach of the first method in Chapter 3, which involved utilizing AI technology, particularly deep reinforcement learning (DRL), to improve the coloring process of GCA so as to avoid color collisions during coloring [C1]. However, during my research, I encountered some problems of using DRL-aided GCA. In particular, the artificial neural networks required for this DRL-aided GCA often needed a specific architecture where the number of neurons in the input and output layers corresponded to the number of clusters in each cell. I believe this design has certain limitations in practical applications.

Firstly, when the number of clusters in a cell is large, it results in a significant increase in the number of neurons in the input and output layers of the neural network, making it difficult to reduce its overall scale. A large neural network would require higher computational complexity and substantial training overhead, which are all impractical. Secondly, considering our system design, the number of clusters in each cell may vary continuously based on requirements.

Therefore, using a neural network with fixed input layer cannot align with our existing system design.

Consequently, in this chapter, the idea of the modified GCA proposed in Chapter 3 has been abandoned and an alternative approach is proposed.

Firstly, the conventional GCA-based IC is applied within each cell in a decentralised manner, solely focusing on intracell IC. During this approach, the occurrence of color collision in the cell-edge area is allowed. Subsequently, efforts are made to eliminate the occurred color collisions as soon as possible after the coloring process.

To address the issue of color collisions, in Section 4.2, I firstly proposed a color-adaptation scheme that is able to slightly adjust the existing coloring results, which make it possible to eliminate the color collision with the neighboring cell.

To effectively utilize the color-adaptation scheme, the proposed color-adaptation scheme is further integrated into a DRL model and formed a DRL-based intercell IC in Section 4.4. The proposed DRL-based intercell IC allows each cell to dynamically and autonomously select the optimal color-adaptation scheme in each color collision situation.

The proposed DRL-based intercell IC and the GCA-based intercell IC are combined together to formed the joint IC in the cellular system with cluster-wise distributed MU-MIMO, which will be presented in Section 4.5.

In Section 4.6, considering the real-time dynamic changes in the environment, the online training strategy have been adopted creatively to enable the proposed joint IC to adapt autonomously to the dynamically changing environment. This online training strategy allows the neural network in joint IC to continually update and adjust its parameters, enabling it to effectively follow the ever-changing environment.

In Section 4.7, in order to control the training overhead required for the online training of the DRL-based intercell IC in the system, I also proposed a strategy to apply the joint IC in the 2-layer IC framework. Through observation, I realized that while the GCA-based intracell IC is necessary for each cell, the DRL-based intercell IC does not need to be activated in every cell. By using non-RT RIC in the first layer to control which cells activate the DRL-based intercell IC, the utilization of the joint IC can be optimized.

In the subsequent sections of this chapter, the aforementioned topics will be sequentially discussed and presented.

4.2 Proposed Color Adaptation Scheme

The proposed color adaptation scheme aims to slightly modify the existing GCA results, so as to make it possible to avoid the color collision with the neighboring cells. Let the coloring result for the kth cluster after GCA be $g_k \in \{0, 1, \cdots, M-1\}$. The proposed set of all the possible color-adaptation actions is defined as $A = \{0, 1, 2, \cdots, M-1\}$.

In each time instant t, each near-RT RIC selects a specific color-adaptation action $a^{(t)}$, after the action $a^{(t)}$ is chosen, the coloring result of each cluster is adjusted based on the modulo operation in time instant $t+1$,

$$g_k^{(t+1)} = \left(g_k^{(t)} + a^{(t)}\right) \bmod M \tag{4.1}$$

One example of the application of the color-adaptation scheme is presented in Figure 4.1. In the cell of interest, the cluster with index of E has color collision with the neighboring cluster in yellow color. Under this scenario, if the color-adaptation action of 3 is adopted, the coloring results will be changed accordingly, resulting in the successful elimination of the color collision.

However, it should be noted that the color-adaptation scheme requires careful selection. Sometimes, reducing color collisions in one area may introduce new color collisions elsewhere. As shown in Figure 4.2, when the color-adaptation action of 1 is chosen, although the color collision near cluster with index E is eliminated, a new color collision near cluster with index A is created. Therefore, while the proposed color-adaptation scheme has the potential to eliminate color collisions, it needs to be applied wisely.

So, how to find the optimal solution? Since the user locations are constantly changing, the user-clusters based on these user locations will be periodically updated. Therefore, a method that can observe the current status of color collisions in real-time and have decision-making capabilities to select the best color-adaptation action based on the observed real-time information is needed.

Under this scenario, the deep reinforcement learning (DRL) which springs up recently overwhelms the traditional optimization methods in both the flexibility and adaptability in dynamic environment. By interacting with the unknown environment, the DRL is able to figure out the solution on its own with limited number of trial and errors. In this study, we try to apply the Deep Q network (DQN) from DRL to dynamically select the color-adaptation action

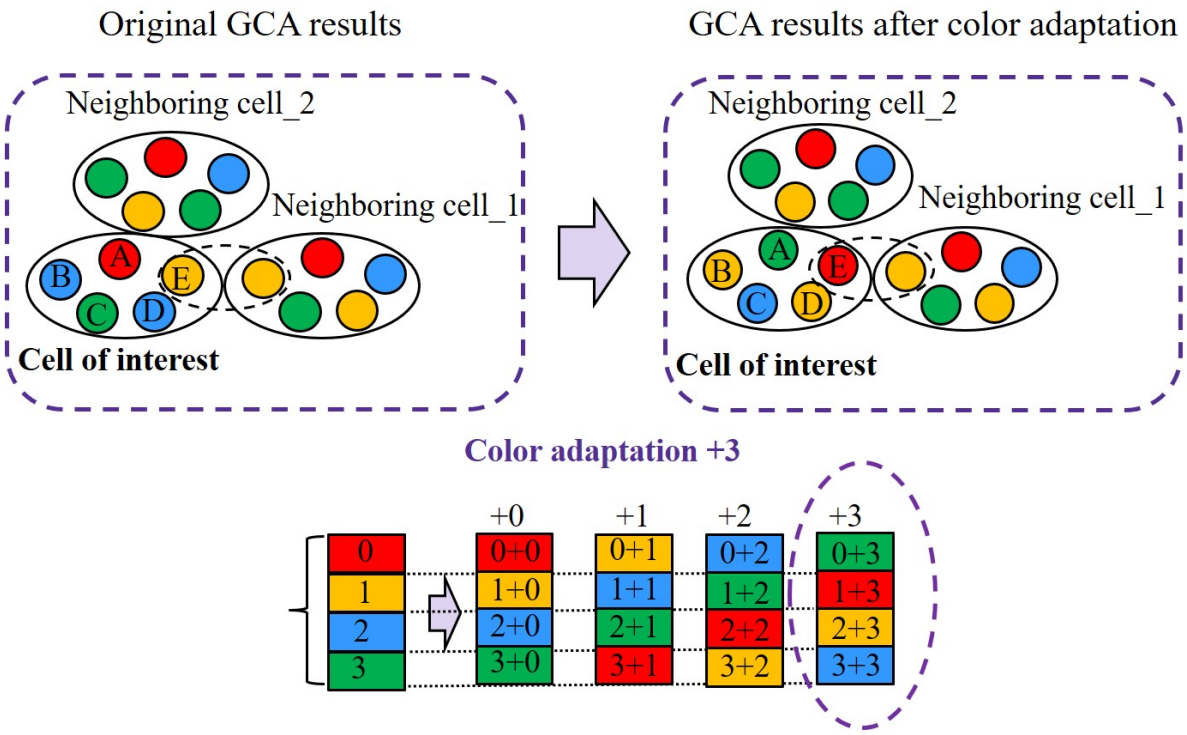

Figure 4.1: One example of an successful application of color-adaptation scheme.

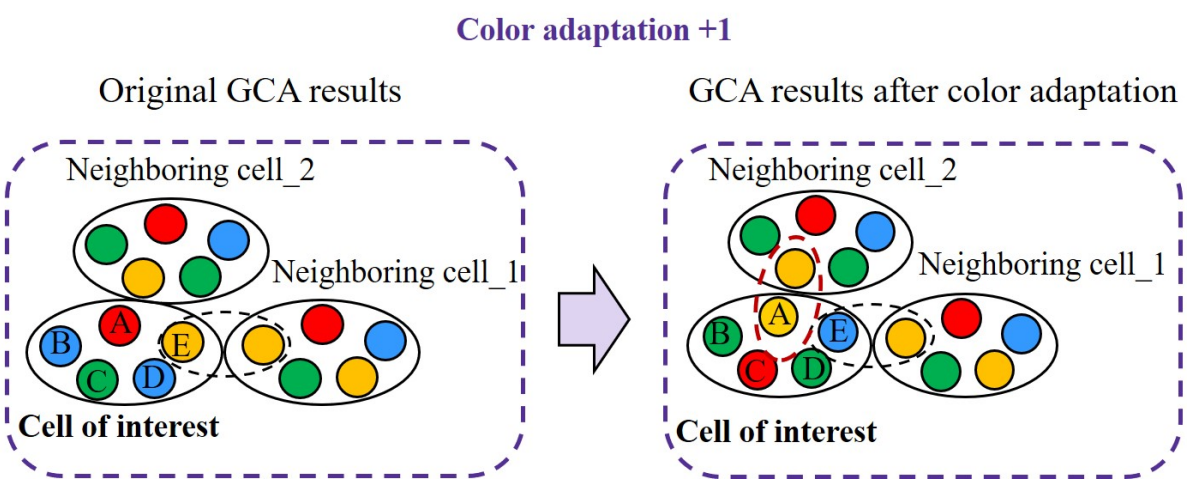

Figure 4.2: One example of an unsuccessful application of the color-adaptation scheme.

by self-learning with only locally observed information, so as to eliminate the color collision, and the corresponding intercell interference.

In Section 4.2, the DQN will first be briefly introduced, and then in Section 4.3, the application of the proposed color-adaptation scheme under the DQN model will be explained in detail.

4.3 Introduction of Deep Reinforcement Learning (DRL)

Reinforcement Learning（RL）is a machine learning approach that aims to enable an agent, or agents, to learn the optimal policy by interacting with the environment in order to maximize cumulative rewards. In RL, the agent observes the state of the environment, takes actions, and receives rewards, gradually learning how to make optimal decisions.

When applying IC in the cellular system with cluster-wise distributed MU-MIMO, we let each near-RT RIC works in a decentralized manner, therefore we adopt the single-agent architecture while each ”agent” corresponds to each near-RT RIC. The goal of each single agent is to optimize its behavior policy through interactions with the environment, aiming to maximize its own expected rewards.

In this study, we adopt the Q-learning algorithm which relies on value functions. It learns the optimal policy by maintaining a table known as the Q-table, which estimates the expected return for each state-action pair as shown in Figure 4.3.

The key idea of Q-learning is to update the Q-value inside the Q-table using the Bellman equation. According to the Bellman equation, the agent updates the Q-value of the current state based on the observed rewards and the Q-value of the next state. Through iterative experience accumulation and Q-value updates, the agent gradually learns the optimal policy to maximize cumulative rewards.

While Deep Reinforcement Learning (DRL) is a combination of the deep learning techniques with RL algorithms. When applying Q learning algorithm in DRL, a deep neural networks, called deep Q network (DQN), is applied to replace the application of Q-table to approximate the Q-value function as shown in Figure 4.4.

A DQN consists of interconnected layers of artificial neurons, organized in input, hidden, and output layers. Each neuron applies a non-linear activation function to its weighted inputs, transforming the information flow throughout the network. The parameters of the neural

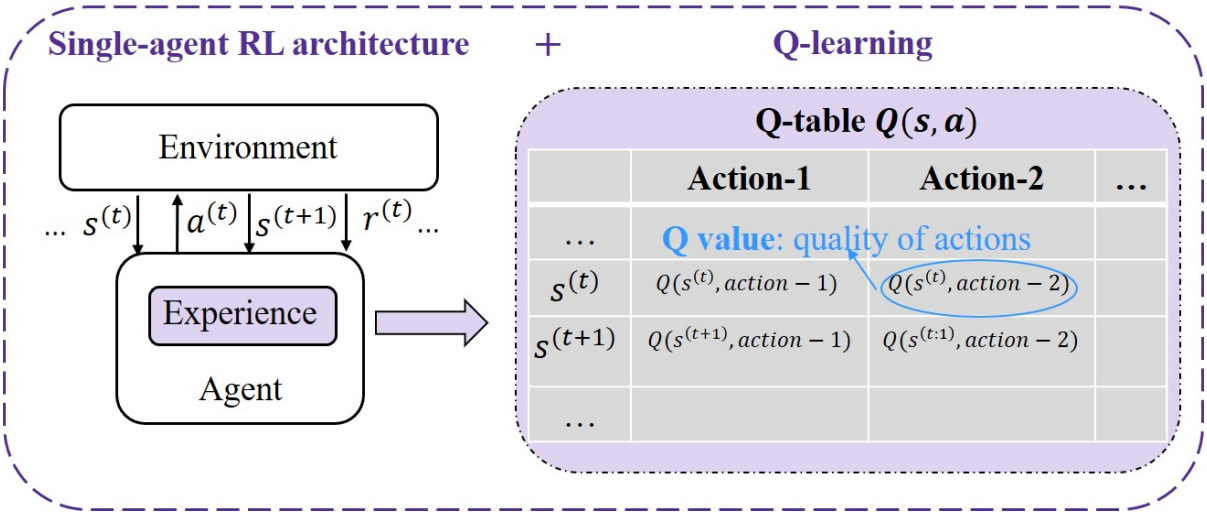

Figure 4.3: The single agent RL architecture based on Q-learning algorithm.

network, including weights and biases, are learned through a process called backpropagation, which adjusts them to minimize the discrepancy between the network's predictions and the desired outputs.

In traditional tabular-based Q-learning, the Q-values are stored and updated in a table structure, which can become impractical or infeasible when dealing with large state spaces. However, in the case of DQN, a deep neural network is used, therefore eliminating the need to store all the data in computer memory. Instead, the data is used to train the DQN model, and once the model is trained, the data can be discarded or deleted. Therefore, compared with tabular-based Q-learning, the DQN can reduce the computer memory usage and access times, making it possible for large-scale problem;

Besides that, the DQN takes the state as input and calculate the outputs of Q-values for each action, therefore once the DQN is well-trained by finite state-action pairs, its generalization ability makes it able to capture patterns and generalize its knowledge to estimate Q-values for unseen states and actions. Therefore, DQN is also applicable to handle continuous and infinite problems.

As a result, the DQN of DRL is more suitable for wireless communication.

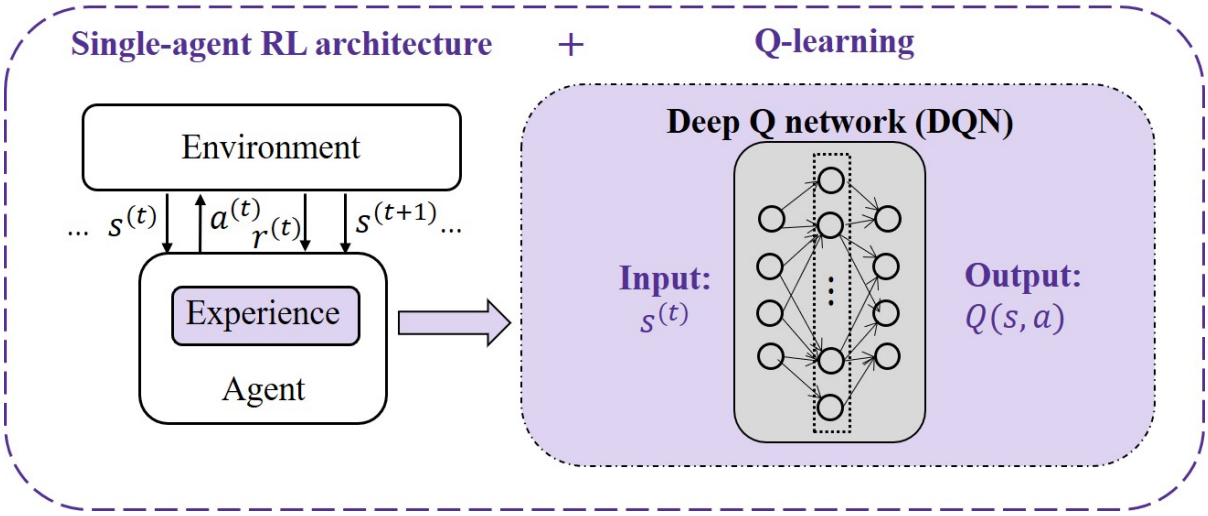

Figure 4.4: The single agent RL architecture based on deep Q network.

4.4 Proposed DRL-based Intercell IC

In this section, how to apply the proposed color-adaptation scheme based on the DRL model is explained, and a DRL-based intercell IC is proposed.

Since we assume each near-RT RIC applies IC in a decentralized framework, we suppose each near-RT RIC is a single agent, and the IC problem in each cell can be modeled as a Markov decision process (MDP), which can be expressed as a triplet $\{S, A, R\}$, where S represents the state space, A represents the action space, and R is the reward function. They are described below.

- **State space**: At time instant t, we define the states for each BS agent as the instantaneous sum capacities of the clusters those belong to κ_m in each cell based on the current coloring result, which is noted as $s^{(t)} = [C_0^{(t)}, C_1^{(t)}, \cdots, C_{M-1}^{(t)}]$.

- **Action space** : The action space A is defined as the proposed color-adaptation scheme as shown in Section 4.2.

  As for the action selection policy (π), we modified the well-known ε-greedy policy [52] to encourage the exploration in the early stage, while focus more on the exploitation in

the later stage. The original ε-greedy policy is noted as

$$a^{(t)} = \begin{cases} \arg\max_{a \in A} Q(s^{(t)}, a), \text{ with probability } \varepsilon \\ \text{Choose a random action, with probability } 1-\varepsilon \end{cases} \tag{4.2}$$

The modified ε-greedy policy is noted as

$$a^{(t)} = \begin{cases} \text{Choose a random action, } 0 < t < t^* \\ \arg\max_{a \in A} Q(s^{(t)}, a), \ t^* < t < T \text{ and with probability } \varepsilon \\ \text{Choose a random action, } , t^* < t < T \text{ and with probability } 1-\varepsilon \end{cases} \tag{4.3}$$

where the ε is designed to be changeable as

$$\varepsilon(t) = \varepsilon_{initial} + \varepsilon_{rate} \times t \tag{4.4}$$

The setting of t^*, $\varepsilon_{initial}$ and ε_{rate} is listed in Table 4.1

- **Reward function** : The reward function is defined as the difference in the change of sum capacity after taking $a^{(t)}$ to change the coloring result and is given as

$$r^{(t+1)} = \sum_{m=0}^{M-1} C_m^{(t+1)} - \sum_{m=0}^{M-1} C_m^{(t)} \tag{4.5}$$

The implementation process of the proposed DRL-based intercell IC is illustrated in Figure 4.5. Each near-RT RIC first estimates the current state $s^{(t)}$ in the time instant t, which is used as the input to the DQN to derive the estimated Q-value of each color-adaptation actions. The color-adaptation action $a^{(t)}$ with the highest value will be selected, which as a consequence, will change the existing coloring results to minimize the occurrence of color collision near cell boundary. The selected $a^{(t)}$ actually serves the next time instant $t + 1$, therefore $s^{(t+1)}$ is estimated again and the reward $r^{(t+1)}$ is defined by the near-RT RIC to evaluate the merit of the selected $a^{(t)}$ by comparing the change in $s^{(t)}$ and $s^{(t+1)}$.

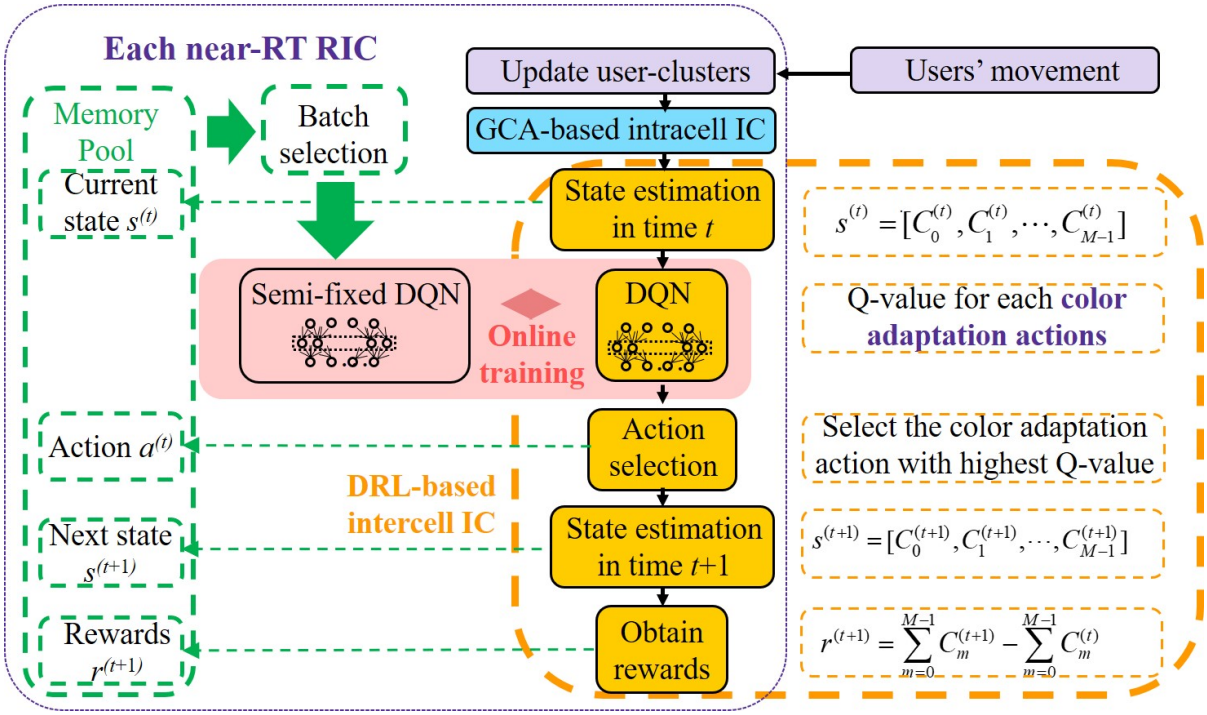

Figure 4.5: The proposed DRL-based intercell IC.

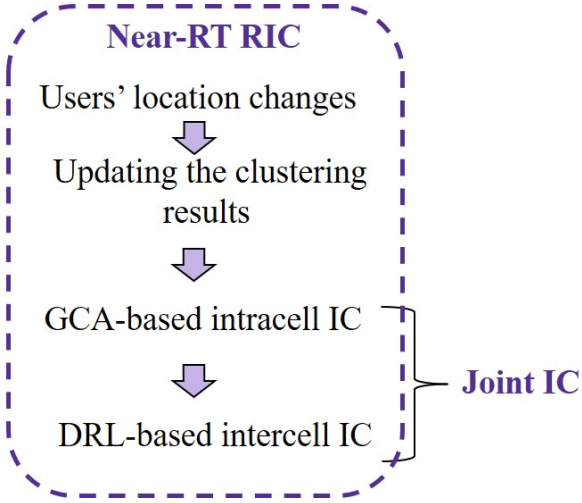

Figure 4.6: The proposed joint IC.

The computational complexity of DQN during implementation process only depends on the complexity of matrix multiplication, therefore it is $O(\sum_{l=1}^{L} n_l n_{l-1})$[52], in which $\mathscr{L} = \{0, \cdots, L\}$ represent the set of layers, $l = 0$ and $l = L$ denote the input layer and output layer respectively, n_l denote the number of neurons of each layer $l \in \mathscr{L}$.

4.5 Proposed Joint IC

Building upon the newly proposed DRL-based intercell IC, a joint IC strategy that combines the GCA-based intracell IC and the DRL-based intercell IC is further proposed as an upgraded version of the existing conventional GCA-based IC.The proposed joint IC strategy, aiming at maximizing the capacity of a cellular system with cluster-wise distributed MU-MIMO in a decentralized manner by combining the GCA and the DRL.

The application of the proposed joint IC is shown in Figure 4.6. Because we suppose each near-RT RIC works in a decentralized manner, so the application of user-clustering and joint IC can only use the locally observed information. The random movement of users leads to periodic updates of user-clusters, which in turn requires the corresponding joint IC to mitigate both intercell interference and intracell interference. The GCA-based intracell IC is applied first

in each cell independently to allocate different sub-bands to the neighboring clusters, therefore successfully mitigate the intracell interference. Then, under the constraint of the existing GCA results, part of cells are selected to turn on the DRL-based intercell IC to dynamically choose one color-adaptation action to adjust the existing coloring result in order to minimize the occurrence of the intercell interference from surrounding cells. In this way, both the intracell interference and the intercell interference can be mitigated.

4.6 Proposed Joint IC Based on Online Training

The proposed joint IC strategy incorporates DRL, allowing it to interact with the environment and gain an understanding of the current color collision status, enabling the selection of appropriate color-adaptation actions to prevent further color collisions. However, as mentioned, the environment is constantly changing. The unpredictable movement of users results in the continual updating of user-clusters, leading to unpredictable changes in the occurrence of color collisions and the colors involved. For example, at this moment, cluster with index A may experience a color collision in red with a neighboring cell, while at the next moment, a green color collision may occur between cluster with index B and another cell. The proposed joint IC with DQN can learn and search for the optimal color adaptation action in a specific environment. However, when facing a continuously changing environment, a fixed DQN will struggle to adapt.

Therefore, the joint IC strategy alone is insufficient to address the interference issues in cellular systems with cluster-wise distributed MU-MIMO. It is crucial to ensure that this newly proposed joint IC strategy can self-adapt to the dynamically changing environment.

In this study, we also proposed a online training strategy to be applied to the proposed joint IC that relies on the real-time data obtained during the implementation process. In the following sections of this section, we will first introduce what is online training and then explain why adopting online training enables environmental adaptability. Furthermore, we will discuss how the online training strategy can be applied in the proposed joint IC.

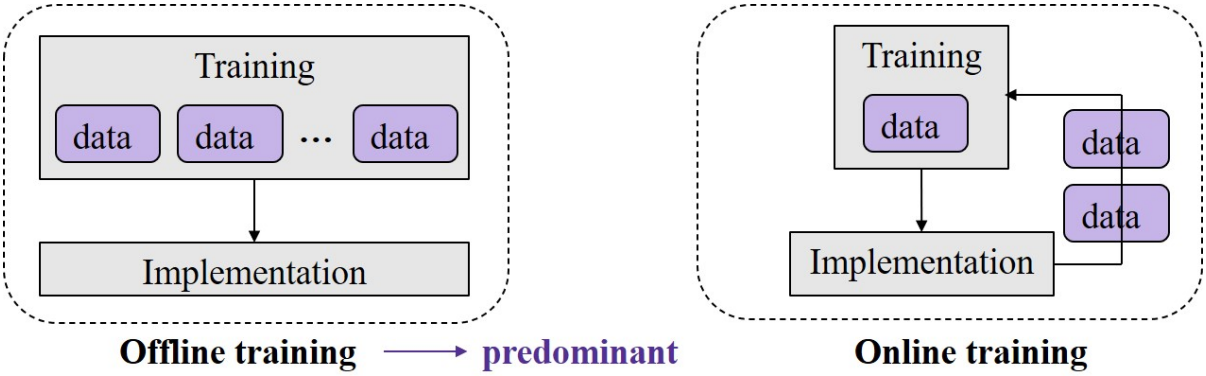

Figure 4.7: The introduction of online training and offline training.

4.6.1 Introduction of Online Training and Offline Training

Online training and offline training are two different training methods. Offline training refers to the training process where all the training data is collected before the training begins, and this collected data is used for training. This method has been widely used in various fields and has established mature techniques and algorithms. In recent years, offline training has also dominated in the applications of communication systems [54][55].

However, a major limitation of offline training is its inability to adapt to dynamically changing environments as it lacks real-time feedback from the environment. In contrast, online training involves training the model in a real-time environment and continuously adjusting its behavior and strategies through interactions with the environment. The advantage of online training lies in its ability to adapt to environmental changes and make timely adjustments, thus providing better adaptability and flexibility.

As shown in Figure 4.7, if the offline training is adopted for joint IC, A large number of datasets need to be prepared in advance, which cannot be satisfied in a dynamic changing environment. While if the online training is adopted, the continuously generated real-time data from real communication processes can be used to train the DQN in the Joint IC. Through constant online training, the parameters of the DQN are updated continuously, enabling it to follow the changing environment and provide real-time solutions. Moreover, online training allows for controlling the data volume to be sufficiently small, thereby effectively managing the

size of the neural network and the training time.

Therefore, DQN is trained online instead of offline in this letter, which guarantees that our proposed joint IC has the ability to adapt to the dynamic environment and react in real time. Then, how to apply online training for joint IC will be explained in detail.

4.6.2 Application of Joint IC Based on Online Training

In order to achieve online training, I have adopted the following strategies.

1. The application of memory replay and batch selection

   To ensure that the DQN can adapt quickly to the changing environment, the DQN needs to be trained with the real-time data obtained from interaction with the dynamic environment. Therefore, a feedback loop between the DQN and the environment which allows the DQN to receive continuous feedback and adjust its actions accordingly is needed.

   In this study, we assume that each cell is equipped with a fixed size of memory pool, in which the state transition sequence $\Delta^{(t)} = (s^{(t)}, a^{(t)}, s^{(t+1)}, r^{(t+1)})$ that happened in latest time instants are stored. Also, the memory pool will be resetted once after the clustering results are updated to weaken the effect of the outdated data. In this way, all the training data can be ensured to be up to date. Because the online training strategy is adopted in this letter, we assume that the wireless environment at $s^{(t)}$ and $s^{(t+1)}$ are different, with future information completely unknown.

   Additionally, a data control mechanism should also be implemented to ensure that during each time of online training only a sufficiently small amount of data is used. This helps in controlling the size of the neural network and reduces the training time, making it feasible for real-time applications.

   Therefore during the online training process, a batch of data D is randomly selected from the memory pool to train the DQN. The application of memory replay and batch selection [52] can effectively eliminate the correlation between training data and improve the data utilization. Meanwhile, it ensures that the training dataset for online training is up-to-date

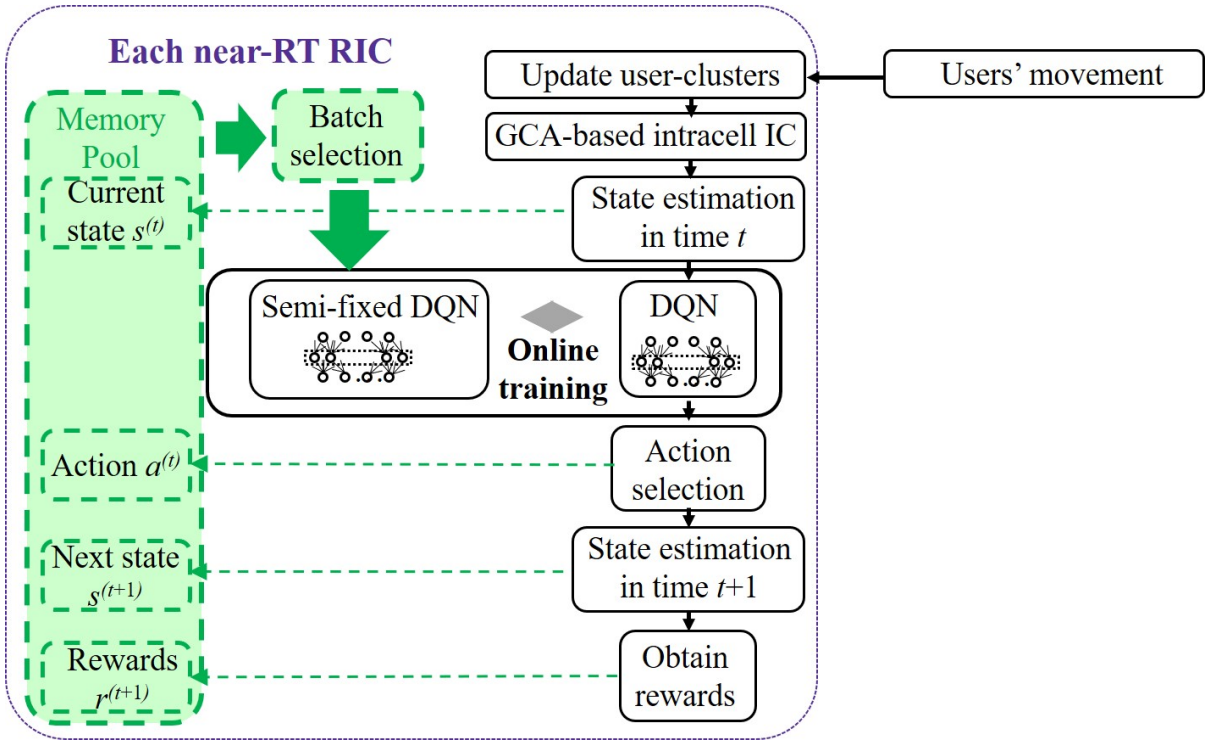

Figure 4.8: The application of memory replay and batch selection for online training.

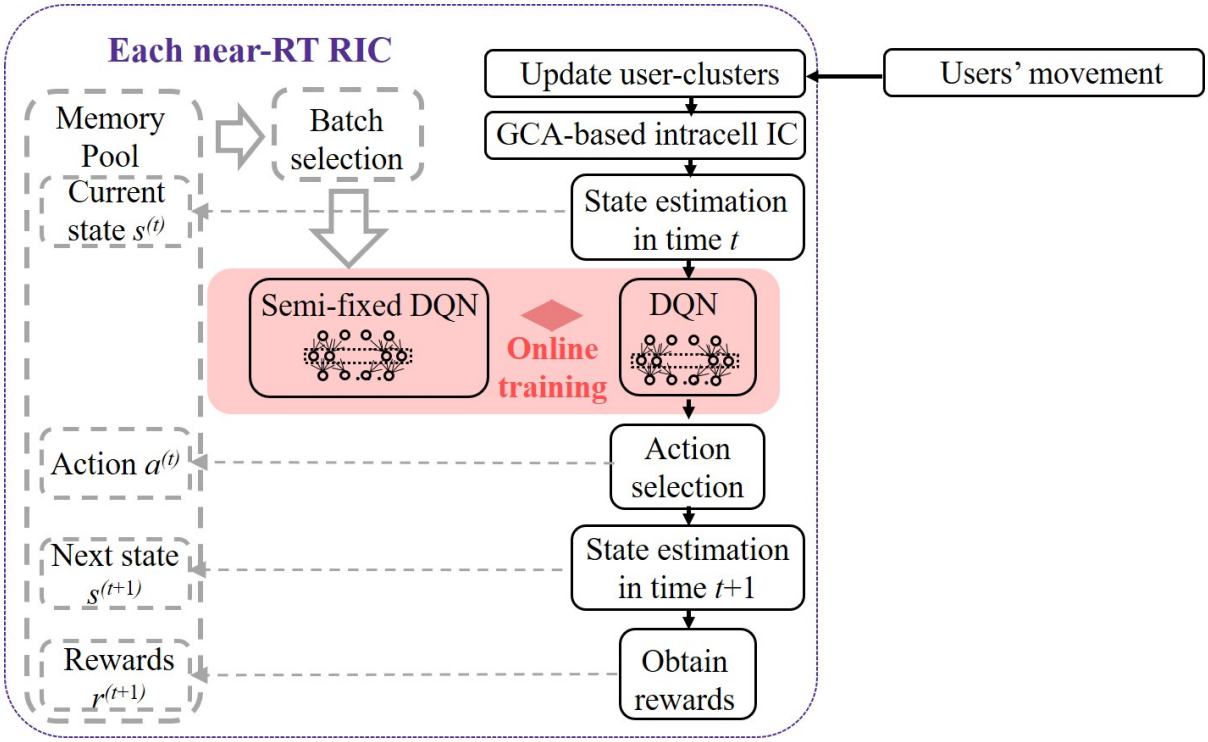

Figure 4.9: The semi-fixed training method in online training.

and also, it greatly reduces the size of dataset during each training episode so as to reduce the training overhead.

2. The application of semi-fixed target Q network

   Another challenge that must be addressed in online training is the fluctuation of data. During online training, the data obtained are only from a very small period of time, so the regularity in the data is poor and usually have significant fluctuations, which can introduce instability and divergence in the learning process. This is particularly relevant in dynamic environments where the data distribution may change over time.

   The fluctuating nature of online training data can lead to large variations in the observed

states, actions, and rewards. As a result, the Q-values estimated by the network based on this data may be highly volatile and subject to frequent changes. Without proper mechanisms to mitigate the impact of these fluctuations, the learning process can become unstable and diverge, hindering the convergence towards an optimal solution.

To address this issue, the fixed target Q technique[52] is commonly used. By using a separate target network with fixed parameters, the fluctuations in the training data are decoupled from the estimation of target Q-values. The target network provides a more stable and consistent set of Q-values for updating the online network. This helps to mitigate the negative effects of data fluctuations and promotes a smoother learning process.

In this study, we adopted a semi-target Q network, in which the target network is instead fixed but periodically copied from the main DQN. The semi-fixed target Q network is able to better mitigate the issue of overestimation and enhances the learning stability while follow the dynamics of environment.

Next, I will explain the process of DQN training after incorporating the semi-target Q network. Since DQN is an extension of the basic Q-learning algorithm [52], which applies the Bellman equation to update the Q value with the learning rate α as

$$\begin{aligned} Q(s^{(t)}, a^{(t)}) \leftarrow & Q(s^{(t)}, a^{(t)}) + \alpha[r^{(t+1)} + \\ & \gamma \max_{a \in A} Q^{'}(s^{(t+1)}, a) - Q(s^{(t)}, a^{(t)})]. \end{aligned} \tag{4.6}$$

When the semi-fixed target network method is applied, in which one local DQN and one semi-fixed DQN coexist. The local DQN updates its weight θ during the online training and calculates the estimated Q value $Q(s^{(t)}, a^{(t)}, \theta)$ (denoted by Q-estimated). While the semi-fixed DQN, with weight $\theta^{'}$ been copied from θ every T^{*} time instants, is to calculate the target Q value $Q(s^{(t+1)}, a^{(t+1)}, \theta^{'})$ (denoted by Q-target). The cooperation of semi-fixed DQN and local DQN can improve the convergence during the DQN training.

In DQN, the Q-target and Q-estimated can be obtained by local DQN and semi-fixed DQN as follows

$$\text{Q-target} = r^{(t+1)} + \gamma \max_{a \in A} Q(s^{(t+1)}, a, \theta') \tag{4.7}$$

$$\text{Q-estimated} = Q(s^{(t)}, a^{(t)}, \theta) \tag{4.8}$$

Therefore, the loss is defined as

$$\text{loss}(\theta) = \sum_{D} (\text{Q-target} - \text{Q-estimated})^2 \tag{4.9}$$

The DQN training process is to minimize the loss by updating the value of θ.

In conclusion, to train the DQN, an experience replay buffer is introduced to store the agent's experiences, including the state, action, reward, and next state. During training, the agent samples mini-batches from the replay buffer to update the neural network weights, utilizing a loss function that minimizes the difference between the predicted Q-values and the target Q-values.

As a result, our proposed joint IC based on online training can naturally explore the unknown environment and find solutions with well adaptability to dynamic environment.

4.7 Proposed Joint IC under 2-layer IC Framework

The design of the joint IC involves activating GCA-based intracell IC in every cell, while selectively activating DRL-based intercell IC in a subset of cells. This is partly due to considerations of computational resources within the system. The proposed joint IC strategy relies on neural networks, and although a trained neural network has relatively low computational complexity during the implementation process, the adoption of online training to adapt to complex and dynamic environments introduces additional training overhead. Therefore, controlling the number of cells that activate DRL-based intercell IC helps manage the training overhead within acceptable limits in the system.

The next question is how to select which cells to activate DRL-based intercell IC. In this study, we propose a strategy to activate DRL-based intercell IC only in non-adjacent cells. There are several reasons for this choice.

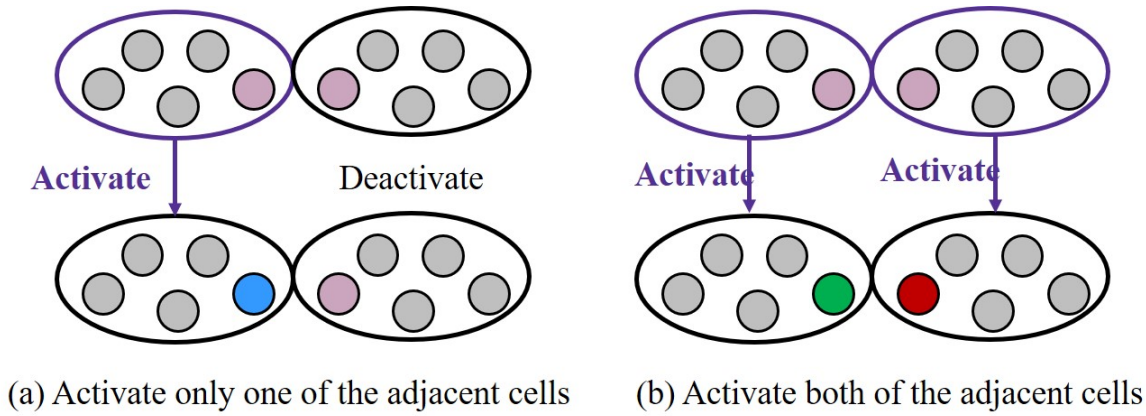

Figure 4.10: The explanation of activating the DRL-based intercell IC only in non-adjacent cells.

1. Color collision is the result of the co-action of two neighboring cells and can be resolved by the color change in either one of them.

2. When adjacent cells are turned on simultaneously, the convergence speed of the DQN will be affected in each cell.

As shown in Figure 4.10, in order to eliminate the color collision,there is no need to let both neighboring cell to change the colors. Moreover, if both adjacent cells activate DRL-based intercell IC simultaneously, they will be in a competitive state, which will inevitably affect the convergence speed of both cells. As a result, selectively activating non-adjacent cells can serve as a viable choice to strike a balance between training overhead and performance.

The next challenge is how to make sure the activation of DRL-based intercell IC in non-adjacent cells while maintaining that each cell are independent to each other. In this study, we applied the 2-layer IC framework proposed in the previous chapter to achieve this goal. Then, a detailed explanation of the joint IC based on the 2-layer IC framework and how it operates under the O-RAN architecture will be explained.

The framework of our proposed joint IC is illustrated in Figure 4.11. The clustering, together with the joint IC (including the GCA-based intracell IC and the DRL-based intercell IC) are designed to be applied on each near-RT RICs in the 2nd layer. During the communication, each

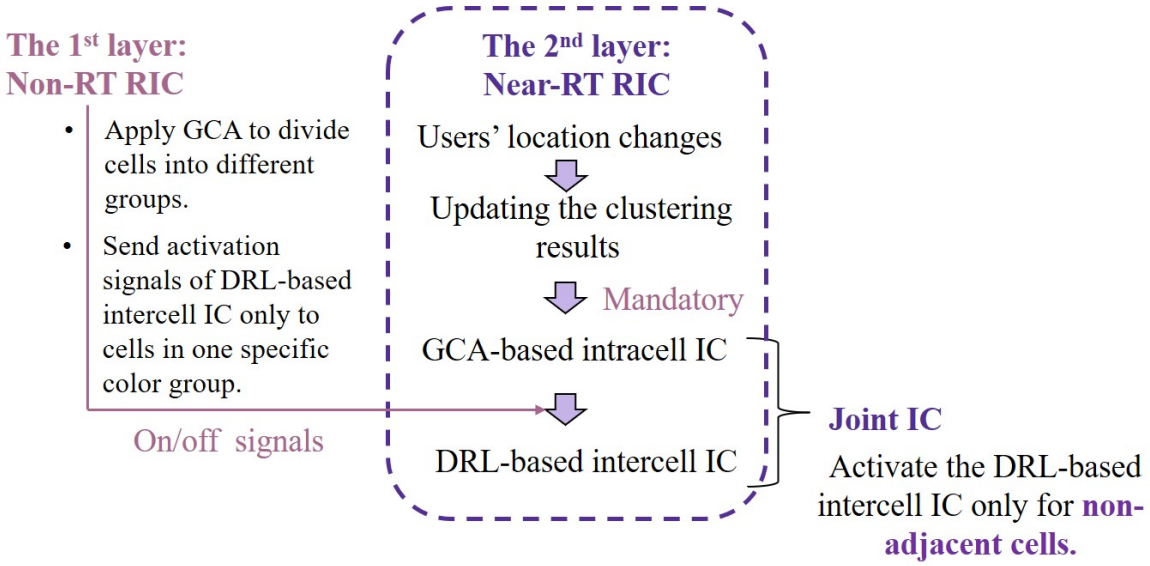

Figure 4.11: The application of joint IC based on 2-layer IC framework.

near-RT RIC updates the clustering results based on the users' movement and associate the DAs according to the principle of proximity. The updating of the clustering results will trigger the GCA-based intracell IC to allocate the different sub-bands to the neighboring clusters to mitigate the intracell interference. After that, the non-RT RIC with its broader system-level view will send guidance information from the 1st layer to the near-RT RICs to turn on some of the non-adjacent cells' DRL-based intercell IC. Then, the selected cells will work independently to mitigate the intercell interference with only the locally observed information.

Figure 4.12 illustrated how the proposed 2-layer IC framework based on joint IC can be applied under O-RAN architecture. In the 1st layer, the RC-GCA proposed in Chapter 3 will still be used as the rApp to divide all the cells into different color groups, and the activation signals will only be sent to cells in one color group via the A1 interface, in this way only the non-adjacent cells will turn on the DRL-based intercell IC. While in the 2nd layer, both the GCA-based intracell IC and the DRL-based intercell IC is applied as the xAPPs.

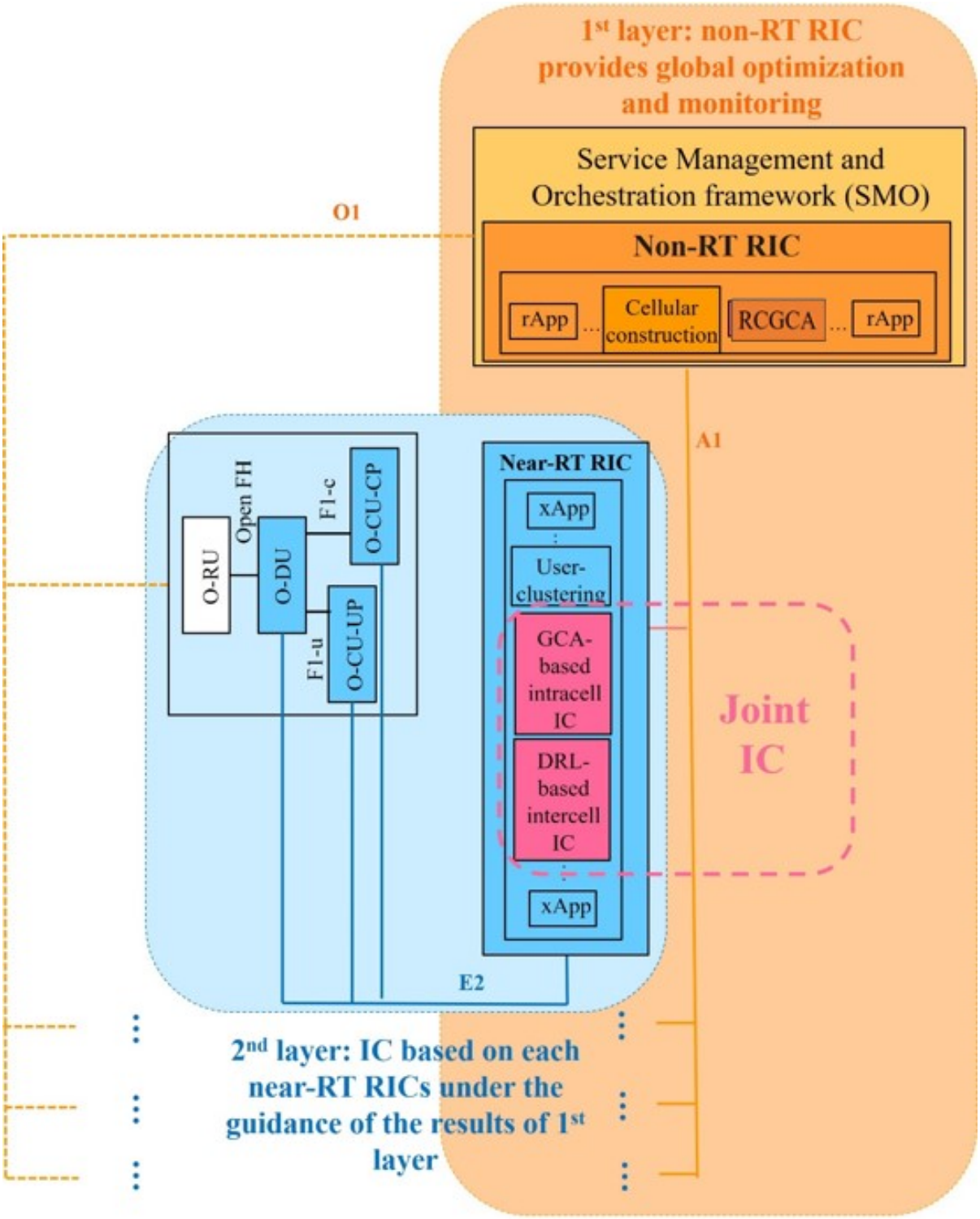

Figure 4.12: The application of joint IC under the O-RAN architecture.

4.8 Simulation Results Analysis

4.8.1 Problem Formulation

In our proposed joint IC, the entire bandwidth is divided into M sub-bands and one of the sub-bands is assigned to each cluster. The set of entire clusters and the set of clusters which are assigned to the mth sub-band in the service area are denoted by κ and κ_m, $m \in \{1, \cdots, M\}$, respectively. In this letter, the numbers of users, DAs, and clusters in κ are denoted by N_U, N_A, and N_C, respectively. While those in the κ_m are denoted by N_U^m, N_A^m, and N_C^m, respectively. The ith user in the kth cluster in κ_m is denoted by $u_{i,k}^m$. Below, the matrices are represented as bold upper-case letters and the superscripts $(i,:)$ and $(:,i)$ represent the ith row and column vectors of the matrix, respectively. Assuming the zero-forcing (ZF) based cluster-wise MU-MIMO to eliminate the multi-user interference within each cluster and by approximating the sum of inter-cluster interference and noise as a complex Gaussian process, the received signal-to-interference plus noise ratio (SINR) of user $u_{i,k}^m$ is given as

$$SINR_{u_{i,k}^m} = \frac{P_k \left\| \mathbf{H}_k^{(i,:)} \mathbf{W}_k^{(:,i)} \right\|^2}{\sum\limits_{l=1, l\neq k}^{N_C^m} P_l \sum\limits_{j=1}^{N_{U,l}^m} \left\| \mathbf{H}_{k,l}^{(j,:)} \mathbf{W}_l^{(:,j)} \right\|^2 + 1}, \tag{4.10}$$

where $\mathbf{W}_k$ and $\mathbf{W}_l$ are the ZF precoder matrices, $\mathbf{H}_k$ and $\mathbf{H}_{k,l}$ are respectively the channel matrix of kth cluster and the interference channel matrix between users in the kth cluster and DAs in the lth cluster in κ_m. $N_{U,k\ or\ l}^m$ denotes the number of users in the kth or l^{th} cluster in κ_m. P_k and P_l are the transmit powers allocated to the kth and l^{th} clusters, respectively and can be expressed as

$$P_{k \text{ or } l} = \frac{N_{U,k\ or\ l}^m P}{\|\mathbf{W}_{k \text{ or } l}\|_F^2}, \tag{4.11}$$

where P is the transmit power-to-noise ratio equal to all N_U users. Using the SINR expression in Eq. (4.10), the user capacity of user $u_{i,k}^m$ can be expressed as

$$C_{u_{i,k}^m} = \frac{1}{M} \log_2(1 + SINR_{u_{i,k}^m}). \tag{4.12}$$

Assigning different sub-bands to different clusters is equivalent to dividing the clusters into different cluster subsets $\{\kappa_m; m \in \{1, \cdots, M\}\}$. Therefore, our goal is to select optimal cluster subset $\kappa_m \subseteq \kappa$ which maximizes the sum capacity. We set our optimization objective as follows:

$$\begin{aligned} &\max_{\kappa_m \subseteq \kappa} \sum_{m=1}^{M} C_m, \\ &\text{s.t. } \forall m \in M, \\ &\quad \bigcup_{m \in M} \kappa_m = \kappa, \text{and } \kappa_n \cap \kappa_m = \emptyset, \forall n \neq m, \end{aligned} \tag{4.13}$$

where

$$C_m = \sum_{k=1}^{N_C^m} \sum_{i=1}^{N_{U,k}^m} C_{u_{i,k}^m} \tag{4.14}$$

Other detailed parameters are shown in Table 4.1.

4.8.2 Comparison of Coloring Results

Figure 4.13 illustrate the coloring results based on the proposed joint IC. Suppose at the beginning (t=0), the clustering results are updated and the GCA-based intracell IC is applied, therefore all the neighboring clusters inside each cell have been allocated different sub-bands, so that the intracell interference can be mitigated. But a lot of color collisions are seen along the cell boundary, thereby causing the intercell interference. While when t=100, due to the implementation of DRL-based intercell IC, the coloring result can be adjusted successfully and thus, minimize the intercell interference.

4.8.3 Sum Capacity Analysis of Activate Cells

In the application of the 2-layer IC framework based on joint IC, the evaluation of capacity improvement is conducted separately due to the presence of some cells activating DRL-based intercell IC while others do not. In this section, we will first analyze the capacity performance and convergence behavior of the cells that activate DRL-based intercell IC.

Table 4.1: PARAMETER SETTINGS

Total number of DAs, N_A	3200
Total number of users, N_U	2400
Total number of clusters, N_C	200
The number of sub-bands, M	4
Pathloss exponent	3.5
Shadowing loss standard deviation in dB	8
P in Eqs. (4.9)	0dB
γ in Eqs. (4.5)	1
$\varepsilon_{initial}$	0.8
ε_{rate}	0.002
t^*	10
Memory size	50
Batch size	10
T^*	50
DQN	3-layer fully connected artificial neural network
Number of neurons in each layer	[256,256,32]

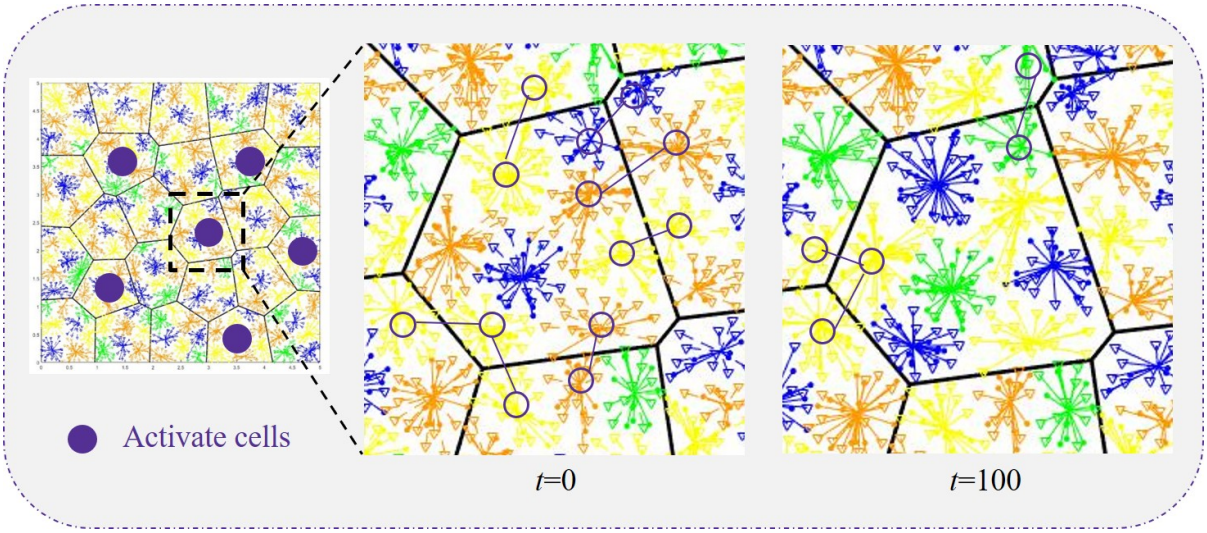

Figure 4.13: Coloring results of joint IC.

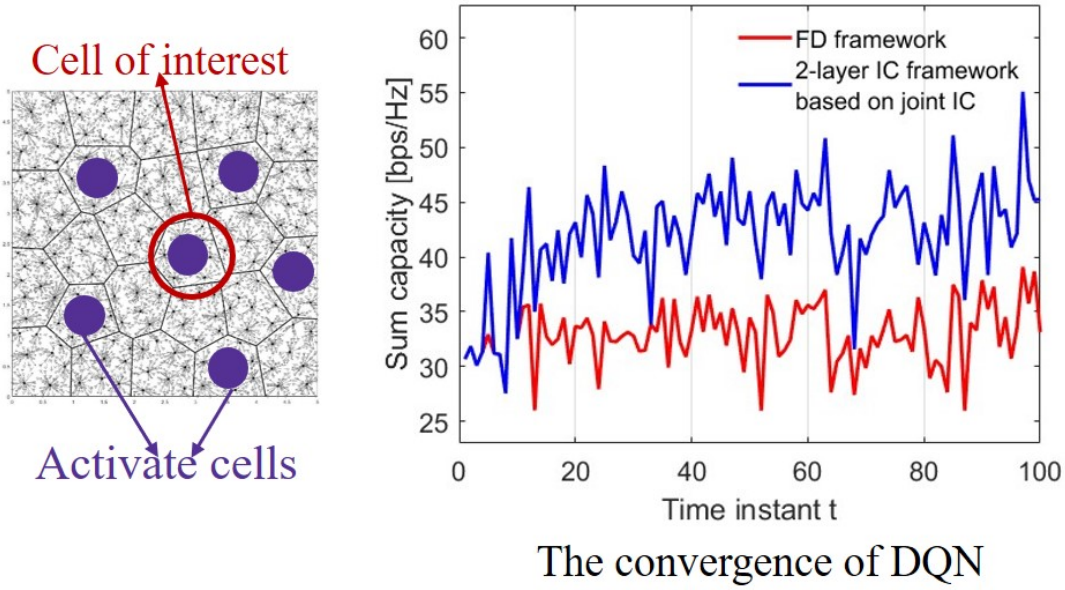

Figure 4.14: Convergence analysis of the activate cells.

In the case shown in Figure 4.14, the cell of interest will be chosen as the activate cell to turn on the DRL-based intercel IC, Therefore, in this scenario, its performance can be regarded as a typical representation of the activated cells.

In Figure 4.14, the sum capacity variation during the beginning 100 time instants for a new updating of clusters when DRL-based intercell IC is applied is illustrated as the blue curve. For comparison, we also provide the case of fully decentralized (FD) framework in red curve. From the results, a clear learning process can be seen when the DRL-based intercell IC is activated, which indicates that the DQN can adapt to the environment, thus providing a promising solution which has higher capacity than the case of FD framework. As for why we choose to divide the entire clustering period into 100 time instants, it is related to the speed of user movement. If the user moves at a faster pace, more time instants are needed. However, if the user consistently moves at a slower speed, fewer time instants are required.

Besides that, to achieve the adaptability of the DRL-based intercell IC to the dynamic environment via online training, the convergence speed of DQN is of vital importance.It is clearly seen from Figure 4.14 that the training only cost a dozen of time instants. This kind of convergence speed of DQN can accommodate the requirements of online training, therefore, convinced that our proposed joint IC based on online training can quickly keep up with the changes in the dynamic environment.

In Figure 4.15, we also plot the cumulative distribution function (CDF) of the sum capacity to evaluate our proposed joint IC when 8 clusters are formed in each cell. It can be clearly observed that the performance of the activated cell in the proposed 2-layer IC framework based on joint IC closely approaches the performance of the fully centralized (FC) framework, where no color collision exists. Therefore, when both the GCA-based intracell IC and the DRL-based intercell IC are activated, the intercell interference and the intracell interference can both be mitigated.

4.8.4 Sum Capacity Analysis of Deactivate Cells

In the case shown in Figure 4.16, the cell of interest will be chosen as the deactivate cell that will not turn on the DRL-based intercel IC, Therefore, in this scenario, its performance can be regarded as a typical representation of the deactivated cells.

By comparing the results in Figure 4.16 and Figure 4.14, it can be observed that there is no

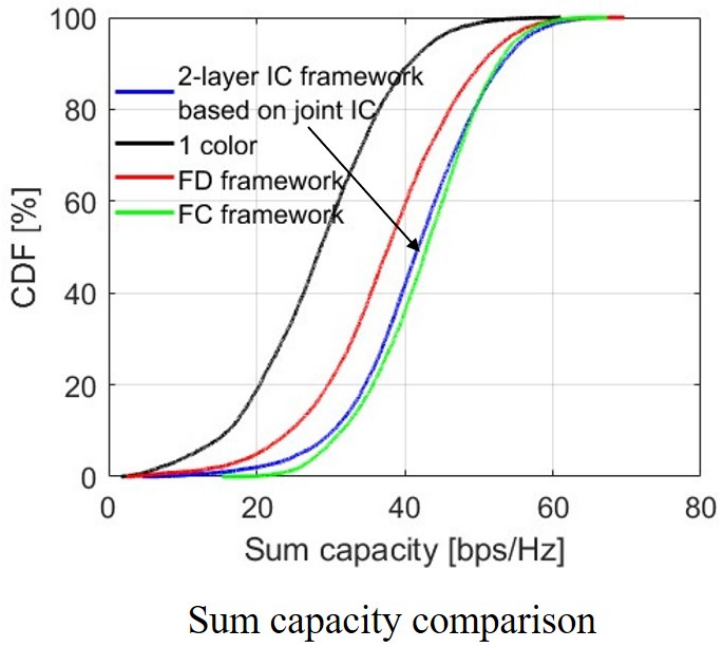

Figure 4.15: CDF of sum capacity achieved by joint IC (activate cell).

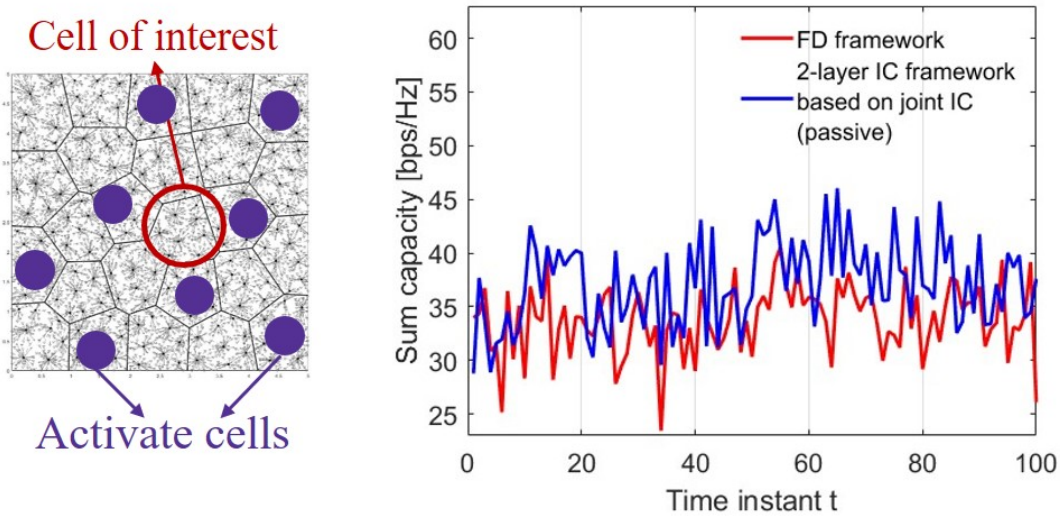

Figure 4.16: Convergence analysis of the deactivate cells.

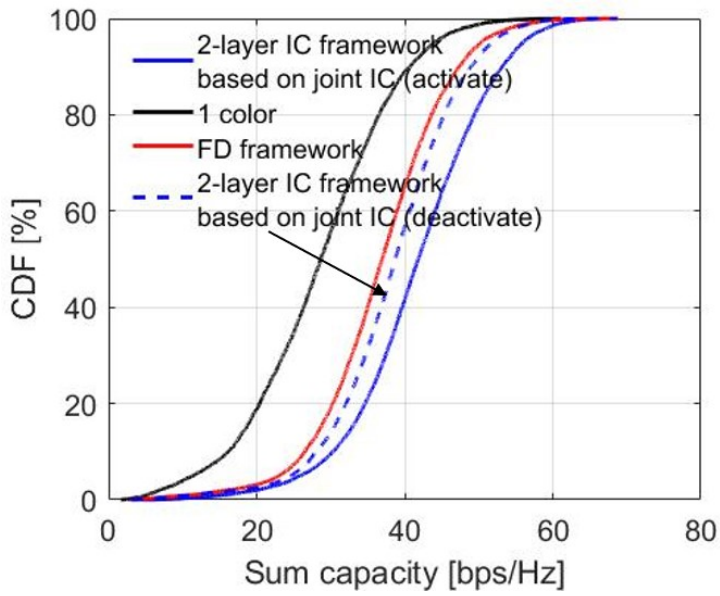

Figure 4.17: CDF of sum capacity achieved by joint IC (deactivate cell).

apparent learning process in the deactivate cell since the coloring results remain unchanged. However, it can be seen that the blue line representing the deactivate cell does show some improvement in capacity compared to the fully centralized (FD) framework represented by the red line. This improvement is attributed to the neighboring cells activating the DRL-based intercell IC, which passively mitigates color collision of the cell of interest.

From the CDF in Figure 4.17, it can be observed that due to the lack of active learning process, the deactivate cell is unable to actively search for its optimal state, which is reflected in the CDF by the deactivate cell's inability to achieve the same level of performance as the activate cell. However, it can also be seen that the results of the deactivate cell have surpassed the performance of the FD framework.

4.8.5 Parameter Study on Impact of Neural Network Size

In this section, the parameter studies on the size of DQN is conducted. The aforementioned simulations were conducted using a fully connected neural network with three hidden layers. The number of neurons in each layer was set to 256, 256, and 32, respectively. In this section,

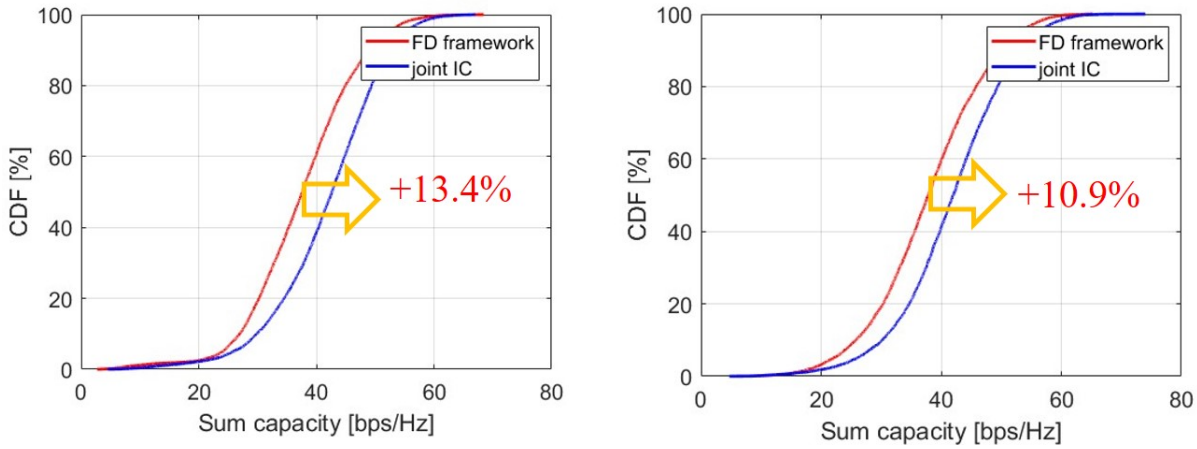

Figure 4.18: CDF of sum capacity achieved by DQN with reduced neurons and layers.

we first compared the impact of the number of neurons. We reduced the number of neurons in each layer of the three hidden layers to 128, 128, and 32, respectively. The simulation results are shown in the Figure 4.18 (left). Compared with the results in Figure 4.15, it can be observed that there is no significant difference, indicating that our previous configuration may have been overly large.

Then the impact of the number of hidden layers is also verified. The original 3-layer hidden layers were reduced to 1 layer, retaining only the last layer with 32 neurons connected to the output layer. From the results in Figure 4.18 (right), it is evident that the capacity at CDF=50% has decreased a lot. This indicates that during the learning process, there were more cases where the optimal solution was not found. It suggests that the current size of DQN may not be sufficient to meet the requirements of the problem scale.

4.8.6 Parameter Study on Impact of Real-time Availability of Training Dataset

In the realm of deep learning, data is often regarded as the essence that breathes “ life ” into the models. Hence, compared to discussing the size of neural networks, it is more crucial to focus on the impact brought by data collection and acquisition. Therefore, in this section, we

will also analyze the importance of real-time data acquisition during online training.

We assume a rapidly changing environment where, at a certain moment, a subset of antennas suddenly becomes inactive due to factors like disasters. We assume that initially each cell has 128 DAs and 64 users, but starting from time instant=101, only 96 antennas are available to serve the 64 users. In addition, for the purpose of better observation, we have chosen a specific scenario that before the environment change, the DQN was trained to choose the color-adaptation action that will maintain the existing coloring results. This choice allows us to observe more clearly the impact of the previously trained DQN when facing a sudden environmental change.

In Section 4.4, we proposed the modified $\epsilon-$ greedy approach to significantly increase the exploration ratio during the early stages of training. This approach aims to ensure the broader collection of real-time data at the moment when facing a sudden updates in clustering results. Additionally, in Section 4.6.2, we discussed the memory replay strategy adopted for online training, which involves fixing memory size and resetting the memory pool after each clustering update. All these measures are used to ensure the timely removal of outdated data, thereby guaranteeing that the data fed into the DQN training process remains up-to-date.

In Figure 4.19, we compare the convergence results with and without the use of the aforementioned memory replay strategy and modified $\epsilon-$ greedy action selection strategy. It can be observed that for the original clustering results (time instant from 1 to 100), after a dozen of time instants of learning, the DQN has learned that the best choice is to maintain the existing coloring scheme, as indicated by the convergence of the red and blue lines in the subsequent time slots. While from time instant=101, where there is a sudden reduction in the number of antennas from 128 to 96 (by randomly removing 32 antennas), necessitating an update in the clustering results. However, the DQN continues to exhibit a preference for the ”no change in coloring results” approach, therefore the online training is needed to update the parameters in DQN tp adapt to the new environment.

Figure 4.19 (left) illustrates the scenario where the memory pool has not been reset, and the $\epsilon-$ greedy action selection strategy has not been modified. From the results, it can be observed that the effectiveness of online training is not satisfactory. Throughout the entire 100 time instants, there is a persistent influence from the previous preference of ”not changing colors.” This situation arises due to two main factors. Firstly, it is because the action selection strategy heavily relies on the pre-trained DQN, resulting in a delay in generating effective training data.

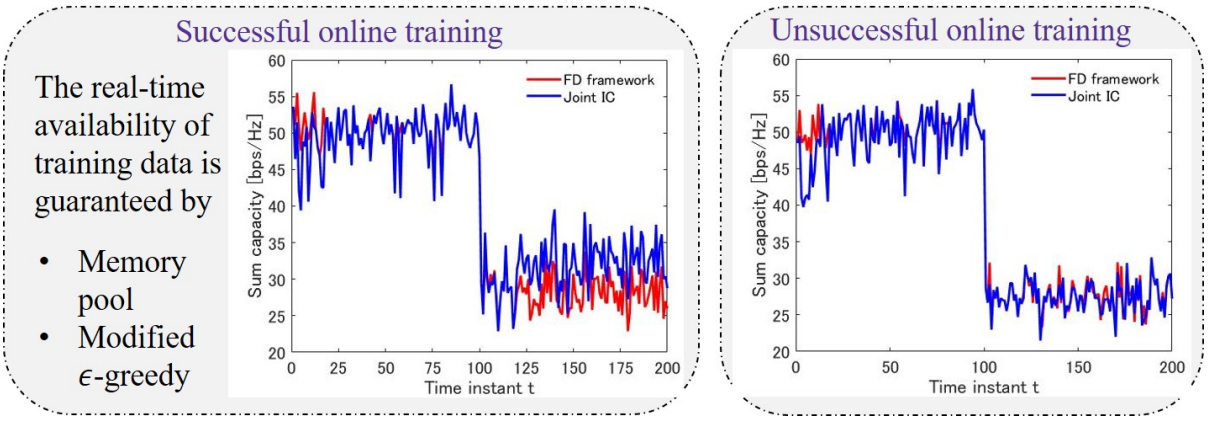

Figure 4.19: The importance of the real-time availability of training dataset.

Secondly, the persistent presence of data from the previous clustering results in the memory pool hampers the immediate impact of newly generated real-time data. This delay prevents the timely selection of newly generated effective data into the training dataset, thereby hindering the overall effectiveness of the online training process.

In contrast, as shown in the Figure 4.19(right), after applying the proposed memory replay strategy and modified $\epsilon-$ greedy action selection strategy, it can be observed that the DQN quickly adapts and successfully learns to select the optimal color adaptation action (which is no longer to maintain the existing coloring results this time) after a short learning period. This leads to a significant improvement in capacity.

The aforementioned memory replay strategy and modified $\epsilon-$ greedy action selection strategy are specifically designed to address the sudden environmental changes during online training. It can be observed that online training and offline training have different requirements in terms of data acquisition. For online training, the quantity of data is not the primary concern, but rather the real-time availability of data is crucial.

4.8.7 Validation of Necessity of Joint IC under the 2-Layer IC Framework

In the previous discussions, we mentioned that our proposed joint IC can work under a fully distributed (FD) manner. However, considering the physical characteristics of color collision and the practical requirements to control the training overhead in the online training, we propose

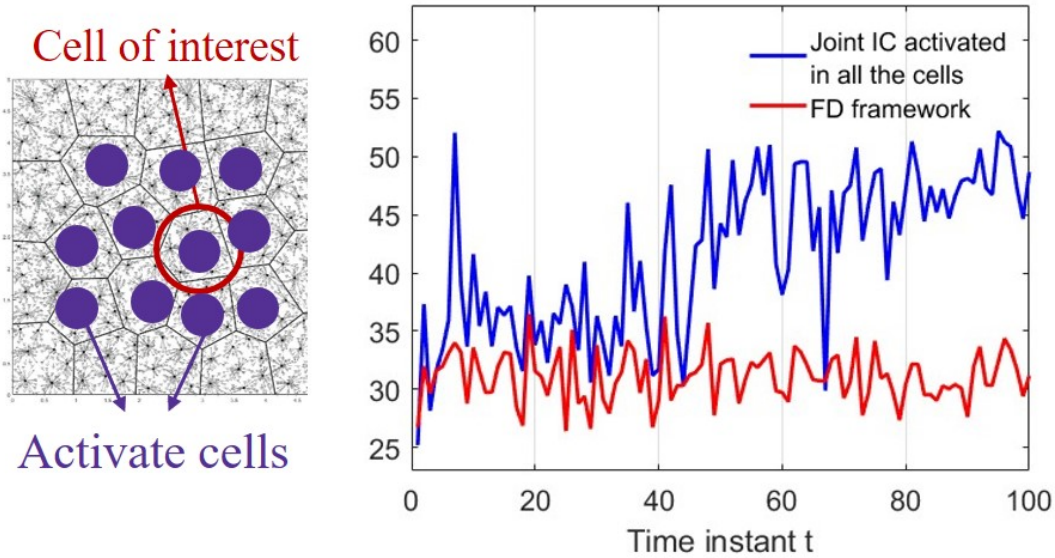

Figure 4.20: Convergence analysis of neighboring cells learning simultaneously.

to apply the joint IC under the 2-layer IC framework. Therefore, in this section, in order to demonstrate the necessity of applying under the the 2-layer IC framework, we further explore the results of applying joint IC based on the FD framework.

From the results in Figure 4.20, it can be observed that if neighboring cells simultaneously activate the DRL-based intercell IC, due to the assumption that each cell works independently as an single agent, there will be a competition among cells during their individual learning process, which leads to a slower convergence rate for each cell.

In online training, the convergence speed directly affects the performance of the system's capacity. If the DQN fails to quickly find the optimal color-adaptation action to mitigate color collision during online training, the results will be as shown in the Figure 4.21. Even if all cells activate the DRL-based intercell interference coordination, the results cannot surpass the performance of activated cells under the 2-layer IC framework. Therefore, both from the perspective of improving capacity and controlling training overhead, applying joint IC based on the 2-layer IC framework to control the number of cells that activate the DRL-based intercell interference coordination have certain advantages. As a preliminary research, this study only provides a simple strategy of applying joint IC under the 2-layer IC framework. More flexible

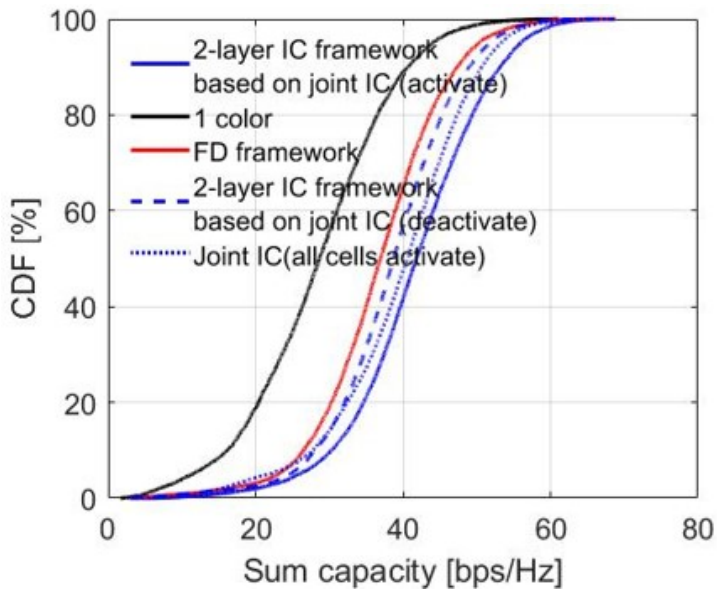

Figure 4.21: CDF of sum capacity achieved by joint IC (all neighboring cells learning together).

and intelligent approaches for applying joint IC based on the 2-layer IC framework require further investigation.

4.9 Summary

In this chapter, in order to incorporate the latest advancements in artificial intelligence (AI) into the traditional application of IC and further enhance the performance of color collision mitigation, the second method called the 2-layer IC framework based on joint IC was proposed. The overall idea of this method is to eliminate the color collision without modifying the coloring process itself. Instead, the existing coloring results are dynamically modified after the coloring process to eliminate color collision, thereby achieving the simultaneous elimination of intracell interference and intercell interference.

To facilitate this idea, the following contributions are made

1. Firstly, a color-adaptation scheme which make it possible to adjust the existing coloring results was proposed. Based on this color-adaptation scheme and the model of DRL,

a DRL-based intercell IC was also proposed to observe the environment in real time and dynamically change the existing coloring results to avoid the color collision. The proposed DRL-based IC was applied together with the original GCA-based intracell IC, thereby together form a joint IC.

2. Secondly, considering the fact that the color collision is dynamically changing according to the movement of users, the DQN applied in the DRL-based intercell IC should be updated accordingly to adapt to the ever-changing environment. Therefore in this study, we also proposed a online training strategy. The proposed joint IC based on online training is able to follow the dynamics of environment in a high mobility environment.

3. Finally, to ensure the convergence speed of DQN and control the training overhead within the system, we have also proposed a strategy to apply joint IC based on the 2-layer IC framework. By effectively selecting the cells to activate DRL-based intercell IC using non-RT RIC in the 1st layer, we can ensure good results in both the activate cell and deactivate cell. Additionally, reducing the usage of DRL-based intercell IC enables the possibility of controlling training overhead.

Chapter 5

Conclusions

In 5G and beyond, the application of distributed MU-MIMO has been of great interest for its ability to solve the problem of radio link blockage caused by the utilization of mm-wave band. In order to solve the prohibitively high computational complexity problem faced by the large-scale distributed MU-MIMO, a cluster-wise distributed MU-MIMO has been developed. However, the application of cluster-wise distributed MU-MIMO has a side effect of introducing additional intracell interference and intercell interference, and the existence of these two types of interference has greatly affected the system capacity. Therefore, this study focused on the interference coordination (IC) in the cellular system with cluster-wise distributed MU-MIMO to increase the system capacity.

In this study, based on the O-RAN architecture, a 2-layer IC framework was proposed and two upgraded GCA-based ICs that can be used under this 2-layer IC framework were also proposed. It was verified that when the two methods been applied under the 2-layer IC framework, both the intercell interference and the intracell interference can be successfully mitigated, and the system capacity can be significantly increased.

This dissertation was divided into 6 chapters.

The Chapter 1 was the introduction, which introduced the background and motivation of this study in detail.

In Chapter 2, the conventional heuristic GCA and the application of GCA-based IC was firstly introduced. Then, the performance of GCA-based IC was evaluated under two commonly used frameworks: fully centralized (FC) and fully decentralized (FD). The verification has

leaded to the fact that the GCA-based IC under FC framework can mitigate both the intracell interference and the intracell interference, but its computational complexity exceeds practical limits. On the other hand, the GCA-based IC under FD framework is computational flexible, but it can only mitigate the intracell interference, leaving intercell interference caused by color collision unresolved. Furthermore, the future requirements for scalability and flexibility for deployment in cellular systems were highlighted. It is highly desirable for cells to operate independently without information exchange between them. Therefore, the problem statement was established: under the condition that each cell operates in a decentralized manner, there has been a pressing need for a novel GCA-based IC that can mitigate intracell interference while considering intercell interference as well.

In Chapter 3, the concept of Fractional Frequency Reuse (FFR) was incorporated into the GCA algorithm, resulting in a modified GCA-based IC approach. The clusters have been categorized into two types: cell-edge clusters and inner-cell clusters. Each type has been colored separately using distinct color options. In order to realize the above-mentioned idea, the following task has been done. Firstly, based on computational geometry (CG), a method to abstract the IC problem as a graph was first proposed, which is able to circumvent the threshold optimization problem of traditional graph construction methods, while at the same time, automatically distinguish the clusters that locates near the cell boundaries. Then, with the constructed graph, a new GCA, named as the restricted conditional GCA (RC-GCA) was also proposed in this chapter, in which it enables the separate coloring of the cell-edge clusters and the inner-cell clusters. Based on RC-GCA, the cell-edge clusters can be colored with restrictions of color options so as to minimize the occurrence of color collisions, while the inner-cell clusters can be colored under conditions so as to self-adapt to the existing cell-edge colors. Finally, based on the O-RAN architecture, a 2-layer IC framework, which relies on the cooperation of non-real-time (non-RT) radio access network intelligent controller (RIC) and near-RT RICs, was also proposed in this chapter. The 2-layer IC framework enables a reasonable allocation of cell-edge color options to each cell. The effectiveness of our proposed 2-layer IC framework based on GCA was verified by the fact that it can further mitigate the intercell interference, building on the successful mitigation of intracell interference, thus enhancing the system capacity even further. It was also demonstrated that the proposed method outperforms the well-known fractional frequency reuse (FFR) scheme, the FD framework and no IC case, and is able to achieve performance comparable to the FC framework.

In Chapter 4, considering the dynamics of the environment and the current progress of AI technologies based on deep learning, the possibility of combining GCA with DRL was explored in depth in this chapter, and a new joint IC method was proposed. The proposed joint IC includes a GCA-based intracell IC and a DRL-based intercell IC. Based on online training, the proposed joint IC can follow the time-varying environment and thus achieve dynamic IC control based on the real-time feedback from the environment. Considering of the training overhead in practical application, a strategy to apply the proposed joint IC under the 2-layer IC framework was also proposed. By selectively activating the DRL-based intercell IC only in non-adjacent cells, not only the capacity enhancement can be guaranteed but also the training overhead can be controlled. The validation of the computer simulation has revealed that our proposed 2-layer IC framework based on joint IC can dramatically increase the capacity and obtain a performance close to the FC framework. At the same time, the analysis of its convergence has proved that the DQN can converge within a dozen of time instants and thus our proposed joint IC can adapt to the fast-changing environment with strong environmental adaptability.

In summary, challenges related to inter-cluster IC in cellular systems with cluster-wise distributed MU-MIMO have been analyzed and addressed. Two GCA-based methods under the 2-layer IC framework were proposed, which effectively meet the requirement for decentralized system operation while significantly enhance system capacity. This research has provided strong support for the application of cluster-wise distributed MU-MIMO in next-generation mobile communication system.

Future Research

In the second method of the 2-layer IC framework based on joint IC, the overall idea is to classify cells into several color groups in the 1st layer. This way, in the 2nd layer, all cells activate GCA-based intracell IC, but only cells belonging to one color group activate DRL-based intercell IC. Therefore, there is still an unresolved question in this study regarding how to select which color group of cells should activate DRL-based intercell IC.

As emphasized in this dissertation, the occurrence of color collisions is highly uncertain. Therefore, the initial intention of this study is to also build a DQN in the non-RT RIC in the 1st layer as well, aiming to dynamically select a certain color group in real time and activate the DRL-based intercell IC only for the cells in the selected cell group.

However, considering that the non-RT RIC can only handle time-insensitive tasks, it is not feasible to upload all training data through the A1 interface to the non-RT RIC to realize the above-mentioned idea. Therefore, a possible way is to adopt the federated learning, which means keeping the training data in each local near-RT RICs and only downloading the model of DQN and a few relevant parameters from the non-RT RIC to each near-RT RICs. Training will then take place within each near-RT RIC. After training is completed, only the updated parameters are uploaded to the non-RT RIC, so that the non-RT RIC only performs a simple parameter assembly process, while a significant amount of computation is still distributed among each local near-RT RIC.

Briefly, the idea of the 2-layer IC framework based on joint IC consists of using a large DQN in a non-RT RIC to control small DQNs in each near-RT RICs, thus enabling full dynamic control of the application of the DRL-based intercell IC to optimize the performance.

Considering the limited time available, this idea could not be implemented during the doctoral period. All the results in this dissertation are based on a fixed color group, that is assuming during the simulation, the selected color group that activate the DRL-based intercell

IC remains unchanged. I believe this idea is promising and deserves further ongoing research in the future.

Acknowledgments

First and foremost, I would like to express my heartfelt gratitude to my supervisor, Prof. Chen Qiang. As a student from a different major, I would never have started this unforgettable journey of doctoral studies without his recognition and support. Throughout my entire doctoral period, Prof. Chen has provided me with meticulous guidance and assistance, for which I am deeply grateful.

Furthermore, I would like to extend special thanks to Prof. Adachi Fumiyuki, who has been instrumental in guiding me through my research endeavors. It is his constant mentorship that has enabled me to successfully complete all of my researches.

Additionally, I would like to express my sincere gratitude to the professors who participated in my thesis defense. I am deeply thankful to Prof. Nishiyama Hiroki, Prof. Suematsu Noriharu, and Prof. Konno Keisuke for their valuable insights and guidance, which have greatly contributed to the refinement and completion of my doctoral dissertation.

Moreover, I would also like to express my sincere appreciation to Prof. Yuan Qiaowei. During my most challenging times, her understanding and encouragement helped me to persevere. Prof. Yuan's care and assistance in both academic and personal aspects have been truly significant to me, and I will always hold them dear in my heart.

I would also like to express my gratitude to all my colleagues in our group. Pursuing doctoral studies alone in a foreign land is undoubtedly challenging, but their presence has transformed countless struggles into cherished memories.

Besides that, I would like to express my heartfelt gratitude to the Tohoku University's Advanced Graduate School Pioneering Research Support Project for the scholarship they provided. Also, I would like to extend my appreciation to the project of「第 5 世代移動通信システムの更なる高度化に向けた研究開発」 and 「Beyond 5G のレジリエンスを実現するネットワーク制御技術の研究開発」for their financial support. Without their generous assistance, I

may not have been able to successfully complete my doctoral program.

Finally, I am immensely grateful to my parents and my boyfriend. Throughout my doctoral journey, I encountered numerous moments of despair, but their unwavering presence provided me with the strength to overcome each and every dark moment.

Bibliography

[1] Cisco, “Cisco visual networking index: Global mobile data traffic forecast update, 2017-2022,” White paper, February, 2019. Available: http://media.mediapost.com/uploads/CiscoForecast.pdf

[2] X. Ge, S. Tu, G. Mao, C. -X. Wang and T. Han, ”5G Ultra-Dense Cellular Networks,” *IEEE Wireless Communications*, vol. 23, no. 1, pp. 72-79, February 2016, doi: 10.1109/MWC.2016.7422408

[3] J. Chen, X. Ge and Q. Ni, ”Coverage and Handoff Analysis of 5G Fractal Small Cell Networks,” *IEEE Transactions on Wireless Communications* , vol. 18, no. 2, pp. 1263-1276, Feb. 2019, doi: 10.1109/TWC.2018.2890662.

[4] D. Gesbert, M. Kountouris, R. W. Heath, C. Chae and T. Salzer, ”Shifting the MIMO Paradigm,” *IEEE Signal Processing Magazine* , vol. 24, no. 5, pp. 36-46, Sept. 2007, doi: 10.1109/MSP.2007.904815.

[5] E. G. Larsson, O. Edfors, F. Tufvesson and T. L. Marzetta, ”Massive MIMO for next generation wireless systems,” *IEEE Communications Magazine* , vol. 52, no. 2, pp. 186-195, February 2014, doi: 10.1109/MCOM.2014.6736761.

[6] M. Shafi, A. F. Molisch, P. J. Smith, and T. Haustein, “5G: A Tutorial Overview of Standards, Trials, Challenges, Deployment, and Practice,” *IEEE Journal on Selected Areas in Communications* , vol. 35, no. 6, pp.

[7] J. Joung, Y. K. Chia and S. Sun,,“Energy-Efficient, Large-Scale Distributed-Antenna System (L-DAS) for Multiple Users,” *IEEE Journal of Selected Topics in Signal Processing*, vol. 8, no. 5, pp. 954-965, Oct. 2014.

[8] S. Xia, C. Ge, Q. Chen and F. Adachi, ”A Study on User-antenna Cluster Formation for Cluster-wise MU-MIMO,” *2020 23rd International Symposium on Wireless Personal Multimedia Communications (WPMC)*, 2020, pp. 1-6, doi: 10.1109/WPMC50192.2020.9309519.

[9] D. Gesbert, S. Hanly, H. Huang, S. Shamai Shitz, O. Simeone and W. Yu,“Multi-Cell MIMO Cooperative Networks: A New Look at Interference,” *IEEE Journal on Selected Areas in Communications*, vol. 28, no. 9, pp. 1380-1408, Dec. 2010.

[10] O-RAN Alliance, ”O-RAN Minimum Viable Plan and Acceleration towards Commercialization”, O-RAN White Paper, June 2021

[11] W. Jiang, B. Han, M. A. Habibi and H. D. Schotten, ”The Road Towards 6G: A Comprehensive Survey,” *IEEE Open Journal of the Communications Society* , vol. 2, pp. 334-366, 2021, doi: 10.1109/OJCOMS.2021.3057679.

[12] A. Garcia-Saavedra and X. Costa-Pérez, ”O-RAN: Disrupting the Virtualized RAN Ecosystem,” *IEEE Communications Standards Magazine* , vol. 5, no. 4, pp. 96-103, December 2021, doi: 10.1109/MCOMSTD.101.2000014.

[13] S. K. Singh, R. Singh and B. Kumbhani, ”The Evolution of Radio Access Network Towards Open-RAN: Challenges and Opportunities,” *2020 IEEE Wireless Communications and Networking Conference Workshops (WCNCW)*, 2020, pp. 1-6, doi: 10.1109/WCNCW48565.2020.9124820.

[14] Q. H. Duong, I. Tamim, B. Jaumard and A. Shami, ”A Column Generation Algorithm for Dedicated-Protection O-RAN VNF Deployment,” *2022 International Wireless Communications and Mobile Computing (IWCMC)*, 2022, pp. 1206-1211, doi: 10.1109/IWCMC55113.2022.9825080.

[15] F. Mungari, ”An RL Approach for Radio Resource Management in the O-RAN Architecture,” *2021 18th Annual IEEE International Conference on Sensing*, Communication, and Networking (SECON), 2021, pp. 1-2, doi: 10.1109/SECON52354.2021.9491579.

[16] H. Lee, J. Cha, D. Kwon, M. Jeong and I. Park, ”Hosting AI/ML Workflows on O-RAN RIC Platform,” *2020 IEEE Globecom Workshops* (GC Wkshps, 2020, pp. 1-6, doi: 10.1109/GCWkshps50303.2020.9367572.

[17] A. K. Singh and K. Khoa Nguyen, ”Joint Selection of Local Trainers and Resource Allocation for Federated Learning in Open RAN Intelligent Controllers,” *2022 IEEE Wireless Communications and Networking Conference (WCNC)*, 2022, pp. 1874-1879, doi: 10.1109/WCNC51071.2022.9771700.

[18] H. Kumar, V. Sapru and S. K. Jaisawal, ”O-RAN based proactive ANR optimization,” *2020 IEEE Globecom Workshops* (GC Wkshps, 2020, pp. 1-4, doi: 10.1109/GCWkshps50303.2020.9367582.

[19] H. Zhang, K. Yang and S. Zhang, ”Resource Allocation Based on Interference Alignment With Clustering for Data Stream Maximization in Dense Small Cell Networks,” *IEEE Access* , vol. 7, pp. 161831-161848, 2019, doi: 10.1109/ACCESS.2019.2951999.

[20] L. Chen, H. Xia, C. Feng and S. Wu, ”Clustering-based co-tier interference coordination in dense small cell networks,” *2015 IEEE 26th Annual International Symposium on Personal, Indoor, and Mobile Radio Communications (PIMRC)*, 2015, pp. 1878-1882, doi: 10.1109/PIMRC.2015.7343605.

[21] D. Qu, Y. Zhou, L. Tian and J. Shi, ”User-Centric QoS-Aware Interference Coordination for Ultra Dense Cellular Networks,” *2016 IEEE Global Communications Conference (GLOBECOM)*, 2016, pp. 1-6, doi: 10.1109/GLOCOM.2016.7842368.

[22] J. Mu, Y. Wei, H. Ma and Y. Li, ”Spectrum Allocation Scheme for Intelligent Partition Based on Machine Learning for Inter-WBAN Interference,” *IEEE Wireless Communications* , vol. 27, no. 5, pp. 32-37, October 2020, doi: 10.1109/MWC.001.1900551.

[23] B. Wang, Y. Sun, N. Zhao and G. Gui, ”Learn to Coloring: Fast Response to Perturbation in UAV-Assisted Disaster Relief Networks,” *IEEE Transactions on Vehicular Technology* , vol. 69, no. 3, pp. 3505-3509, March 2020, doi: 10.1109/TVT.2020.2967124.

[24] Ericsson, “R1-050764: Inter-cell interference handling for E-UTRA,” 3GPP TSG RAN WG1 Meeting #42, Aug. 2005.

[25] 3GPP TSG RAN WG1, “ Soft frequency reuse scheme for UTRAN LTE, ” R1-050507, Athens, Greece, May 2005.

[26] M. Qian, W. Hardjawana, Y. Li, B. Vucetic, X. Yang and J. Shi, ”Adaptive Soft Frequency Reuse Scheme for Wireless Cellular Networks,” *IEEE Transactions on Vehicular Technology* , vol. 64, no. 1, pp. 118-131, Jan. 2015, doi: 10.1109/TVT.2014.2321187.

[27] L. Yang, T. J. Lim, J. Zhao and M. Motani, ”Modeling and Analysis of HetNets With Interference Management Using Poisson Cluster Process,” *IEEE Transactions on Vehicular Technology* , vol. 70, no. 11, pp. 12039-12054, Nov. 2021, doi: 10.1109/TVT.2021.3114739.

[28] L. Eslami, G. Mirjalily and T. N. Davidson, ”Spectrum-Efficient QoS-Aware Resource Assignment for FFR-Based D2D-Enabled Heterogeneous Networks,” *IEEE Access* , vol. 8, pp. 218186-218198, 2020, doi: 10.1109/ACCESS.2020.3041770.

[29] A. D. Firouzabadi, A. M. Rabiei and M. Vehkaperä, ”Fractional Frequency Reuse in Random Hybrid FD/HD Small Cell Networks With Fractional Power Control,” *IEEE Transactions on Wireless Communications* , vol. 20, no. 10, pp. 6691-6705, Oct. 2021, doi: 10.1109/TWC.2021.3075987.

[30] M. Song, H. Shan, H. H. Yang and T. Q. S. Quek, ”Joint Optimization of Fractional Frequency Reuse and Cell Clustering for Dynamic TDD Small Cell Networks,” *IEEE Transactions on Wireless Communications* , vol. 21, no. 1, pp. 398-412, Jan. 2022, doi: 10.1109/TWC.2021.3096383.

[31] M. Nafees, J. Thompson and M. Safari, ”Multi-Tier Variable Height UAV Networks: User Coverage and Throughput Optimization,” *IEEE Access* , vol. 9, pp. 119684-119699, 2021, doi: 10.1109/ACCESS.2021.3107674.

[32] X. Li, Z. Liu, N. Qin and S. Jin, ”FFR Based Joint 3D Beamforming Interference Coordination for Multi-Cell FD-MIMO Downlink Transmission Systems,” *IEEE Transactions on Vehicular Technology* , vol. 69, no. 3, pp. 3105-3118, March 2020, doi: 10.1109/TVT.2020.2968095.

[33] T. Saito and F. Adachi, ”De-Centralized Adaptive 2-Step Inter-cell Interference Coordination in Distributed MIMO,” *2018 24th Asia-Pacific Conference on Communications (APCC)*, 2018, pp. 224-228, doi: 10.1109/APCC.2018.8633471.

[34] M. Simsek, M. Bennis and İ. Güvenç,“Learning Based Frequency- and Time-Domain Inter-Cell Interference Coordination in HetNets,” *IEEE Trans.actions on Vehi.cular Technology*, vol. 64, no. 10, pp. 4589-4602, Oct. 2015.

[35] Y. Wang, G. Feng, Y. Sun, S. Qin and Y. -C. Liang,“Decentralized Learning Based Indoor Interference Mitigation for 5G-and-Beyond Systems,” *IEEE Transactions on Vehicular Technology*, vol. 69, no. 10, pp. 12124-12135, Oct. 2020.

[36] M. Yan, J. Yang, K. Chen, Y. Sun and G. Feng, “Self-Imitation Learning-Based Inter-Cell Interference Coordination in Autonomous HetNets,” *IEEE Transactions on Network and Service Management*, vol. 18, no. 4, pp. 4589-4601, Dec. 2021.

[37] M. Aslan and N. A. Baykan , ”A Performance Comparison of Graph Coloring Algorithms”, *International Journal of Intelligent Systems and Applications in Engineering* , vol. 4, no. Special Issue-1, pp. 1-7, Dec. 2016, doi:10.18201/ijisae.273053.

[38] Q. Du and T. Wong, “Numerical Studies of MacQueen’s k-Means Algorithm for Computing the Centroidal Voronoi Tessellations,” *Computer & Mathematics with Applications* , Vol. 44, pp. 511-523, Aug. 2002, doi: 10.1016/S0898-1221(02)00165-7

[39] J. A. Hartigan and M. A. Wong, “Algorithm AS 136: A k-means clustering algorithm,” *Journal of the Royal Statistical Society. Series C (Applied Statistics)* , vol. 28, no. 1, pp. 100–108, 1979, https://doi.org/10.2307/2346830.

[40] Q. H. Spencer, A. L. Swindlehurst, and M. Haardt, “Zero-Forcing Methods for Downlink Spatial Multiplexing in Multiuser MIMO Channels,” *IEEE Transactions on Signal Processing* , Vol. 52, pp. 461-471, Jan. 2004, doi: 10.1109/TSP.2003.821107.

[41] C. Ge, S. Xia, Q. Chen and F. Adachi, ”2-step Graph Coloring Algorithm for Cluster-wise Distributed MU-MIMO in Ultra-dense RAN,” *2020 23rd International Symposium on Wireless Personal Multimedia Communications (WPMC)*, 2020, pp. 1-6, doi: 10.1109/WPMC50192.2020.9309477.

[42] M. de Berg, O. Cheong, M. van Kreveld, and M. Overmars, *Computational Geometry: Algorithm and Applications*, Springer Berlin Heidelberg, Jan. 2008, doi:10.1007/978-3-540-77974-2.

[43] A. Pravin Renold and S. Chandrakala, “Convex-Hull-Based Boundary Detection in Unattended Wireless Sensor Networks,” *IEEE Sensors Letters* , Vol. 1, pp. 2475-1472, Aug. 2017, doi: 10.1109/LSENS.2017.2731200.

[44] H. Edelsbrunner, D. G. Kirkpatrick, and R. Seidel, “On the Shape of a Set of Points in the Plane,” *IEEE Transaction on Information Theory* , Vol. 29, pp. 551-559, July 1983, doi: 10.1109/TIT.1983.1056714

[45] A S. Asratian, T M. J. Denley, R. Häggkvist, “Bipartite Graphs and their Applications,” *Cambridge Tracts in Mathematics, Cambridge University Press* , 1998, doi:10.1017/CBO9780511984068.

[46] R. L. Graham and P. Hell, “On the History of the Minimum Spanning Tree Problem,” *Annals of the History of Computing* , Vol. 7, No. 1, pp. 43-57, Jan.-March 1985, doi: 10.1109/MAHC.1985.10011.

[47] Y. Meng, Y. Dong, X. Liu and Y. Zhao, ”An Interference-Aware Resource Allocation Scheme for Connectivity Improvement in Vehicular Networks,” *IEEE Access* , vol. 6, pp. 51319-51328, 2018, doi: 10.1109/ACCESS.2018.2867745.

[48] M. K. Dholey, D. Sinha, S. Mukherjee, A. K. Das and S. K. Sahana, ”A Novel Broadcast Network Design for Routing in Mobile Ad-Hoc Network,” *IEEE Access* , vol. 8, pp. 188269-188283, 2020, doi: 10.1109/ACCESS.2020.3030802.

[49] V. Freschi and E. Lattanzi, “A Prim–Dijkstra Algorithm for Multihop Calibration of Networked Embedded Systems,” *IEEE Internet of Things Journal* , Vol. 8, No. 14, pp. 11320-11328, 15 July, 2021, doi: 10.1109/JIOT.2021.3051270.

[50] C. Ge, S. Xia, Q. Chen and F. Adachi, ”An Improved Method in Graph Coloring Algorithm for Interference Coordination in Cluster-wise Ultra-dense RAN,” *2020 International Symposium on Antennas and Propagation (ISAP)*, 2021, pp. 293-294, doi: 10.23919/ISAP47053.2021.9391334.

[51] A. S. Abdalla, P. S. Upadhyaya, V. K. Shah and V. Marojevic, ”Toward Next Generation Open Radio Access Networks–What O-RAN Can and Cannot Do!,” *IEEE Network (early access)*, doi: 10.1109/MNET.108.2100659.

[52] V. Mnih, K. kavukcuoglu, D. Silver. et al,“Human-level control through deep reinforcement learning,” *Nature*, vol. 518, pp. 529–533, 2015. doi: 10.1038/nature14236

[53] C. Ge, S. Xia, Q. Chen and F. Adachi, “2-layer Interference Coordination Framework Based on Graph Coloring Algorithm for A Cellular System with Distributed MU-MIMO,” *IEEE Transactions on Vehicular Technology*, 2022. doi: 10.1109/TVT.2022.3219411.

[54] Y. Qian, J. Xu, S. Zhu, W. Xu, L. Fan and G. K. Karagiannidis,“Learning to Optimize Resource Assignment for Task Offloading in Mobile Edge Computing, ” *IEEE Communications Letters*, vol. 26, no. 6, pp. 1303-1307, Jun. 2022. doi: 10.1109/LCOMM.2022.3159742.

[55] J. Xu, P. Zhu, J. Li and X. You,“Deep Learning-Based Pilot Design for Multi-User Distributed Massive MIMO Systems,” *IEEE Wireless Communications Letters*, vol. 8, no. 4, pp. 1016-1019, Aug. 2019. doi: 10.1109/LWC.2019.2904229.

List of Publications

I Journal Papers

[J1] C. Ge, S. Xia, Q. Chen and F. Adachi, ”Learning Based on Graph: A Joint Interference Coordination for Cluster-Wise Distributed MU-MIMO,” in IEEE Communications Letters, vol. 27, no. 3, pp. 871-875, March 2023, doi: 10.1109/LCOMM.2023.3239605.

[J2] C. Ge, S. Xia, Q. Chen and F. Adachi, ”2-Layer Interference Coordination Framework Based on Graph Coloring Algorithm for a Cellular System With Distributed MU-MIMO,” in IEEE Transactions on Vehicular Technology, vol. 72, no. 3, pp. 3557-3568, March 2023, doi: 10.1109/TVT.2022.3219411.

[J3] C. Ge, S. Xia, Q. Chen, and F. Adachi, “A graph coloring-based interference coordination algorithm for cluster-wise ultra-dense RAN, ” IEICE Communications Express, vol.10, No.2, 99-104, 2021.

II Conference Papers with Peer Review

[C1] C. Ge, S. Xia, Q. Chen, and F. Adachi, “Reinforcement Learning-based Interference Coordination for Distributed MU-MIMO,” 2021 24rd International Symposium on Wireless Personal Multimedia Communications (WPMC2021),14-16 Dec. 2021, Okayama.

[C2] C. Ge, S. Xia, Q. Chen, and F. Adachi,” Graph Coloring-based Interference Coordination for Ultra-dense Cellular Network with Distributed MU-MIMO, ” The 2021 IEEE 94th Vehicular Technology Conference (VTC2021-Fall), 27-30 Sep. 2021.

[C3] C. Ge, S. Xia, Q. Chen, and F. Adachi, “An Improved Method in Graph Coloring Algorithm for Interference Coordination in Cluster-wise Ultra-dense RAN,” 2020 International Symposium on Antennas and Propagation (ISAP2021),25-28 Jan. 2021.

[C4] C. Ge, S. Xia, Q. Chen, and F. Adachi, “2-Step Graph Coloring Algorithm for cluster-wise Distributed MU-MIMO in Ultra-dense RAN,” 2020 23rd International Symposium on Wireless Personal Multimedia Communications (WPMC2020),19-26 Oct. 2020.

III Conference Papers without Peer Review

[R1] C. Ge, S. Xia, Q. Chen, and F. Adachi,” A Joint Interference Coordination based on Graph Coloring Algorithm and Deep Reinforcement Learning for Cluster-wise Distributed MU-MIMO,” IEICE Technical Report, vol. 122, no. 399, pp. 66-71, Mar. 2023.

[R2] C. Ge, S. Xia, Q. Chen, and F. Adachi,” Robustness of Reinforcement Learning-based Interference Coordination for Distributed MU-MIMO,” IEICE General Conference 2022, online, 15-18 Mar. 2022

[R3] C. Ge, S. Xia, Q. Chen, and F. Adachi,” Reinforcement Learning-based Graph Coloring Algorithm for Interference Coordination in Distributed MU-MIMO”, IEICE Technical Report, Vol. 121, no. 234, pp. 69-74, 10-12 Nov. 2021, Nagasaki.

[R4] C. Ge, S. Xia, Q. Chen, and F. Adachi,” 2-step RCN-GCA for Interference Coordination for Multicell Distributed MU-MIMO in Ultra-dense RAN”, IEICE Technical Report, Vol. 120, no. 404, Mar. 2021

[R5] C. Ge, S. Xia, Q. Chen, and F. Adachi,” Cell-edge Classification for 2-step Interference Coordination in Multi-cell Distributed MU-MIMO Ultra-dense RAN,” IEICE General Conference 2021, online, Mar. 2021

[R6] C. Ge, S. Xia, Q. Chen, and F. Adachi, “The influence of different clustering method on graph coloring algorithm in Ultra-dense RAN,” Proc. IEICE Society Conference 2020, online, 15-18 Sept. 2020.

[R7] C. Ge, S. Xia, Q. Chen, and F. Adachi,” A graph coloring based interference coordination algorithm for ultra-dense RAN ”, 2020 年度電気関係学会東北支部連合大会, Aug. 27, 2020

[R8] C. Ge, S. Xia, Q. Chen, and F. Adachi,”2-Steps Graph Coloring Algorithm for Interference Coordination in 5G Advanced Ultra-dense RAN ”, IEICE Technical Report, Vol. 120, no. 29, May 2020

List of Awards

[1] GE CHANG, IEEE Sendai WIE Best Paper Award 2020, for the paper of “A graph coloring-based interference coordination algorithm for ultra-dense RAN” by C. Ge, S. Xia, Q. Chen, and F. Adachi.

[2] GE CHANG, WPMC2021 IEEE VTS-T/J Student Paper Award, for the paper of “Reinforcement Learning-based Interference Coordination for Distributed MU-MIMO” by C. Ge, S. Xia, Q. Chen, and F. Adachi, IEEE VTS Tokyo/Japan Chapter, 16 Dec. 2021.